

Instituto Tecnológico y de Estudios Superiores de Monterrey

Campus Monterrey

School of Engineering and Sciences



**OPTIMIZATION OF DISTRIBUTION NETWORKS USING  
EVOLUTIONARY ALGORITHMS**

A dissertation presented by

**Juan Pablo Avilés Arévalo**

Submitted to the

School of Engineering and Sciences

in partial fulfillment of the requirements for the degree of

**Doctor of Philosophy**

**In**

**Engineering Science**

Major in Electrical Engineering

Monterrey Nuevo León, December 1<sup>st</sup>, 2018



# Instituto Tecnológico y de Estudios Superiores de Monterrey

## Campus Monterrey

### School of Engineering and Sciences

The committee members, hereby, certify that have read the thesis presented by Juan Pablo Avilés and that it is fully adequate in scope and quality as a partial requirement for the degree of Doctor of Philosophy in Engineering Science, with a major in Electrical Engineering.



Dr. Osvaldo Micheloud  
Tecnológico de Monterrey  
School of Engineering and Sciences  
Principal Advisor



Dr. Gerardo Escobar  
Tecnológico de Monterrey  
School of Engineering and Sciences  
Reading committee member



Dr. Jonathan Mayo  
Tecnológico de Monterrey  
School of Engineering and Sciences  
Co-advisor



Dr. Daniel Guillen  
Tecnológico de Monterrey  
School of Engineering and Sciences  
Reading committee member



Dr. Nathan Johnson  
Arizona State University  
Ira A. Fulton Schools of Engineering  
Reading committee member



Dr. Rubén Morales Menéndez  
Dean of Graduate Studies  
School of Engineering and Sciences



Monterrey Nuevo León, December 1<sup>st</sup>, 2018

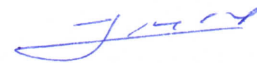




## **Declaration of Authorship**

I, Juan Pablo Avilés Arévalo, declare that this dissertation titled, 'OPTIMIZATION OF DISTRIBUTION NETWORKS USING EVOLUTIONARY ALGORITHMS', and the work presented in it are my own. Additionally, I confirm that:

- This work was done wholly or mainly while in candidature for a research degree at this University.
- Where any part of this thesis has previously been submitted for a degree or any other qualification at this University or any other institution, this has been clearly stated.
- Where I have consulted the published work of others, this is always clearly attributed.
- Where I have quoted from the work of others, the source is always given. With the exception of such quotations, this thesis is entirely my own work.
- I have acknowledged all main sources of help.
- Where the thesis is based on work done by myself jointly with others, I have made clear exactly what was done by others and what I have contributed myself.



Juan Pablo Avilés Arévalo  
Monterrey Nuevo León, December 1<sup>st</sup>, 2018.



## Acknowledgements

Firstly, I would like to express my sincere gratitude to my advisor Dr. Osvaldo Micheloud for the continuous support of my Ph.D. study and related research, for his patience, motivation, and immense knowledge. His guidance helped me in all the time of research and writing of this thesis. I could not have imagined having a better advisor and mentor for my Ph.D. study.

Besides my advisor, I would like to thank the rest of my thesis committee: Dr. Jonathan Mayo, Dr. Gerardo Escobar, Dr. Daniel Guillen, and Dr. Nathan Johnson, for their insightful comments and encouragement, but also for the hard question which incited me to widen my research from various perspectives.

My sincere thanks also go to Dr. Nathan Johnson who provided me an opportunity to join their team as an intern, and who gave me access to the LEAPS laboratory and research facilities. Without their precious support it would not be possible to complement this work.

I am grateful to my brothers and parents, Leslye, Franco, Carmen, and Juan, who have provided me through moral and emotional support in my life. Thanks to Ana, for her patience and immeasurable love during these years. I am also grateful to my other family members and friends who have supported me along the way.

A very special gratitude goes out to the “Instituto de Fomento al Talento Humano” and to SENECYT for providing the scholarship for this doctoral study.

And finally, last but by no means least, also to everyone in the “Consortio Empresarial”, it was great sharing a space with all of you during the last five years. You can count on my friendship and support always.

Thanks to everyone for your support!



*No te rindas, aún estas a tiempo  
de alcanzar y comenzar de nuevo,  
aceptar tus sombras, enterrar tus miedos,  
liberar el lastre, retomar el vuelo.  
No te rindas que la vida es eso,  
continuar el viaje,  
perseguir tus sueños,  
destrabar el tiempo,  
correr los escombros y destapar el cielo.*

*“No te rindas” – Mario Benedetti.*



# OPTIMIZATION OF DISTRIBUTION NETWORKS USING EVOLUTIONARY ALGORITHMS

by

Juan Pablo Avilés Arévalo

## Abstract

One of the biggest problems that a distribution network (DN) must face is the constant increase in load demand, which eventually will cause the degradation of its optimal operation. To overcome these challenges the distribution network usually is oversized or reinforced, however, although this is a quick and practical solution, it is not necessarily the most economical and efficient one. For this reason, it is desirable to implement an optimization algorithm to improve the network without increasing investment costs. The optimization of a power distribution network is not an easy task, because this is the most extensive part of the entire electrical system. Due to this extension, along with the high complexity of the topology, and some quality parameters that must be respected, the entire design or improvement of a distribution network can be considered as an extremely hard combinatorial, non-convex, and non-linear optimization problem, difficult to solve by conventional methods.

For these reasons, we propose a *Two-Stage Multiobjective Evolutionary Approach* (TS-MOEAP) capable to design and optimize distribution networks, at primary and secondary levels. Due to the complexity of the optimization problem, the approach is implemented in two stages, that can be summarized as follows:

*Stage-1.* Optimal placement and sizing of generation units, as well as optimal branch routing and conductor sizing. For this purpose, an *Improved Particle Swarm Optimization* technique (IPSO) combined with a greedy algorithm is introduced.

*Stage-2.* Optimal network reconfiguration. For this, an *Improved Nondominated Sorting Genetic Algorithm with a Heuristic Mutation Operator* (INSGA-HO) is presented, aiming at minimizing the total power loss and investment cost of the system.

Finally, to complement the optimization process, the software DER-CAM will be used to find optimal investment solutions for *Distributed Energy Resources* (DER). Both algorithms are successfully applied to design and optimize real distribution networks that presented several problems, concluding that the combination of these approaches -network reconfiguration with optimal installation of DERs- can converge toward better configurations than other algorithms.





## List of Figures

South America projected average growth of electricity demand.....	2
The basic structure of the electric power system.....	4
Typical Layout of an electric distribution system.....	5
General structure of TS-MOEAP. ....	15
Flow-diagram of the thesis.....	18
The general pseudocode of an evolutionary algorithm. ....	20
The general scheme of an evolutionary algorithm. ....	20
General pseudocode of the GA with a numerical example.....	24
Illustration of the Pareto front and dominance concept. ....	26
NSGA-II procedure. ....	27
MOEA-D procedure. ....	28
Representation of a distribution network.....	30
Model construction by using PRIM.....	31
Obtainment of the GMR and GMD using ETAP.....	32
System model for the power flow analysis. ....	34
Optimal placement of DTs/DGs by the IPSO. ....	43
IPSO-PRIM operation.....	44
Optimal result after Stage-1 of TS-MOEA.....	46
General flowchart of the IPSO-PRIM algorithm. ....	46
LVDN design with/without quality issues. ....	47
Curves for the fitness, power losses and quality issues. ....	48
LVDN design considering branch overcurrents.....	48
LVDN design regarding voltage drops and overcurrents.....	49
Nondominated sorting and crowding distance procedure. ....	52
Pseudocode of the Nondominated Sorting.....	54
Crowding distance calculation. ....	55
Creation of a random population R. ....	56
Heuristic mutation operation. ....	57
INSGA-HO process. ....	58
TS-MOEAP operation.....	59
Pseudocode of TS-MOEAP. ....	61
Flowchart of TS-MOEAP. ....	62
Application of TS-MOEAP to design an off-grid electrification project. ....	64
Geographical coordinates of the case studies. ....	65
TS-MOEAP evolution process and results for CM1.....	66
Optimal configuration for CM2 by TS-MOEAP. ....	68
TS-MOEAP convergence curve.....	68
Non-optimal results for CM2 .....	69

Demand profile of a residential user. ....	72
Test system LVDN1. ....	72
Random configuration from the first generation. ....	74
Best result for LVDN1 found by TS-MOEAP. ....	74
Different results before and after the optimization for LVDN1. ....	75
Algorithm comparisons for total investment cost, power loss, and quality issues. ....	77
Pareto fronts of MOEA/D and INSGA-HO for the test system LVDN1. ....	78
Test system LVDN2. ....	79
Best result for LVDN2 found by TS-MOEAP. ....	81
Results for LVDN2, before and after the optimization. ....	81
Different results before and after the optimization for LVDN2. ....	82
Entire set of possible solutions found by TS-MOEAP. ....	83
Test system MVDN1. ....	84
Test system MVDN2. ....	85
Best result for MVDN1 found by TS-MOEAP. ....	86
Evolutionary process for the reconfiguration of MVDN1. ....	86
Pareto front of MVDN1 obtained by TS-MOEAP. ....	87
Best result for MVDN2 found by TS-MOEAP. ....	88
Optimal power flow for MVDN2. ....	88
Obtaining GPS coordinates, using the device's GPS or an excel file. ....	90
First glance of the network, with the activation of branch restrictions. ....	90
Changing parameters for the network design. ....	91
Setting the size of conductors and the location of transformer manually. ....	91
Network design by the IPSO-PRIM algorithm. ....	92
Example of a network presenting some problems. ....	93
Overall input and output structure of DER-CAM. ....	96
Scenario 1, base case. ....	97
Summary of results for the base case. ....	98
Summary of results for the base case with induction stoves and without DERs. ....	99
Summary of results for the base case with induction stoves and DERs. ....	99
Installation of DERs for the base case with induction stoves. ....	100
Electricity dispatch for the base case with induction stoves and DERs. ....	100
MVDN2 optimized by TS-MOEAP and DER-CAM. ....	101
MVDN2 optimized by DER-CAM. ....	101
Electricity dispatch for the optimized network with induction stoves and DERs. ....	102
Load profiles of the utility and load factors. ....	102
Electricity dispatch implementing load shifting and peak shaving. ....	103
Comparison of scenarios, with/without DERs. ....	104
Test system MVDN2-LVDN1, improved by TS-MOEAP and DER-CAM. ....	104
Daily solar radiation and average temperature of the test area. ....	111
Diagram of the city, for the case studies LVDN1 and LVDN2. ....	113

## List of Tables

Impedance for the most important conductors used in DNs. ....	33
Available conductors with their amapcities and costs. ....	37
Available transformers with their costs. ....	37
Considered inverters and batteries. ....	38
Nomenclature. ....	65
TS-MOEAP results for CM1 and CM2. ....	67
Results for different DG placement in CM2-Gs. ....	67
TS-MOEAP vs centralized/decentralized models. ....	69
TS-MOEAP vs Single Objective/Standard Operators. ....	70
Quality issues of the test system LVDN1. ....	73
Geographical and technical constraints of LVDN1. ....	73
Results for the test system LVDN1, before and after the optimization. ....	76
Algorithm comparisons for LVDN1. ....	79
Quality issues of the test system LVDN2. ....	80
Geographical and technical constraints of LVDN2. ....	80
Results for the network T4. ....	81
State information for network T2 before the optimization. ....	82
Results for MVDN1, before and after the optimization. ....	85
Results for MVDN2, before and after the optimization. ....	87
Solar radiation of the test area. ....	111
Active and reactive loads per node of the test system LVDN1. ....	115



# Contents

Abstract.....	vii
List of Figures.....	ix
List of Tables .....	xi
Abbreviations and Notations .....	xv
Chapter 1.....	1
Introduction	
1.1. Distribution Network Planning .....	1
1.2. Distribution Network Structure and Overview .....	3
1.3. Quality Issues, Power Losses, and Possible Solutions .....	8
1.4. Optimization Challenges .....	10
1.5. Objectives and Hypothesis.....	13
1.6. A Two-Stage Multiobjective Evolutionary Approach .....	14
Chapter 2.....	19
Evolutionary Algorithms	
2.1. What is an Evolutionary Algorithm? .....	19
2.2. The Components of Evolutionary Algorithms .....	21
2.3. Evolutionary Algorithm Variants.....	22
2.4. Multiobjective Evolutionary Algorithms.....	25
2.5. Summary .....	28
Chapter 3.....	29
Construction and Evaluation of a DN Model	
3.1. Representation and Model Construction.....	29
3.2. Evaluation of the Model.....	31
3.3. Economic Evaluation .....	36
3.4. Summary .....	38
Chapter 4.....	39
Stage-1 of TS-MOEAP (IPSO – PRIM)	
4.1. Objective Functions for the Evolutionary Algorithms .....	39

4.2.	Implementation of Stage-1 (IPSO – PRIM) .....	43
4.3.	IPSO-PRIM Complete Algorithm .....	46
4.4.	Simulations and Results for the IPSO-PRIM Algorithm.....	47
4.5.	Summary .....	50
Chapter 5.....		51
	Stage-2 of TS-MOEAP (INSGA – HO)	
5.1.	Reformulation of the Objective Functions in Terms of Constraints .....	51
5.2.	Implementation of Stage-2 (INSGA-HO).....	52
5.3.	Summary of TS-MOEAP .....	59
5.4.	Complete Algorithm of TS-MOEAP (INSGA-HO/IPSO) .....	60
5.5.	Main Contributions of the Proposal .....	60
Chapter 6.....		63
	Implementation of TS - MOEAP	
6.1.	Optimal Design of Off-Grid Electrification Projects with DG.....	63
6.2.	Optimal Condition Restoration of Secondary Distribution Networks .....	71
6.3.	Optimal Reconfiguration of Primary Distribution Networks .....	83
6.4.	Implementation of the IPSO-PRIM Algorithm in Android-Java .....	89
6.5.	Summary .....	92
Chapter 7.....		95
	Network Optimization using DER-CAM	
7.1.	DER-CAM.....	95
7.2.	Implementation of DER-CAM for the Case Study MVDN2 .....	97
7.3.	Summary .....	105
Chapter 8.....		107
	Conclusions and Future Work	
Appendix A.....		111
	Solar Radiation for the Case Studies CM1 y CM2	
Appendix B .....		113
	Diagram of the Urban Area for the Case Studies LVDN1 and LVDN2	

Appendix C .....	115
Active and Reactive Loads for the Test System LVDN1	
Appendix D .....	117
Java Code for the IPSO Algorithm	
Published Papers .....	119
Curriculum Vitae .....	121
References .....	123

## Abbreviations and Notations

### Abbreviations

---

DN	Distribution Network
TS-MOEAP	Two-Stage Multiobjective Evolutionary Approach
IPSO	Improved Particle Swarm Optimization
INSGA-HO	Improved Nondominated Sorting Genetic Algorithm with a Heuristic Mutation Operator
LVDN	Low Voltage Distribution Network
MVDN	Medium Voltage Distribution Network
DG	Distributed Generation
DER	Distributed Energy Resources
RES	Renewable Energy Source
NR	Network Reconfiguration
DT	Distribution Transformer
GMR	Geometric Mean Radius
GMD	Geometric Mean Diameter
EA	Evolutionary Algorithm
SDN	Secondary Distribution Network
DPG	Distributed Photovoltaic Generation

---

## Notations

---

$\chi_i^{(t)}$	Particle's position
$v_i^{(t)}$	Particle's velocity
$<$	Operator of dominance
$\lambda^j$	Weight vectors
$\mathbb{Z}^+$	Set of positive integers
$c_i$	Chromosome
$G_k$	Group of loads
$d_{ij}$	Euclidean distance
$u_i$	Node
$U_{ij}$	Branch between nodes $i$ and $j$
$f_1'(c)$	Objective function for power losses
$f_2'(c)$	Objective function for investment costs
$\mathcal{D}$	Crowding distance operator
$\mathcal{H}$	Heuristic mutation operator

---



# Chapter 1

## Introduction

In this chapter, we provide a general introduction to the challenges of designing and optimizing distribution networks, and we briefly study their structure, common technical issues, and conventional design. Due to the complexity that presents these type of combinatorial optimization problems, we present and justify the implementation of a Two-Stage Multi-objective Evolutionary Approach (TS-MOEAP) to design and optimize distribution networks.

### 1.1. Distribution Network Planning

A power distribution network is the most extensive part of the entire electrical system and consists of Low Voltage (LV) and Medium Voltage (MV) networks. Its extension hinders its planning, since it is necessary to respect certain quality parameters towards the final consumer, maintaining adequate levels of reliability.

In the LV network planning the designer must find the optimal network topology, for later set the optimal capacity and placement of distribution transformers. At this level, the design must be done minimizing investment costs and line power losses.

In the MV network planning, the designer must identify the location and size of distribution substations and MV feeders. Also, the optimal path and size for the conductors must be found to feed all distribution transformers. The objective at the MV level is to minimize the total investment cost along with line power losses, to improve reliability indices [1].

During the planning procedure several constraints should be satisfied, for example, the bus voltage magnitude should be maintained within a standard range and the branch currents must not exceed the ampacity of conductors. Furthermore, the capacity of transformers and MV feeders must not be exceeded. Apart from these constraints, the planning must consider line loss reduction as well as load growth and peak loads, particularly for urban and rural areas. To meet all these requirements, the networks could incorporate more equipment and reinforce their structure (e.g. transformers and conductors) what causes the increase of investment costs, however, the utilities always try to minimize their budgets, which

are inversely proportional to the robustness of the network. Therefore, network planning become a complex multiobjective optimization problem.

In practical distribution networks, the demand grows gradually, for example for South America the projected average growth of electricity demand for the 2010-2022 horizon are Bolivia 6.3%; Chile 5.3%; Colombia 3.5%; Ecuador 5.5%; and Peru 6.7% [2]. The projected load profiles for these countries are shown in Figure 1.1.

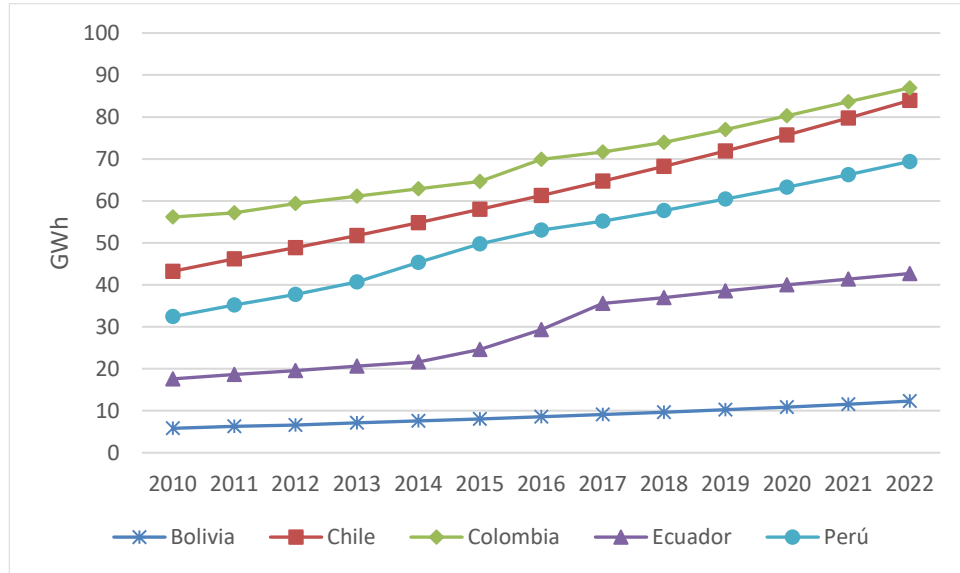


Figure 1.1. South America projected average growth of electricity demand.

This load growth eventually causes degradation of optimal operating conditions of the distribution networks, therefore the electrical system must be modernized and improved very often. However, current commercial software such as HOMER and DER-CAM only serves to optimize existing networks through the implementation of distributed generation and they do not apply to design and reconfigure the network topology. Other software such as ETAP help us to design distribution networks but all the decisions must be taken by the designer, i.e. ETAP is only an evaluation software.

Due to the discrete and nonlinear nature of the entire distribution network planning, conventional optimization methods are not suitable to solve these problems. Therefore, the best option is to implement metaheuristic-based methods which can deal with the particularities of the design.

## **1.2. Distribution Network Structure and Overview**

### **1.2.1. Electric Power Distribution**

Electric power distribution is the final stage in the delivery of electric power; it carries electricity from the transmission system to individual consumers. Distribution substations connect to the transmission system and lower the transmission voltage to medium voltage ranging between 5 kV and 35 kV, with the use of transformers. Primary distribution lines carry this medium voltage power to distribution transformers located near the customer's premises. Distribution transformers again lower the voltage to the utilization voltage used by lighting, industrial equipment or household appliances. Often several customers are supplied from one transformer through secondary distribution lines. Commercial and residential customers are connected to the secondary distribution lines through service drops. Customers demanding a much larger amount of power may be connected directly to the primary distribution level or the sub-transmission level [3].

Electric power distribution systems are designed to serve their customers with reliable and high-quality power. The most common distribution system consists of simple radial circuits (feeders) that can be overhead, underground, or a combination. From the distribution substation, feeders carry the power to the end customers, forming the medium-voltage or primary network, operated at a medium voltage level. Feeders range in length from a few kilometers to several tens of kilometers. As they must supply all customers in the designated distribution area, they often curve and branch along the assigned corridors. A substation typically supplies 3–30 feeders.

Distribution transformers or secondary transformers, placed along feeders, convert the voltage from the medium to a low voltage level, suitable for direct consumption by end customers. Typically, a rural primary feeder supplies up to 50 distribution transformers, spread over a wide region, but the number can vary depending on configuration. They are sited on pole tops, cellars or designated small plots. From these transformers, low-voltage or secondary network branches off to the customer connections at customer premises, equipped with electricity meters [4].

Figure 1.2 shows the basic structure of the electric power system with the typical voltage level for each stage. In the following, we describe the characteristics of primary and secondary lines.

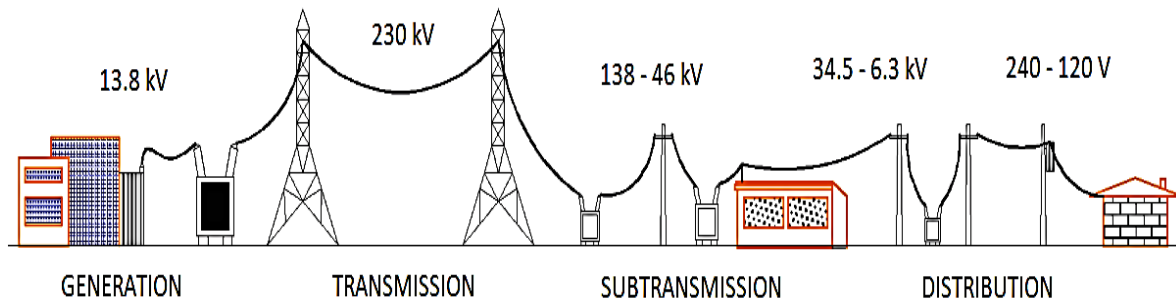


Figure 1.2. The basic structure of the electric power system.

### a) Primary distribution lines

Primary distribution voltages range from 5 kV to 35 kV (phase-to-phase). The higher the voltage, the lower the current, and thus the lower the resistive losses on these lines. However, higher voltages require taller poles (or more expensive undergrounding technology), so there is a cost/efficiency tradeoff. Only large consumers are fed directly from distribution voltages; most utility customers are connected to a distribution transformer, which reduces the distribution voltage to the "*utilization voltage*".

For primary lines, we have two types of configurations, radial or meshed. A radial system is arranged like a tree where each customer has one source of supply. A meshed system has multiple sources of supply operating in parallel. Meshed networks are used for concentrated loads and radial systems are commonly used in rural or suburban areas. Long feeders experience voltage drops (power factor distortion) requiring capacitors or voltage regulators to be installed. Reconfiguration, by opening or closing specific switches, represents one of the most important measures which can improve the operational performance of a distribution system. The optimization problem through the reconfiguration of a power distribution system was introduced by Merlin and Back (1975) [5] with the main objective to minimize active power losses.

### b) Secondary distribution lines

A low-voltage network or secondary network is a part of electric power distribution which carries electric energy from distribution transformers to electricity meters of end customers. Secondary networks are operated at a low voltage level, which is typically equal to the mains voltage of electric appliances. Most modern secondary networks are operated at AC rated

voltage of 100 – 127 or 220 – 240 V, at the frequency of 50 or 60 Hz. The operating voltage establishes the number of phases (three-phase or single-phase) and the required reliability dictates the topology and configuration of the network. The simplest form is a radial service drop line from the transformer to the customer premises. Electric wiring can be realized by overhead power lines or underground power cables, or their mixture.

Urban distribution is mainly underground, sometimes in common utility ducts. Rural distribution is mostly above ground with utility poles, and suburban distribution is a mix. Closer to the customer, a distribution transformer steps the primary distribution power down to a low-voltage secondary circuit for residential customers. The power comes to the customer via a service drop and an electricity meter. The final circuit in an urban system may be less than (15 m) but may be over 300 feet (90 m) for rural customers [4].

Figure 1.3 shows a typical layout of a distribution network, composed of a medium-voltage network (green line) and a low-voltage network (blue line). The secondary network, presented in a radial form, shows a three-phase (urban network) and single-phase (rural network) connections.

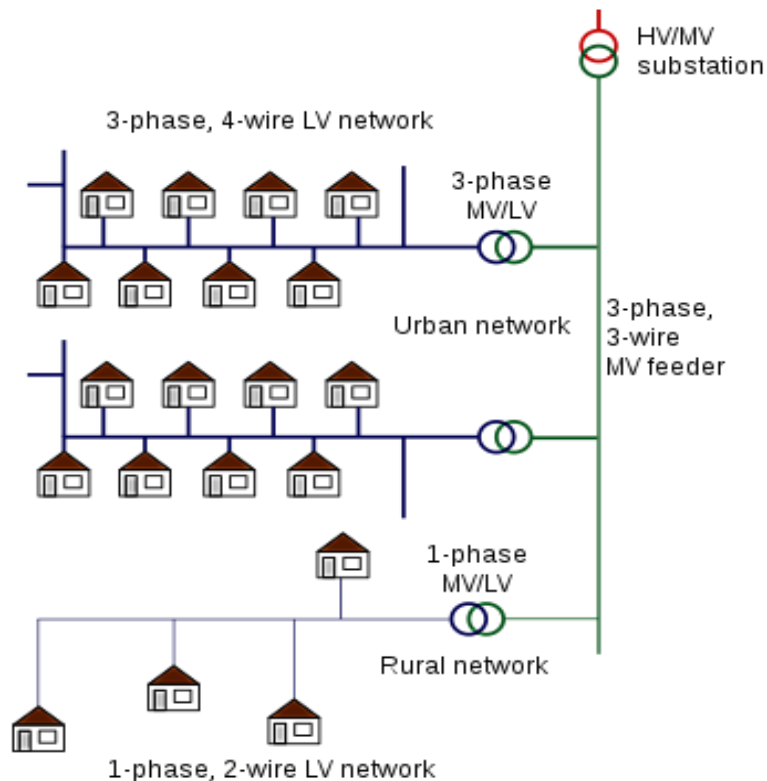


Figure 1.3. Typical Layout of an electric distribution system [6].

### **1.2.2. Conventional Design of Distribution Networks**

In this section, we briefly explain how LV and MV distribution networks are designed following the regulations of the utility company EERSSA [7] from Ecuador. According to this manual, the general procedure is as follows:

#### **a) Design of LV Networks**

- i. To begin the design, a georeferenced topographic survey must first be carried out under the WGS84 UTM coordinate system, to define the location of users and utility poles.
- ii. Depending on whether it is a rural or urban area, define a single-phase or three-phase system and the level of tension, e.g. 240/120 V or 220/127 V.
- iii. Identify if there are especial loads above 10 kVA. If this is the case, the special consumer must install his own transformer.
- iv. Calculate the Maximum Projected Demand (MPD) considering the installed capacity per user, the number of users, and a coincidence factor. For residential loads, the consumer demand is established by the utility company with a projection of 10 years.
- v. Calculate the capacity of Distribution Transformers (DTs) using the MPD and an overload factor (according to the installed capacity of residential users).
- vi. Establish the route for the conductors and place the DT at a node, regarding the designer's criteria.
- vii. Calculate the voltage drop (VD). For secondary lines in rural areas the VD must not exceed 5.5 %, and for urban areas must not exceed the 4.5 %.
- viii. If the VD exceeds the limit, change the position of the transformer or the size of the conductors.

#### **b) Design of MV Networks**

Once the LV network has been designed, we proceed to design the MV network as follows:

- i. First, the designer must choose the route for the medium voltage lines.

- ii. Choose the voltage level (13.8/7.97 kV or 22/12.7 kV) and the configuration of the network such as single-phase, two-phase or three-phase. The MV network must be projected for 15 years.
- iii. Determine the conductor considering the loads and the allowable voltage drop (3.5% for urban areas and 7% for rural areas). The utility must provide the voltage drop value and the power losses at the starting point of the project. The conductor must be ACSR.
- iv. Install fuse switches on all three-phase and single-phase branches that derive from a primary feeder.
- v. If the technical requirements and voltage drops are not met, select another path or another feeder.

### 1.2.3. Distributed Generation

As this research also covers the optimal localization of distributed generation, a brief explanation of this topic is necessary. Distributed generation (DG), also known as distributed energy, on-site generation or decentralized generation is electrical generation and storage performed by a variety of small grid-connected devices referred to as distributed energy resources (DER) [8].

Distributed generation employs small-scale technologies to produce electricity close to the end users. DG technologies often consist of modular generators, and they offer several potential benefits. In many cases, distributed generators can provide lower-cost electricity, higher power reliability, and more security with fewer environmental consequences than can traditional power generators.

DG systems typically use renewable energy sources, including small hydro, biomass, biogas, solar power, wind power, and geothermal power, and increasingly play an important role in the electric power distribution system. Among the services provided by the DGs, we have *reduction in peak power requirements*, *provision of ancillary services*, *emergency power supply* and *diversification of energy sources*. These services may lead to the reduction of power losses in transmission and distribution lines, increase the reliability of the systems (working in isolated mode), minimize the growing congestion and correct poor power quality that results from a variety of factors, including poor switching operations in the network, voltage dips, interruptions, transients, and network disturbances from loads.

### 1.3. Quality Issues, Power Losses, and Possible Solutions

Within the design and optimization of distribution networks, several constraints must be considered to deliver quality power to end users. Among the most important quality issues (QI) that we must avoid in the network design are:

- *Voltage Drop*: a decrease in voltage along a conductor due to its impedance, through which current is flowing. Voltage drop is considered as a long-time voltage variation caused by an excess of loads, thin electrical conductor, or poor power factor.
- *Branch Overcurrent*: a larger than intended electric current through a conductor, leading to excessive generation of heat. Possible causes for overcurrent include short circuits, excessive load, incorrect design, or a ground fault.
- *Overloaded Transformer/Generator*: caused by the rapid expansion of the network/loads without adequate capacity planning. An overloaded transformer presents an obstacle to future plant expansion and heavily overloaded transformers can over-heat and pose a potential fire hazard.

To avoid these problems, constraints for voltage magnitudes, the ampacity of conductors, and the maximum capacity for transformers/generators must be introduced at the beginning of the design. For the case of islanded networks, the capacity of the battery banks should also be considered as a constraint.

Apart from the power quality, the DN must be designed to minimize power losses and investment costs. To minimize power losses, the structure of the network can be reinforced, and during this process, the power quality and reliability of the system are improved as well. The disadvantage is that reinforcing the network also increases investment costs, therefore, the design problem can be considered as a complex combinatorial multi-objective optimization problem, where the main objectives to minimize are power losses and investment costs.

In the following, we describe the causes of power losses in distribution networks and what are the alternatives to minimize them.

#### 1.3.1. Power Losses in Distribution Networks

Electricity losses occur at each stage of the power distribution process, beginning with the step-up transformers that connect power plants to the transmission system and ending with the customer wiring beyond the retail meter. System average line losses are in the range of



6 to 10 percent of the total power generated on most utility grids. The largest amounts of these losses occur in primary and secondary distribution networks and can be classified as either technical or non-technical losses.

#### a) Technical Losses

Occur when the energy is dissipated by the equipment and conductors of the network. Some losses, called “core” or “no-load” losses, are incurred to energize transformers in substations and on the distribution system. A larger share is labeled “resistive” or “copper” losses. These losses reflect the resistance of the materials themselves to the flow of electricity. Core losses are typically 25 to 30 percent of total distribution losses and do not increase (or decrease) with changes in load [9]. Resistive losses are analogous to friction losses in the lines and transformers. As loads increase, the wires get hotter, the material becomes more resistive, and line losses increase. For this reason, resistive losses increase exponentially to the current ( $I^2R$ ) and are typically 70 to 75 percent of the technical losses in a distribution system [9]. Among the causes of technical losses are inefficient equipment, inadequate size of conductors, long distribution lines, load imbalance among the phases, low power factor, overloading of lines, transformers installed far from the load centers, and inadequate size of transformers.

#### b) Non-Technical Losses

The non-technical losses also referred to as commercial losses, are those related to unmetered supplies, incorrect billing, untimely billing, wrong tariff, defective meters and energy thefts.

### 1.3.2. Alternatives to Minimize Power Losses and Quality Issues

Some potential methods for dealing with power losses include:

- *Replacing old equipment:* Installing cables with a higher power rating and updating distribution transformers can reduce the total power loss and voltage drops.
- *Right-sizing transformers:* Transformers operate most efficiently when they are at 80-100% of maximum capacity. Underloaded transformers are inefficient due to core

losses. A careful analysis is needed to determine when it would make sense financially to upsize, downsize, or shut off a transformer.

- *Phase balancing*: Considering that resistive losses are a nonlinear function of current, balancing the current delivered through each phase line can reduce the total losses of the system. An analysis of customer loads and circuit geometry can be used to determine the best way to rebalance the loads on each phase.
- *Demand management*: Customer demand can be reduced by offering rewards for reducing power consumption during peak periods. Because loss is a nonlinear function of current flow, even modest reductions in power usage at peak periods can have a substantial effect on total loss.
- *Voltage optimization*: By carefully re-adjusting voltage levels in a network it may be possible to reduce the current flow in parts of the network, decreasing the total resistive loss of the system.
- *Feeder Restructuring*: The topology of the network can be changed by opening or closing specific switches to minimize active power losses.
- *DG Implementation*: As DG systems generate power locally to fulfill customer demands, appropriate size and placement of DG can drastically reduce power losses.
- *Capacitor Placement*: Capacitor banks are installed in power distribution systems for voltage support, power factor correction, reactive power control, loss reduction, system capacity increase, and billing charge reduction.

Identifying the best method for reducing power losses can be challenging, due to the complexity of the network topology, the mixture of discrete variables (transformers, capacitors, and DG placement) and the set of nonlinear equations. However, recent proposals are implementing metaheuristic methods to overcome these inconveniences, since evolutionary algorithms are ideal to solve this kind of combinatorial optimization problems.

## **1.4. Optimization Challenges**

One of the biggest problems that utility companies face is the constant increase in load demand with the increasing penetration of distributed generation (DG) and renewable energy sources (RES). Furthermore, they must mitigate other problems such as voltage devia-

tions, power quality issues, and system reliability. To overcome these challenges, the distribution network (DN) usually is oversized, however, although this is a quick and practical solution, it is not necessarily the most economical and efficient one.

Since distribution networks display high complexity in terms of their topology, their optimal planning is not an easy task. For the design must be considered the optimal number, placement, and size of generation plants, in order to feed all users under strict power quality requirements. Furthermore, the system must be designed to minimize power losses and investment costs. This problem becomes even more challenging when DG is involved. Additional difficulties include the consideration of non-uniform loads, the future projection of user growth, the remote location of RES, and geographical constraints.

This has brought new opportunities to improve electrical systems. For instance, *optimal placement* and adequate *size estimation* of DGs, with a suitable *network configuration* can improve an electrical system by reducing power losses, excessive generation, and overall costs. These goals can potentially improve the service quality, reliability and voltage profiles provided to end customers and enable the integration of RES to the grid [10-14]. In the following, a bibliographic review of these two research directions is presented.

#### **1.4.1. Network Reconfiguration**

Among the methods used to improve distribution systems, *Network Reconfiguration* (NR) [15] is a well-known technique that consists in changing the topology of the network by opening or closing existing switches, aimed to find a new radial configuration where one or more objectives can be minimized [16]. Common issues treated by NR are the minimization of power losses or voltage deviations, for which different meta-heuristic methods such as biogeography-based optimization (BBO) [17]; selective particle swarm (SPSO) [18]; genetic algorithms (GA) [19, 20] and ant colony algorithms (ACA) [21], have been applied (e.g. in 12.66 kV systems). However, due to the complexity of such combinatorial optimization problem, these heuristic methods require considerable time to converge to a solution, therefore compensation techniques for switch exchange or simplifications in the power flow calculation [14, 22] can be applied to reduce the computational time. Although these optimization methods offer satisfactory results, the location of DGs must be pre-established.

The use of NR with a single-objective function does not ensure the resolution of all the quality issues in the network, therefore multi-objective approaches are preferred. For example, in [23], a multi-objective differential evolution algorithm (DE) is presented for optimal NR, minimizing power losses and voltage deviations. Despite the satisfactory results, the drawback is the use of scalarization, which requires a new weighting when the user's preferences change. Moreover, other approaches such as [24, 25] and [26] solve these multi-objective optimization problems using fuzzy logic. However, the drawback of these methods is the proper tuning of membership function parameters (MF) when the algorithm is intended to be applied to other systems. As we argue in this paper, to avoid these disadvantages, in [27], a nondominated sorting particle swarm optimizer (NSPSO) is presented for NR.

#### **1.4.2. Optimal Placement and Sizing of Distributed Generation**

Another well-known method to optimize DNs is the *Optimal Placement and Sizing* of distributed generation (DG) (e.g. see [10, 28]) for a given network topology. The implementation of new generators, in radial distribution systems, could minimize the total power loss, reactive power flow, and voltage deviation. For example, in [29] and [30] a krill herd algorithm (KHA) and a symbiotic organism search (SOS) are implemented to minimize total power losses through optimal placement of DGs. In [31], a combination of NR and DG optimal placement is tested for power loss reduction, however, voltage deviation and branch overcurrents are not considered. In [32], a two-stage evolutionary optimization method is implemented for multi-year expansion planning of primary distribution systems (e.g. 20 kV), although only the investment cost is considered. In [33], a multi-objective approach for optimal placement of DGs and capacitors is presented, with the goal of minimizing the real power loss and the net reactive power flow of 12.66 kV systems. Although satisfactory results are achieved, the number of DGs to install must be pre-specified. Finally, in [34] an improved nondominated sorting genetic algorithm (INSGA) is proposed to minimize power losses, voltage deviations, and to improve the voltage stability of primary distribution networks, combining optimal placement and sizing of DGs.

Other proposals focus on the improvement of the network through the *optimal placement of distributed generation and capacitors*. For example, in [35], a multi-objective approach is used to minimize the real power loss and the net reactive power flow, by means of optimal placement and sizing of DGs and capacitors and in [36], the power quality of DNs is improved by optimal sitting, sizing, and harmonic tuning orders of LC filters.

Even though a simultaneous solution of the two research directions outlined above is highly desirable, we can find only a few contributions with this aim, e.g. [37-39]. Particularly in [37], a meta-heuristic method based on a greedy randomized adaptive search procedure (GRASP) is used to design off-grid electrification systems with distributed generation. However, a non-trivial computational effort is demanded as the complexity of the system increases. In [38], a genetic algorithm-based tool is tested to solve a dynamic multistage planning that aims at sizing and locating substations in distribution networks. This algorithm generates satisfactory results, as long as a set of plausible substation locations and branch interconnections are provided *a priori*. In [39], a model for active distribution systems expansion planning based on genetic algorithms is presented, where DG integration is considered together with network reconfiguration. The possible drawback of this model is that only considers the minimization of a single objective function based on costs and cannot guarantee the network radiality and accomplishment of power quality parameters.

## 1.5. Objectives and Hypothesis

- *Main Objective:*

Get an approach to optimize or design primary and secondary distribution networks, considering the problems caused by the growing demand.

- *Secondary Objectives:*
  - i. The algorithm must be able to design from scratch off-grid electrification projects or optimize existing networks with several quality issues.
  - ii. The approach must combine the advantages of network reconfiguration and optimal placement of distributed generation.
  - iii. The approach must be able to solve a multiobjective, combinatorial, nonconvex, and non-linear optimization problem, so-called distribution network design.
  - iv. The algorithm must find the optimal topology of the network, dividing the users into groups and selecting the optimal path of the conductors.
  - v. Once the topology has been defined, the algorithm must select the optimal capacity and placement of transformers/distributed generators. The algorithm must also consider the optimal size of conductors.

- vi. The algorithm must design the network under strict power quality requirements trying to minimize power losses and investment costs.
- vii. To complement the network optimization a second algorithm such as DER-CAM can be implemented after the network reconfiguration.

- *Hypothesis:*

An evolutionary approach, based on the concepts of network reconfiguration and optimal placement of distributed generation, can optimize or help with the design of distribution networks, mitigating quality issues, power losses and excessive investment costs caused by the growing demand.

## **1.6. A Two-Stage Multiobjective Evolutionary Approach**

### **1.6.1. The Proposal**

Considering all the arguments described in section 1.1 (regarding the planning of distribution networks), the optimization challenges presented in section 1.4, and the required objectives of section 1.5, we propose a Two-Stage Multiobjective Evolutionary Approach (TS-MOEAP) to design and optimize distribution networks, at primary and secondary levels. The approach is implemented in two stages, due to the complexity of the entire optimization problem, which is nonconvex, nonlinear and mixed-integer. TS-MOEAP will be able to improve a DN which may have several problems or to design a DN from scratch. Each stage can be summarized as follows:

- *Stage-1: Optimal placement and sizing of DTs/DGs*, as well as optimal *branch routing* and *conductor sizing*. For this purpose, a particle swarm optimization technique and a greedy algorithm can be used to minimize power losses and quality issues.
- *Stage-2: Optimal network reconfiguration*. For this, a genetic algorithm or a more complex variant of it, can be implemented to find the optimal topology of the network, aiming at minimizing the total power loss and investment cost of the system.

The proposed structure permits to find the optimal network topology and the optimal number of DTs/DGs with their capacity and best location. Furthermore, the algorithm must design

the system under power quality requirements, network radiality, and geographical constraints. The approach uses GPS coordinates as input data and develops a network topology from scratch, driven by overall costs and power losses minimization.

Figure 1.4 shows the general structure of TS-MOEAP. Genetic algorithms were selected for the Stage-2 since they can work with discrete variables, and their genetic operators can be adapted to modify the structure of the network. A particle swarm optimization technique was chosen for Stage-1 for its simplicity and outstanding performance, being ideal to be used as a sub-optimization function within the general algorithm.

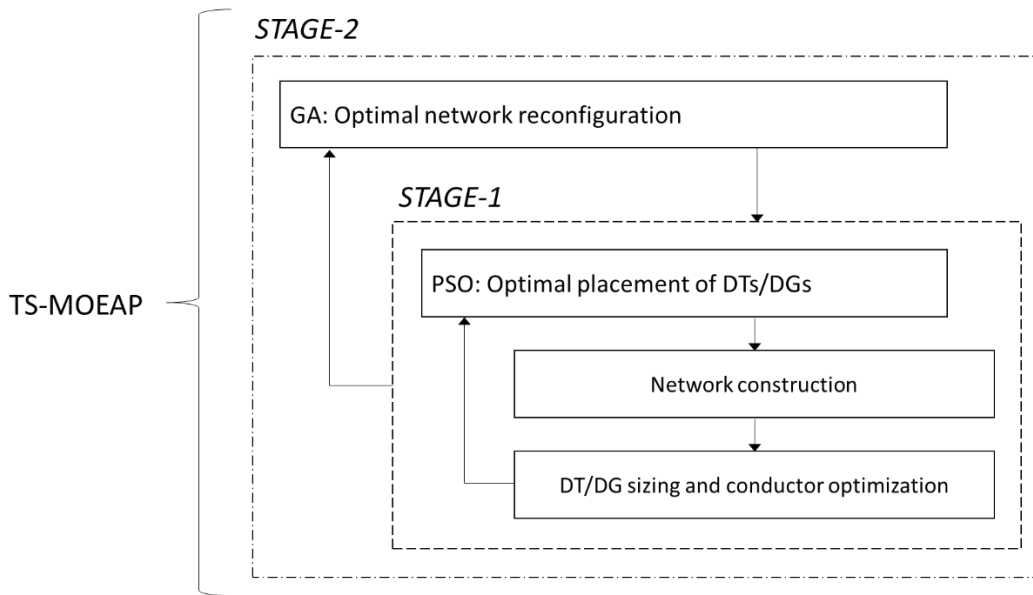


Figure 1.4. General structure of TS-MOEAP.

We must emphasize that the hybrid algorithm must be able to design a DN from scratch or restore the optimal condition of existing networks, therefore TS-MOEAP can be implemented to solve some problems that other authors have not been able to do it. For example, *the design from scratch of small off-grid networks with DGs*, since unlike grid-connected systems, off-grid projects have more freedom to locate DGs in different points of the network, even small generation units can be installed at each house. This implies a greater number of possible configurations, becoming a hard-combinatorial optimization problem, difficult to solve with conventional methods.

Also, TS-MOEAP will be applied to *restore the optimal condition of distribution networks*, particularly for secondary lines which present several quality issues, since no proposals have been made on this subject before. Although some works in section 1.4 focus on power loss

reduction, voltage deviation, cost minimization, and other quality issues, they only consider primary distribution lines. For the case of LVDNs, different considerations must be taken, e.g. there are no switches as in MV lines, and contrary to DGs, DTs can be easily changed in quantity and location. Moreover, due to a high  $R/X$  ratio LVDNs have more  $I^2R$  losses than primary distribution lines, this implies that the conductor's size must be considered in the optimization problem. All this has made it difficult to find a method to optimize LVDNs, but as explained later, our proposal can solve this type of problems.

Furthermore, to expand the performance of TS-MOEAP an *Improved Nondominated Sorting Genetic Algorithm with a Heuristic Mutation Operator* (INSGA-HO) is proposed for Stage-2. This multiobjective evolutionary algorithm has been designed especially for the optimization of DNs, therefore it can overcome state of the art algorithms such as: a Nondominated Sorting Genetic Algorithm II (NSGA-II) [40] and a Multiobjective Evolutionary Algorithm Based on Decomposition (MOEA-D) [41]. For the Stage-1, an *Improved Particle Swarm Optimization* technique (IPSO) is presented to overcome the computational time of a conventional PSO, reducing the amount of power flow analysis required to evaluate the particles.

As will be shown later, the combination of the INSGA-HO with the IPSO gets better results than other mentioned algorithms in this thesis. To prove this performance, six real cases are considered: a) two rural communities that need off-grid electrification projects with photovoltaic units and battery banks, b) two urban secondary networks with several quality issues due to an excessive demand of energy, and c) two primary networks that need a reconfiguration to support a new topology and to minimize power losses.

### **1.6.2. Outline of Thesis**

We now describe the contents of this thesis:

- *Chapter 2.* Basic concepts about evolutionary algorithms and multiobjective optimization are shown in this chapter. The description of a GA, PSO, NSGA-II, and MOEA-D are detailed, to understand, in a better way, the algorithms proposed in this thesis.
- *Chapter 3.* We explain how the topology of the distribution network is built by means of a greedy algorithm (PRIM). Also, it is explained how the network is evaluated



through a power flow analysis and an investment cost function. Furthermore, it explains the sizing of DTs and DGs and the selection of optimal conductors. This chapter is a key component before implementing the optimization approach.

- *Chapter 4.* In this chapter it is introduced the first stage of TS-MOEAP. Here we explain how a particle swarm optimization technique is applied to find the optimal placement of distribution transformers or distributed generation. Also, it is explained how the IPSO acts in networks with several quality issues.
- *Chapter 5.* In this chapter, it is introduced the second stage of TS-MOEAP. Here is explained the attributes of the INSGA-HO algorithm and how it is applied for optimal network reconfiguration. Also, the total structure of the INSGA-HO/IPSO algorithm is presented in detail with a flowchart and a pseudocode.
- *Chapter 6.* We present the implementation of TS-MOEAP for real applications, from designing a network from scratch to optimizing existing low and medium voltage networks (MVDN). Several scenarios are tested and some comparisons against other algorithms are presented. Also, an app developed on Android is introduced to help in the design of LVDN.
- *Chapter 7.* In this chapter, we introduce DER-CAM for the optimization of distribution networks by Implementing DERs. Different scenarios are tested for a real case study to verify the advantages of installing DERs. At the end of this chapter, we present the test system optimized by TS- MOEAP and DER-CAM.
- *Chapter 8.* We provide some general conclusions and future research directions.

*Appendix A* contains the data of the solar radiation of some case studies.

*Appendix B* shows the urban area of the case studies that need improvement.

*Appendix C* shows the active and reactive loads for a secondary distribution network.

*Appendix D* shows part of the code of the android app.

Finally, the following flow-diagram illustrates the content and organization of the material of this thesis.

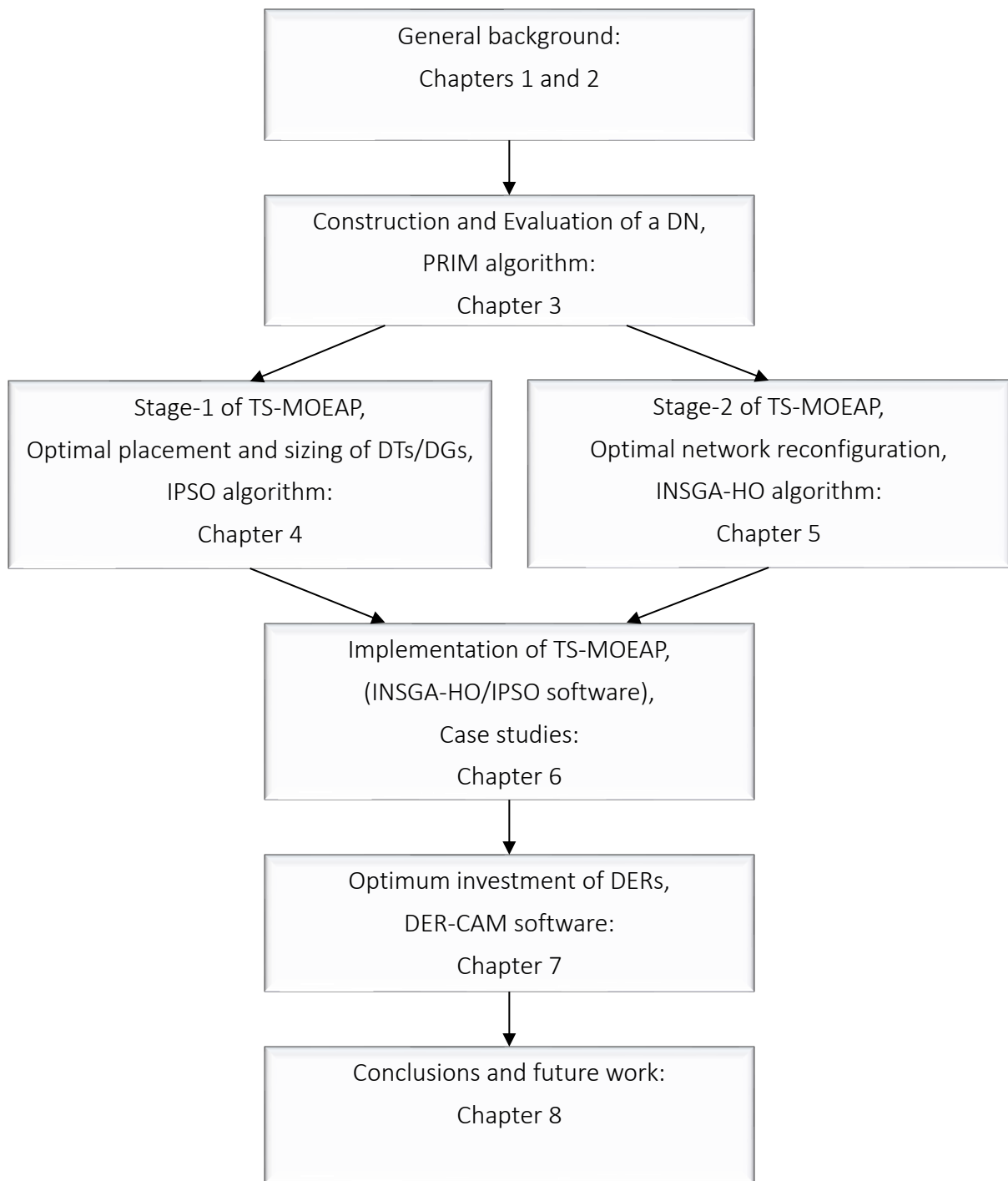


Figure 1.5. Flow-diagram of the thesis

## Chapter 2

# Evolutionary Algorithms

The aim of this chapter is to describe what an evolutionary algorithm (EA) is, to better understand the proposal of this thesis and the algorithms that compose it. In order to give a unifying view, we present a general scheme that forms the common basis for all the different variants of evolutionary algorithms. The main components of EAs are detailed, explaining their role in the optimization process. Finally, we describe the application of evolutionary techniques to solve a complex class of problems, namely multiobjective optimization.

### 2.1. What is an Evolutionary Algorithm?

An evolutionary algorithm can be defined as a population-based metaheuristic optimization method, which uses mechanisms inspired by biological evolution such as reproduction, mutation, recombination, and selection, to find a solution to a problem (see chapter 3 of [42]). The common underlying idea behind this concept is as follows: given a population of individuals within some environment that has limited resources, competition for those resources causes the survival of the fittest and a rise in the fitness of the population.

Given a quality function to be maximized, we can randomly generate a set of candidate solutions to then get a fitness of each one applying the quality function (the higher the better). On the basis of these fitness values, some of the better candidates are chosen to seed the next generation. This is done by applying recombination and mutation to them. Recombination is an operator that is applied to two or more candidate solutions (the parents), mixing their information to produce one or more new individuals (the children). Mutation is an operator applied at random over a few individuals to change their fitness. Therefore, the constant application of recombination and mutation on the parents leads to the creation of a set of new candidates (the offspring). These then compete, based on their fitness, with the old ones for a place in the next generation.

The process described above can be iterated until a candidate with sufficient quality is found, or until some stop criterion is satisfied. So, the two main concepts that form the basis of evolutionary algorithms are:

- *Variation Operators* (recombination and mutation), create the necessary diversity within the population.
- *Selection*, which increases the mean quality of solutions in the population.

The combined application of variation and selection leads to improving fitness values in consecutive populations, where can exist an optimal solution to our problem.

The general scheme of an evolutionary algorithm is given in pseudocode in Figure 2.1 and is shown as a flow chart in Figure 2.2.

---

```

1: BEGIN
2:   INITIALIZE population with random candidate solutions;
3:   EVALUATE each candidate;
4:   REPEAT UNTIL (Termination condition is satisfied) DO
5:     SELECT parents;
6:     RECOMBINE pair of parents;
7:     MUTATE the resulting offspring;
8:     EVALUATE new candidates;
9:     SELECT individuals for the next generation;
10:  END
11: END

```

---

Figure 2.1. The general pseudocode of an evolutionary algorithm.

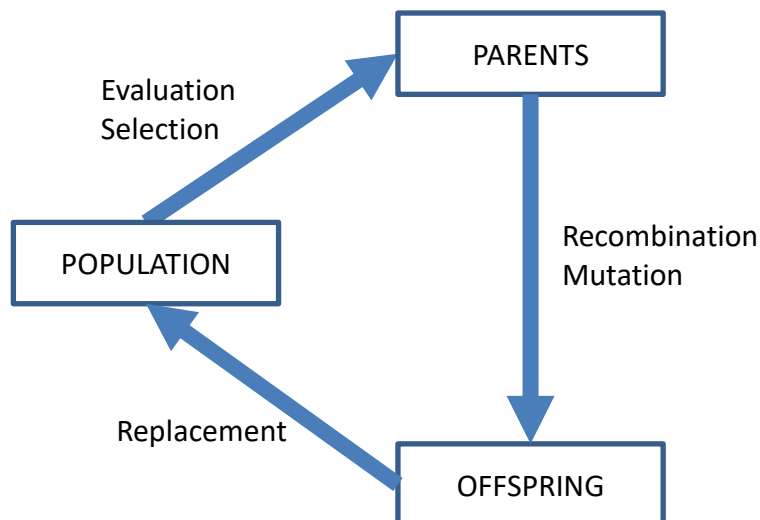


Figure 2.2. The general scheme of an evolutionary algorithm.

## 2.2. The Components of Evolutionary Algorithms

There are different components and operators of EAs that we must specify to create a complete runnable algorithm. Among the most important are:

- *Representation*: It serves to link the “real world” to the “EA world”. Here we define how possible solutions should be specified and stored in a way that can be manipulated by the different operators in the EA. The physical solutions within the original problem are called *phenotypes* (e.g. the network topology), while their encoding, that is the individuals within the EA are referred to as *genotypes* (e.g., an integer vector). We must note that the whole evolutionary search takes place in the genotype space.
- *Evaluation Function*: From the problem-solving perspective, it represents the task to be solved in the EA. Technically, it is a function or procedure (e.g. a power flow) that assigns a quality measure to genotypes (e.g. the power loss of the system).
- *Population*: A population holds a set of possible solutions, expressed in genotype form. The population has a defined size, and the individuals that compose it do not change or adapt.
- *Selection*: This operator selects the best individuals from the current population to become them in parents of the next generation. The selection is based on the quality of the individuals, thus high-quality individuals have more chance to become parents than those with low quality.
- *Recombination*: According to the type of representation this can be also named as *crossover*. This operator swaps information from two parents to get one or two offspring genotypes. The choices of what parts (genes) of each parent are combined depend on random selections.
- *Mutation*: This operator is applied to a few genotypes of the offspring to deliver slightly modified mutants, in order to improve the gene pool. Commonly, the decisions to change a part of the chromosome is taken at random, however for some practical problems this operator can find the weak spot of an individual and improve it by performing specific changes on its chromosome.
- *Replacement*: Similar to the *selection*, this operator is based on the quality of individuals. Its role is to keep the size of the population, selecting individuals from the old or new generation.

## 2.3. Evolutionary Algorithm Variants

An evolutionary algorithm can have different variants based on the type of representation, and how the variation operators are applied. Technically, one representation might be preferable to others if it matches the given problem. Among the most important variants we have:

- *Genetic Algorithms (GA)*: This is the most popular type of EA. It uses a binary representation, fitness proportionate selection, a low probability of mutation, and an emphasis on genetically inspired recombination.
- *Evolution Strategies (ES)*: This method uses vectors to represent the genotypes and implements *self-adaptation* of strategy parameters such as the mutation. The selection is stochastic.
- *Evolutionary Programming (EP)*: This method implements real-valued vectors for the representation, and not uses recombination. In EP each parent generates exactly one offspring via mutation and has self-adaptation of mutation step sizes.
- *Genetic Programming (GP)*: This differs from other EAs in that uses trees for the representation of chromosomes. Its recombination implements exchange of subtrees and the mutation performs random changes in the trees.
- *Learning Classifier System (LCS)*: Here the solution is a set of classifiers (rules or conditions) rather than parse trees. LCS is used primarily in applications where the objective is to evolve a system, regarding the inputs to such system.
- *Differential Evolution (DE)*: This method uses real-valued vectors for the representation of genotypes, and its mutation is based on the difference of two random vectors whose result is added to a third vector.
- *Particle Swarm Optimization (PSO)*: This algorithm is inspired by social behavior of bird flocking or fish schooling, where each element (particle) is a possible solution. These particles depend on three factors: individual best position, global best position, and inertia. The PSO does not use the crossover and its mutation is defined through a vector addition.

Considering that the elementary model of TS-MOEAP is based on a GA and a PSO, in the following, we present in detail these two algorithms.

### 2.3.1. Particle Swarm Optimization

The PSO is a swarm intelligence technique inspired by social behavior of bird flocking or fish schooling. It solves a problem by moving particles (candidate solutions) around in the search-space, according to simple mathematical formulae over the particle's position (1) and velocity (2) [43].

$$\chi_i^{(t+1)} = \chi_i^{(t)} + v_i^{(t+1)} \quad (1)$$

$$v_i^{(t+1)} = \underbrace{\gamma \cdot v_i^{(t)}}_{\text{inertia}} + \underbrace{\alpha \cdot r_1 \cdot [\vartheta_i - \chi_i^{(t)}]}_{\text{cognitive behaviour}} + \underbrace{\beta \cdot r_2 \cdot [\sigma - \chi_i^{(t)}]}_{\text{social behaviour}} \quad (2)$$

Each particle's movement is influenced by its cognitive behavior, social behavior and inertia, as expressed in equation (2), where  $\vartheta_i$  is the local best-known position of the particle and  $\sigma$  is the best-known position among all particles. For both equations,  $v_i^{(t)}$  is the current velocity of the particle and  $\chi_i^{(t)}$  is its position for the iteration ( $t$ ).  $\gamma$ ,  $\alpha$ , and  $\beta$  are weights to calibrate the inertia, cognitive behavior, and social behavior, respectively.  $r_{1,2}$  are random values between [0,1]. In the optimization process,  $\gamma$  can change dynamically to improve the exploration of the search space. In the beginning, it can take a higher value (typically 0.9) to allow the particles to move freely around the searching space, to later narrow the search using a lower inertia.  $\alpha$  and  $\beta$  can be modified (typically between 1-2) to improve the local search by each particle or to give greater importance to the optimum found by the entire group.

### 2.3.2. Genetic Algorithm

The GA is a meta-heuristic optimization method inspired by natural evolution [42]. It is based on a population that evolves with the aid of four genetic operators:

- i. *Representation*: Each possible solution must be represented as a *string* (chromosome), containing the relevant information to be evaluated. For this purpose, a *binary* or *integer vector* representation can be implemented.
- ii. *Selection*: This operator creates a new generation by selecting the best individuals from an older population. The selection can be *proportional*, by *ranking*, implementing *selection probabilities*, or by *tournament selection*.

- iii. *Recombination*: This operator swaps chromosome segments (genes) between two individuals to create an offspring. The recombination can be an *n-point crossover*, *uniform crossover*, *arithmetic recombination* and *blend crossover*.
- iv. *Mutation*: Commonly this operator causes random changes on the alleles of few chromosomes, in order to improve the diversity of the gene pool. The mutation can be by *bitwise*, *swapping*, *insertion*, *scramble* and *inversion*. *Heuristic-based methods* can also be applied to perform specific changes on the alleles of the chromosomes in order to improve the quality of the solution.

To better interpret the action of each genetic operator, Figure 2.3 shows the general pseudocode of a GA with a numerical example. In this case, the objective function to minimize is  $f(x) = x^2$ .

---

```

1: BEGIN
2: Initialize population with random candidate solutions
       $x_1 = 25; \quad x_2 = 30; \quad x_3 = 12$ 
3: Evaluate each candidate using  $f(x) = x^2$ 
       $f(x_1) = 625; \quad f(x_2) = 900; \quad f(x_3) = 144;$ 
4: REPEAT UNTIL the diversity of individuals is higher than an established error
5:   Selection operator takes the candidates with best fitness
       $\min f(x) \rightarrow x_1 \text{ and } x_3$ 
6:   Representation operator converts the phenotypes to genotypes
       $x_1 = [1 \ 1 \ 0 \ 0 \ 1]; \quad x_3 = [0 \ 1 \ 1 \ 0 \ 0]$ 
7:   Crossover operator selects two random crossover points to interchange gene blocks
       $\left. \begin{array}{l} x_1 = [1 \ 1 \ 0 \ 0 \ 1] \\ x_3 = [0 \ 1 \ 1 \ 0 \ 0] \end{array} \right\} \quad \begin{array}{l} x_{13} = [1 \ 1 \ 1 \ 0 \ 1] \\ x_{31} = [0 \ 1 \ 0 \ 0 \ 0] \end{array}$ 
8:   Mutation operator flips bits at random
       $x_{13} = [1 \ 1 \ 1 \ 0 \ 1] \rightarrow x_{m13} = [0 \ 1 \ 1 \ 0 \ 1]$ 
9:   Representation operator converts the genotypes to phenotypes
       $x_{m13} = 13; \quad x_{31} = 8;$ 
10:  Evaluate the new candidates
12: END
13: END

```

---

Figure 2.3. General pseudocode of the GA with a numerical example.



## 2.4. Multiobjective Evolutionary Algorithms

In this section, we describe the application of evolutionary algorithms to solve multiobjective problems (MOPs), where the quality of a candidate solution is defined by its performance in relation to several conflicting objectives.

In practice, many problems (that are multiobjective) have been transformed into *single-objective functions*, in order to make the optimization tractable. A popular alternative to do this is assigning a weight (usually fixed) to each objective and then combine these scores into a single fitness score. This weighted sum approach is called *Scalarization*, but suffers from the following drawbacks:

- For applications where their characteristics are changing repeatedly, we should modify these weights in order to get acceptable results in each scenario.
- In scalarization, we assume that we can capture all the user's preferences, without even know the range of possible solutions.

For these reasons, it is preferred to use methods that can find a diverse set of high-quality solutions without the need to convert the multiobjective problem into a single-objective function. EA-based methods intended to solve multiobjective problems are based on the concept of *Dominance and Pareto Optimality* and have a proven ability to identify high-quality solutions in high-dimensional search spaces, containing difficult features such as nonconvexity, discontinuities, and multiple constraints. Therefore, in the following, we will describe this concept and present two novel methods, NSGA-II [40] and MOEA-D [41], for multiobjective optimization problems.

### 2.4.1. Dominance and Pareto Optimality

If we expressed a multiobjective optimization problem as follows:

$$\min f_i(x), \quad i = 1, 2, \dots, N_{obj}, \quad x \in \Pi \quad (3)$$

where  $f_i(x)$  is the  $i$ th objective function,  $\Pi$  is the feasible searching space, and  $N_{obj}$  is the number of objectives, a solution  $x_1$  is said to dominate  $x_2$  (denoted by  $x_1 < x_2$ ) if and only if

$$\forall i, j \in \{1, 2, \dots, N_{obj}\}: f_i(x_1) \leq f_i(x_2) \wedge f_j(x_1) < f_j(x_2). \quad (4)$$

A solution is called *nondominated* if this is not dominated by any other. The set of all non-dominated solutions is called the *Pareto front*. These concepts are illustrated in Figure 2.4, where the  $x$  and  $y$ -axes represent two conflicting objectives subject to constraints. If the optimization problem is to minimize both objectives (lower is better), we can say that point  $A$  dominates point  $D$  and all other points in the blue area.  $A$  and  $C$  do not dominate each other, and the blue line represents the Pareto front, where  $A$  is a nondominated point. Solutions under and to the left of the line, such as  $B$ , are infeasible.

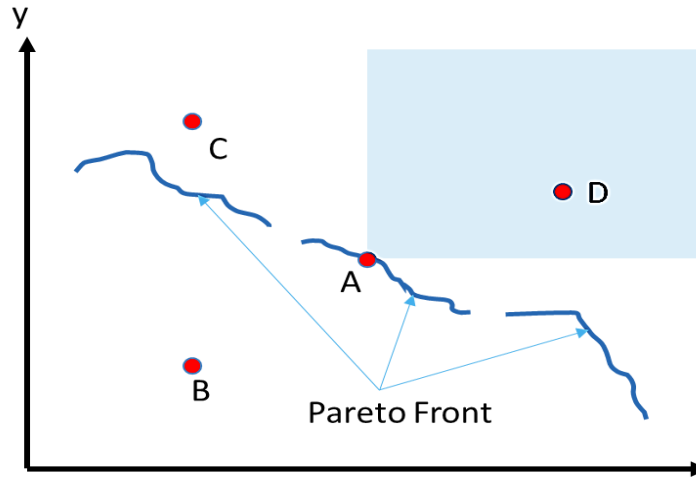


Figure 2.4. Illustration of the Pareto front and dominance concept.

#### 2.4.2. Nondominated Sorting Genetic Algorithm II (NSGA-II)

NSGA-II is a multiobjective evolutionary algorithm that uses nondominated sorting, an elitist approach, and a crowded-comparison method in order to find multiple solutions to a problem [40]. For a better understanding, the procedure of this algorithm is illustrated in Figure 2.5 and it will be detailed as follows: this algorithm takes a population  $R^{(t)}$  and sorts it in fronts based on nondomination. The first front ( $F_1$ ) is composed of nondominated individuals (the so-called Pareto front), and the second front ( $F_2$ ) is composed by individuals dominated only by the first front, and so on. Each individual is assigned with a *rank* according to the front that it belongs, this is, individuals in the first front have rank 1, individuals in the second front have rank 2, and so on. Additionally, each individual is assigned with a crowding distance value, which is a measure of how close an individual is to its nearest neighbors in the same front. The larger this value, the fewer solutions reside in the vicinity of this point. This parameter is used to maintain diversity among the solutions.

From the sorted population  $R^{(t)}$ , a new population  $P^{(t+1)}$  is obtained by accepting individuals from progressively inferior fronts until it is full (size  $N$ ). If not, all individuals from the last considered front ( $\mathcal{F}_r$ ) can be accepted based on their crowding distance (the larger the better). Then, from  $P^{(t+1)}$ , some individuals are selected to be parents through a tournament selection based on the rank and the crowding distance. Between two solutions with different nondomination ranks, it is preferred the solution with the lower rank. Otherwise, if both solutions belong to the same front, then the solution with a greater crowding distance is selected. The selected population generates an offspring  $Q^{(t+1)}$  using conventional crossover and mutation operators.

Finally, the current population  $P^{(t+1)}$  and the offspring  $Q^{(t+1)}$  are merged to form  $R^{(t+1)}$  (size  $2N$ ), to repeat the entire process until converge to a set of optimal solutions.

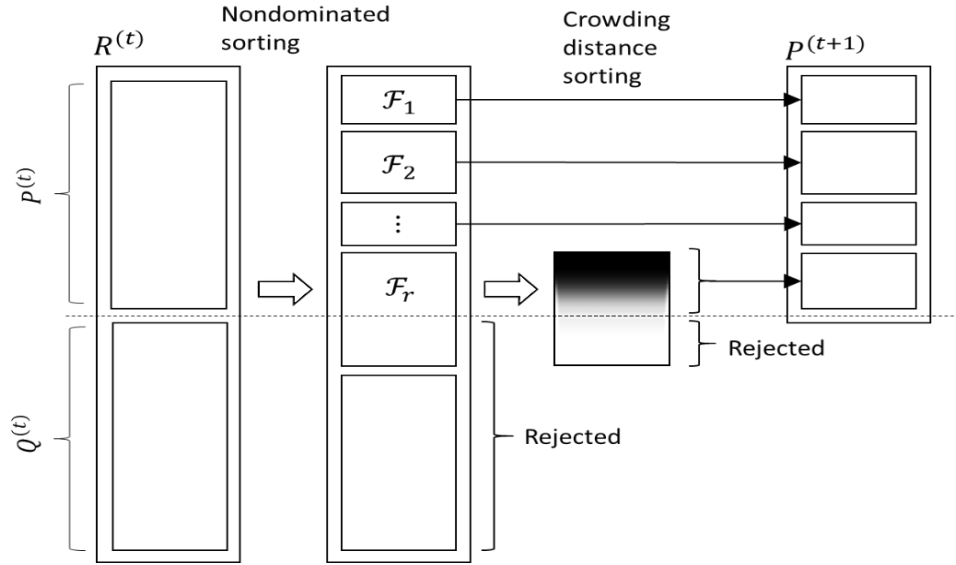


Figure 2.5. NSGA-II procedure.

### 2.4.3. Evolutionary Algorithm Based on Decomposition (MOEA-D)

MOEA-D is an algorithm that combines features from the single-objective weighted sum approach and the population-based approaches. Its aim is to distribute the population evenly along the current approximation to the Pareto front.

MOEA-D starts by evenly distributing a set of  $N$  weight vectors (i.e.  $\lambda^1, \lambda^2, \dots, \lambda^N$ ) in the objective space and then for each builds a list of its  $T$  closest neighbors (using Euclidean distances), please see Figure 2.6. Then, it creates an evolves a population of  $N$  individuals, each

associated with one of the weight vectors, which it uses to calculate a single fitness value  $g$  of the  $j$ th subproblem, implementing a decomposition approach as *Tchebycheff*:

$$g(x|\lambda^j, z^*) = \max_{1 \leq i \leq m} \{\lambda_i^j \cdot |f_i(x) - z_i^*|\}, \quad x \in \Pi \quad (5)$$

$$z_i^* = \min\{f_i(x) | x \in \Pi\} \quad (6)$$

where  $m$  is the number of objectives,  $\lambda^j = (\lambda_1^j, \dots, \lambda_m^j)^T$  are the weight vectors,  $z_i^*$  is a reference point, and  $f_i(x)$  is the quality of each objective.

MOEA-D minimizes all these  $N$  scalar subproblems simultaneously in a single run. We must note that  $g$  is continuous of  $\lambda$ , and the optimal solution of  $g(x|\lambda^i, z^*)$  should be close to that of  $g(x|\lambda^j, z^*)$  if  $\lambda^i$  and  $\lambda^j$  are close each other. Therefore, any information about these  $g$ 's with weight vectors close to  $\lambda^i$  should be helpful for optimizing  $g(x|\lambda^i, z^*)$ . Finally the population is composed of the best solutions found so far for each subproblem.

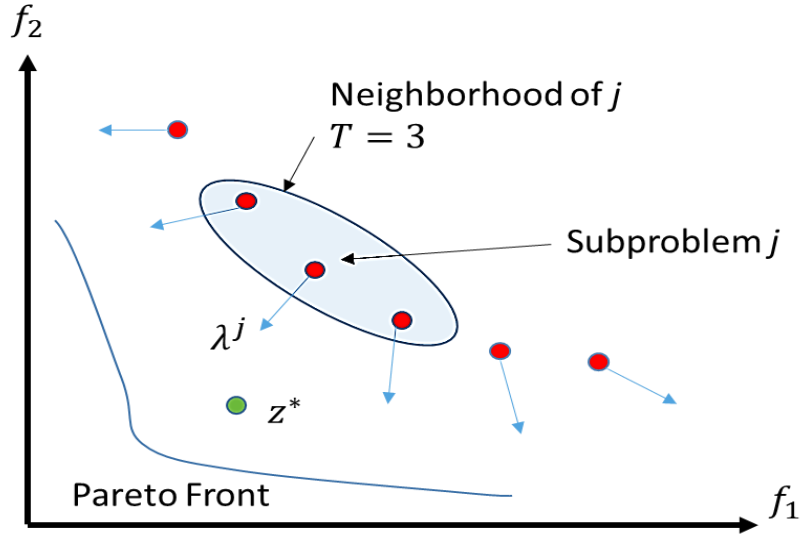


Figure 2.6. MOEA-D procedure.

## 2.5. Summary

We have introduced fundamental concepts of evolutionary algorithms, used to develop TS-MOEAP. In particular, genetic algorithms, particle swarm optimization, and multiobjective evolutionary methods (NSGA-II and MOEA-D) were reviewed.

## Chapter 3

### Construction and Evaluation of a DN Model

This chapter is a key component before implementing the optimization approach, because here we explain how a network model can be obtained to evaluate the possible configurations. In addition, it is explained how the network is represented as a genotype to be manipulated for the different optimization algorithms, and how the possible configurations are evaluated through a power flow and an investment cost function.

#### 3.1. Representation and Model Construction

The most difficult part of implementing an evolutionary algorithm is to find a proper system representation that meets all its characteristics. The algorithm starts by creating an initial random population, on which each individual is a possible configuration of the system. In our case, as the DN is composed of several groups of loads connected to different feeders, we can apply an integer vector representation such as:

$$c_i = [p_{i1} \ p_{i2} \ p_{i3} \ \dots \ p_{i\mu}]; \ p_{ij} \in \mathbb{Z}^+; \ i = 1, 2, \dots, N \quad (7)$$

where  $p_{ij}$  is the group number of the loads,  $N$  is the size of the population and  $\mu$  is the total number of users in the chromosome  $c_i$ . Therefore, as each *user* (called as  $u_j$ ) can belong to any group/set ( $G_k$ ) within a *configuration/chromosome* (as shown in Figure 3.1), we can represent the entire population by a matrix, whose  $p_{ij}$  values denote the group number of the  $j$ th user in the  $i$ th chromosome, i.e.

$$\text{Population} = \begin{matrix} & u_1 & u_2 & u_3 & \dots & u_\mu \\ \begin{matrix} c_1 \\ c_2 \\ \vdots \\ c_N \end{matrix} & \begin{bmatrix} p_{11} & p_{12} & p_{13} & \dots & p_{1\mu} \\ p_{21} & p_{22} & p_{23} & \dots & p_{2\mu} \\ \vdots & \vdots & \vdots & \ddots & \vdots \\ p_{N1} & p_{N2} & p_{N3} & \dots & p_{N\mu} \end{bmatrix} \end{matrix} \quad (8)$$

For example, the system configurations of Figure 3.1 can be represented by  $c_1$  and  $c_2$  respectively, as follows:

$$\begin{array}{c}
u_1 \ u_2 \ u_3 \ u_4 \ u_5 \ u_6 \ u_7 \ u_8 \ u_9 \ u_{10} \ u_{11} \\
c_1 \begin{bmatrix} 1 & 1 & 1 & 1 & 3 & 3 & 2 & 2 & 2 & 2 & 2 \end{bmatrix} \\
c_2 \begin{bmatrix} 1 & 1 & 1 & 1 & 2 & 2 & 1 & 2 & 3 & 2 & 3 \end{bmatrix}
\end{array} \tag{9}$$

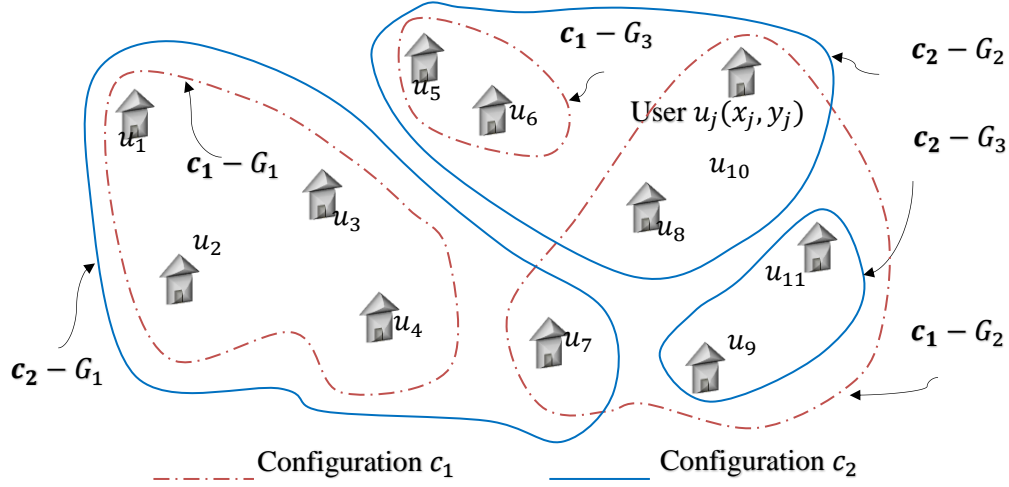


Figure 3.1. Representation of a distribution network.

We must note that the users are sorted in ascending order with respect to the x-GPS coordinate, and this order is maintained throughout the entire process, i.e.  $\{u_1 \ u_2 \ ... \ u_\mu\}$ , where  $u_i(x_i, y_i)$ .

Once we have the representation of the network, the next step is to build the model. From  $c_i$  we can get the  $G_k$  sets, selecting the  $u_i$  elements with the same group number, e.g.

$$\begin{aligned}
c_1 &= [1 \ 1 \ 1 \ 1 \ 3 \ 3 \ 2 \ 2 \ 2 \ 2 \ 2] \rightarrow \begin{aligned} G_1 &= [u_1 \ u_2 \ u_3 \ u_4] \\ G_2 &= [u_7 \ u_8 \ u_9 \ u_{10} \ u_{11}] \\ G_3 &= [u_5 \ u_6]. \end{aligned}
\end{aligned} \tag{10}$$

Considering that, each  $G_k$  set represents a real network; this must be built in radial form. To do this, the network can be considered as a weighted undirected graph from which we can obtain a minimum spanning tree using a greedy algorithm. A well-known method is *PRIM* [44], which takes a graph as input and finds the subset of edges/branches ( $U_{ij}$ ) which will form a tree (the network) with the minimum amount of weight (wire length).

The algorithm starts by calculating the Euclidean distance  $d_{ij}$  between all the  $u_i$  nodes contained in  $G_k$ , using their  $(x_i, y_i)$  GPS coordinates, i.e.

$$\begin{matrix} & u_1 & u_2 & \cdots & u_\psi \\ \begin{matrix} u_1 \\ u_2 \\ \vdots \\ u_\psi \end{matrix} & \begin{bmatrix} 0 & d_{12} & \cdots & d_{1\psi} \\ d_{21} & 0 & \cdots & d_{2\psi} \\ \vdots & \vdots & \ddots & \vdots \\ d_{\psi 1} & d_{\psi 2} & \cdots & 0 \end{bmatrix} \end{matrix} \quad (11)$$

where  $\psi$  is the length of each set  $G_k$  and  $d_{ij}$  is represented as

$$d_{ij_{i \neq j}} = \sqrt{(x_i - x_j)^2 + (y_i - y_j)^2}. \quad (12)$$

If within  $G_k$  there are two nodes ( $u_i, u_j$ ) that can form a restricted branch  $U_{ij}^{rst} \in \Gamma$ , a penalty  $w$  can be applied to  $d_{ij}$  to avoid selecting that specific branch, i.e.,

$$[U_{ij} = U_{ij}^{rst}] \Rightarrow [d_{ij} = d_{ij} + w]. \quad (13)$$

After that, PRIM operates by building the network one node at a time, from an arbitrary starting node  $u_i$ , adding at each step the shortest branch  $U_{ij}$ , until all nodes are included in the network. This process is illustrated in Figure 3.2.

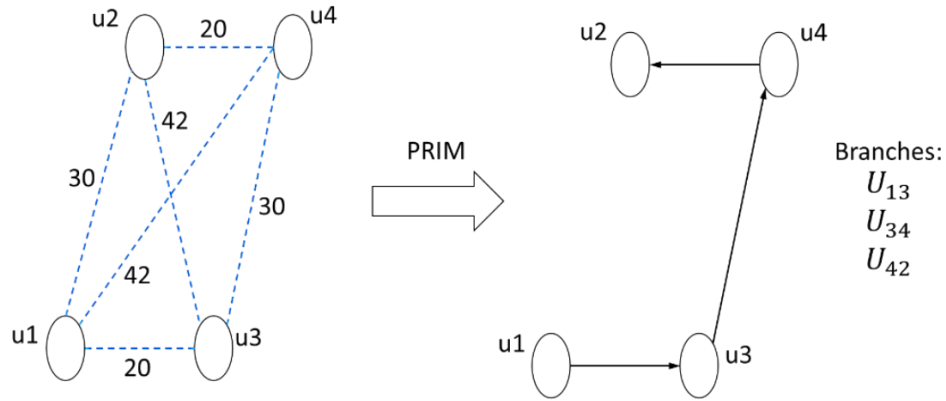


Figure 3.2. Model construction by using PRIM.

### 3.2. Evaluation of the Model

To know if a possible configuration is technically correct we must run a power flow study. This is of great importance in the planning, and design of power systems, as well as in determining the best-operating conditions of existing systems. The most important information obtained from a power flow study is the magnitude and phase angle of the voltage at each

bus bar, and the real and reactive power flowing through each line. We can use these results to evaluate the performance of the network and establish the desired objective functions.

To solve a power flow problem, it is possible to use the self- and mutual admittances that compose an admittance matrix  $Y_{BUS}$ , or the impedances that composes the  $Z_{BUS}$ . In our case, we focus our attention on the methods that use admittances, and where the distribution lines are represented by per-phase nominal- $\pi$  equivalent circuits. In the following, we are going to describe how the admittance matrix is calculated, how the *power-flow equations* are obtained, and how the set of non-linear equations are solved by using an iterative method such as *Gauss-Seidel*. In the last part of this chapter, we briefly explain how a distribution network can be evaluated economically.

### 3.2.1. Calculation of the Admittance Matrix

The first step before calculating the admittance matrix is to obtain the reactance per length ( $\Omega/\text{km}$ ) of the cables that we are going to use in the system. For this, we need the Geometric Mean Radius (GMR) regarding the type of conductor and number of strands and the Geometric Mean Diameter (GMD) regarding the layout of conductors and their spacing. These two parameters can be obtained using ETAP, as shown in Figure 3.3, where a 2 AWG ACSR conductor type Sparrow with 6 strands is taken as an example.

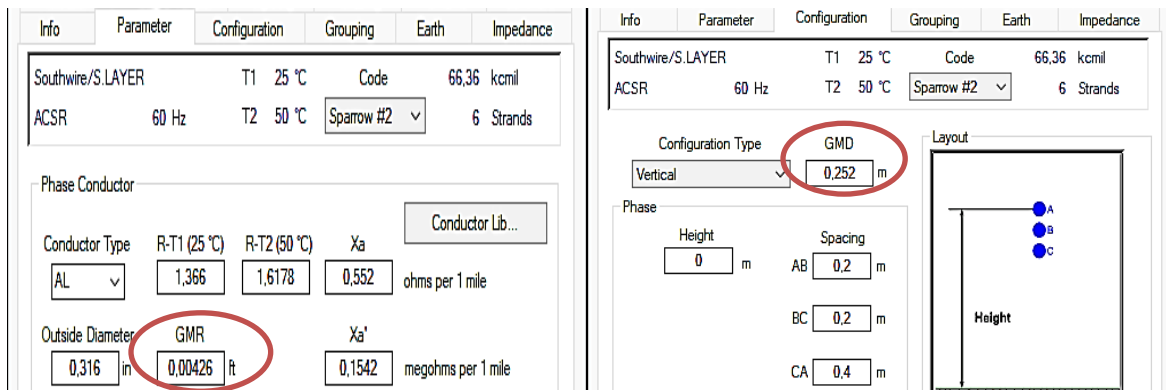


Figure 3.3. Obtainment of the GMR and GMD using ETAP.

Then, the reactance for each conductor can be calculated using the following equation:

$$XL = 0.00126 \cdot f \cdot \ln \left( \frac{GMD}{GMR} \right) \quad (14)$$



where  $f$  is the frequency of the system. Therefore, the impedance for the most important conductors used in distribution networks, at low and medium voltage levels, can be established as:

Table 3.1. Impedance for the most important conductors used in DNs.

Impedance $ZL$ [ $\Omega/\text{km}$ ]			
Three Phase			Single Phase
Conductor type	Low voltage networks	Medium voltage networks	Low voltage networks
2 AWG, Sparrow	1.0105+0.3907i	1.0105+0.5273i	2.021+0.6588i
1/0 AWG, Raven	0.6470+0.3589i	0.6470+0.3233i	1.294+0.5951i
2/0 AWG, Quail	0.5302+0.3520i	0.5302+0.4829i	1.0604+0.5814i
3/0 AWG, Pigeon	0.3963+0.3409i	0.3963+0.4692i	0.7927+0.5591i

With these values, a subroutine can calculate the  $y_{ij}$  admittance for each branch of the network, multiplying their length by  $1/ZL_{ij}$ , according to the type of selected conductor. Finally, the  $Y_{BUS}$  (15) can be calculated using these  $y_{ij}$  admittances to compute the elements in the matrix by means of (16) and (17), where  $n$  is the total number of bus bars. The  $Y_{ii}$  elements are the self-admittances, and the  $Y_{ij}$  elements represent the mutual admittances between the nodes  $i$  and  $j$ .

We should note that this process is performed automatically thanks to PRIM, which finds the branches of the network and their respective lengths. So, PRIM and the calculation of the admittance matrix are implemented whenever it is required to evaluate the network, being the most used subroutines within the optimization algorithm.

$$Y_{BUS} = \begin{bmatrix} Y_{11} & \cdots & Y_{1n} \\ \vdots & \ddots & \vdots \\ Y_{n1} & \cdots & Y_{nn} \end{bmatrix} \quad (15)$$

$$Y_{ii} = \sum_{j=0}^n y_{ij} \quad (16)$$

$$Y_{ij} = -y_{ij} \quad (17)$$

### 3.2.2. Power Flow Equations

Taking as reference the system shown in Figure 3.4, the sum of currents in the  $k$ -bus can be established as

$$I_k = y_{k0} V_k + y_{k1}(V_k - V_1) + y_{k2}(V_k - V_2) \dots + y_{kn}(V_k - V_n) \quad (18)$$

which can be rewritten using summations as follows:

$$I_k = V_k \sum_{j=0}^n y_{kj} - \sum_{j=1}^n y_{kj} V_j \quad (19)$$

$$I_k = V_k Y_{kk} + \sum_{\substack{j=1 \\ j \neq k}}^n Y_{kj} V_j \quad (20)$$

where  $\sum_{j=0}^n y_{kj} = Y_{kk}$  represents the sum of all admittances connected to the node  $k$  including any Shunt admittance, and  $-y_{kj} = Y_{kj}$  represents the mutual admittance between the nodes  $k$  and  $j$ .

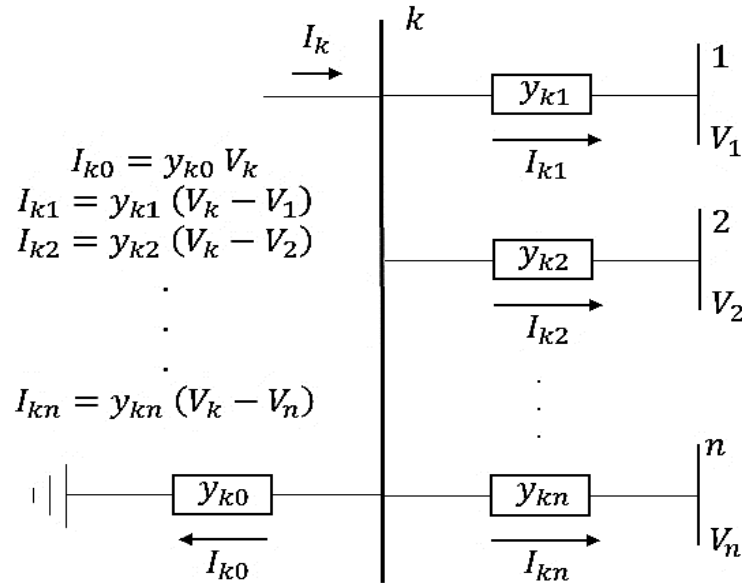


Figure 3.4. System model for the power flow analysis.

Now supposing a system of  $n$  bars, these equations can be represented in matrix form as  $YV = I$  (21), where  $Y$  is the admittance matrix.

$$\begin{bmatrix} Y_{11} & \dots & Y_{1n} \\ \vdots & \ddots & \vdots \\ Y_{n1} & \dots & Y_{nn} \end{bmatrix} \begin{bmatrix} V_1 \\ \vdots \\ V_n \end{bmatrix} = \begin{bmatrix} I_1 \\ \vdots \\ I_n \end{bmatrix} \quad (21)$$

Now, the power that is injected into the bar  $k$  can be represented by

$$S_k = V_k I_k^* \rightarrow S_k^* = V_k^* I_k \quad (22)$$

and replacing (20) in (22) we have

$$S_k^* = V_k^* \left[ V_k Y_{kk} - \sum_{\substack{j=1 \\ j \neq k}}^n Y_{kj} V_j \right] = P_k - jQ_k \quad (23)$$

From (23) we can obtain the voltage of the  $k$ -node by rewriting this equation as

$$V_k = \frac{1}{Y_{kk}} \left[ \frac{P_k - jQ_k}{V_k^*} + \sum_{\substack{j=1 \\ j \neq k}}^n Y_{kj} V_j \right] \quad (24)$$

In the case that the admittance matrix is singular, a value can be assigned to one of the variables so that the others are expressed as a function of it, making the system linearly independent, with which a solution can be found by using an iterative method. In our case, we must assume a known value of voltage (magnitude and phase angle) in one of the bars, i.e. we must define a *Slack bus*.

### 3.2.3. The Gauss-Seidel Method

To solve the set of non-linear equations formed with the voltages (24) of each  $k$ -bus, we can implement an iterative method such as Gauss-Seidel. Its operation is as follows: for a system of  $n$  non-linear equations with  $n$  unknowns, we proceed to clear one of the variables as shown in (25).

$$\begin{cases} x_1^{(i+1)} = g_1(x_1^{(i)}, x_2^{(i)}, \dots, x_n^{(i)}) \\ x_2^{(i+1)} = g_2(x_1^{(i+1)}, x_2^{(i)}, \dots, x_n^{(i)}) \\ x_n^{(i+1)} = g_n(x_1^{(i+1)}, x_2^{(i+1)}, \dots, x_{n-1}^{(i+1)}, x_n^{(i)}) \end{cases} \quad (25)$$

Then, initial values are assigned to each one of the unknown variables of the problem to find a new value in the immediate iteration. In this way, it will converge more quickly to the solution. The iterative process must be stopped if the error between two consecutive iterations is less than an established tolerance, i.e.  $|x^{i+1} - x^i| < tol$ .

To implement the Gauss-Seidel method, we must consider the type of bus bars of the system, which in our case are PQ type. Therefore, we know the active and reactive powers injected into the nodes and the unknown variables will be the magnitude and phase angle of the voltage at each node. Considering this, we can clear the voltage variable using the equation (24) and reordering the summation as follows:

$$V_k^{(i+1)} = \frac{1}{Y_{kk}} \left[ \frac{P_k - jQ_k}{V_k^{*(i)}} + \sum_{j=1}^{k-1} Y_{kj} V_j^{(i+1)} + \sum_{j=k+1}^n Y_{kj} V_j^{(i)} \right] \quad (26)$$

where  $(i)$  indicates the value of the previous iteration, and  $(P_k, Q_k)$  are the total values of the active and reactive powers (27) injected to each  $k$ -node.

$$\begin{aligned} P_k &= P_{gen_k} - P_{load_k} \\ Q_k &= Q_{gen_k} - Q_{load_k} \end{aligned} \quad (27)$$

After each iteration, the voltage value of each bus bar is successively improved, so it is necessary to verify the convergence using the error between two consecutive calculated values, i.e.

$$|V^{(i+1)} - V^{(i)}| < tol. \quad (28)$$

The Slack bar does not merit any calculation because the magnitude and phase angle of the voltage are already specified, therefore this node does not contribute with unknowns.

Finally, knowing the voltages of each node in the system, we can determine the current and power flow through each line applying the following equations:

$$I_{ij} = Y_{ij}(V_i - V_j) \quad (29)$$

$$S_{ij} = V_{ij} I_{ij}^* = P_{ij} + jQ_{ij} \quad (30)$$

which will allow us to evaluate the network in a technical way.

### 3.3. Economic Evaluation

Once the technical part of the system is evaluated, we must proceed with its economic evaluation based on the type, number, size, and capacity of its components. In our case, the

total investment cost will be calculated considering conductors, insulators, transformers, DG units (photovoltaic generation), and storage units (battery banks).

For the economic analysis, we must select available commercial equipment, therefore, it is important to calculate the required capacity before the selection of the most suitable unit.

For electrical conductors, we must select them considering their ampacity and the current through the line. In our case we are going to use the conductors shown in Table 3.2.

Table 3.2. Available conductors with their ampacities and costs [45].

Conductor type	Ampacity [A]	Cost [\$/m]
2 AWG, Sparrow	184	0.70
1/0 AWG, Raven	242	1.09
2/0 AWG, Quail	276	1.40
3/0 AWG, Pigeon	315	1.71

In the case of transformers, their capacity can be calculated using the following equation:

$$CAP_{DT} = (H^{0.91} \cdot P_{UD} + L \cdot P_{SL}) \cdot \xi \quad (31)$$

where  $H$  is the total number of houses connected to the transformer and  $P_{UD}$  is the projected unit demand according to the type of users.  $L$  is the number of street lights and  $P_{SL}$  is their power.  $\xi$  is an overload factor usually used by utility companies for DT sizing. Once  $CAP_{DT}$  is calculated, this value is compared with a list of available commercial transformers (see Table 3.3) and the closest one is selected.

For insulators, at LV level we consider the type 53-2, and for MV level of type UP, each one with a price of \$15 and \$18 USD [45], respectively.

Table 3.3. Available transformers with their costs [45].

Transformer capacity [kVA]	Cost [\$ USD]
30	3100
50	3800
75	4200
100	4800

For the case where we need a DN with *distributed photovoltaic generation* (DPG), the required capacity for a small photovoltaic system can be calculated by

$$CAP_{pV} = h^{0.91} \cdot E \cdot \varepsilon / (30 \cdot \Lambda) \quad (32)$$

where  $h$  is the number of users,  $E$  is the average energy consumption per month (kWh/month),  $\varepsilon$  is a compensation factor for power losses, and  $\Lambda$  is the average solar radiation. Furthermore, if the system requires a battery bank, this can be calculated by

$$CAP_{Batt} = CAP_{PV} \cdot RD \cdot \Lambda \cdot \frac{1000}{V_{in} \cdot \epsilon} \quad (33)$$

where  $RD$  is the number of reserve days,  $V_{in}$  is the input voltage for the inverter, and  $\epsilon$  is the discharge rate. Finally, these results can be compared with commercial equipment and those that can supply the required demand will be chosen. For our case study, the considered inverters and batteries are shown in Table 3.4. We must note that for the DPG sizing, photovoltaic panels of 240 W ( $I_p = 8.19$  Adc,  $V_p = 29.3$  Vdc) and a cost of \$ 250 are considered.

Table 3.4. Considered inverters and batteries [46, 47].

Equipment	Characteristics	Capacities	Price/U.
Inverters	$V_{in} = 340 - 500$ Vdc $V_{bat} = 348$ Vdc $V_{out} = 240$ Vac $Eff = 0.98$ %	5.5 kW	\$ 1675
		10 kW	\$ 2925
		12.5 kW	\$ 3285
		15 kW	\$ 3665
		20 kW	\$ 4215
Batteries	48 V $Disch. R. = 0.8$	24 Ah	\$ 310
		40 Ah	\$ 475
		60 Ah	\$ 645
		90 Ah	\$ 725
		120 Ah	\$ 925

After the selection of the commercial equipment, we can calculate the total investment cost by adding individual expenses of each element, i.e.

$$Total\ Investment\ Cost = CGU + CSB + CCO + CIN \quad (34)$$

where  $CGU$  is the total cost of DGs or DTs,  $CSB$  is the total cost of storage units (if they exist),  $CCO$  is the total cost of conductors, and  $CIN$  is the total costs of insulators. This equation will be more detailed in chapter 4 according to the type of system to solve.

### 3.4. Summary

In this chapter we have explained how the DN is constructed and evaluated by means of a greedy algorithm and a power flow with an economic analysis.

## Chapter 4

### Stage-1 of TS-MOEAP (IPSO – PRIM)

In this chapter, it is explained how the first stage of TS-MOEAP is applied to optimize a radial distribution network by selecting the *optimal placement and capacity of DGs/DTs*, as well as the optimal *branch routing and conductor sizing*. Here we explain in detail the formulation of the entire problem and how the IPSO-PRIM algorithm is applied to build the network and optimize it, minimizing power losses and quality issues. At the end of this chapter, some simulations are presented to prove the performance of the first-optimization stage.

#### 4.1. Objective Functions for the Evolutionary Algorithms

The intention of our proposal, *in the real world*, is to design or restore the optimal condition of DNs, by applying optimal network reconfiguration and optimal placement of DTs/DGs. In particular, we need to reinforce the structure of the network or install new equipment, i.e. increasing the capacity and number of their components (transformers, conductors, DGs) or changing their topology. A variable that is directly related to this reinforcement is the power loss (greater reinforcement causes fewer power losses), therefore this can be applied in the optimization model as one of the objective functions.

On the other hand, while the network is reinforced and expanded, the expenses also increase and considering that distribution companies always want to minimize this variable, the total investment cost can be considered as the second objective function. Therefore, we can say that the combination of optimal reconfiguration of DNs with optimal placement of DTs/DGs is a complex combinatorial, non-convex, and non-linear optimization problem with the purpose of identifying an optimal network configuration ( $c$ ) to minimize power losses ( $f_1$ ) and investment costs ( $f_2$ ), expressed as

$$\text{minimize}[f_1(c), f_2(c)], \quad c \in \Pi \quad (35)$$

where  $\Pi$  is a feasible solution space. In the following we describe each objective function and the constraints of the optimization problem.

#### 4.1.1. Minimization of Power Losses

The first objective of our problem is the minimization of power losses of the entire system (see Sec. 9.1 of [48]), expressed as

$$\text{minimize } f_1(c) = \text{minimize } \sum_{n=1}^{\eta} g_{ij}(V_i^2 + V_j^2 - 2V_i V_j \cos \theta_{ij}) \quad (36)$$

where  $\eta$  is the total number of branches,  $(i, j)$  are the nodes of a branch, and  $g_{ij}$  is the conductance between the respective nodes.  $V_i$  and  $V_j$  are the voltage magnitudes at each node and  $\theta_{ij}$  is the difference between phase angles of the respective voltages.

#### 4.1.2. Minimization of Investment Cost

The second objective is the minimization of the total investment cost. For the case of a traditional distribution network (using DTs), the objective function can be expressed as

$$\text{minimize } f_2^{DT}(c) = \text{minimize } \left( \sum_{n=1}^{\lambda} q_n p_n + \sum_{n=1}^{\varsigma} l_n \varrho_n + \mu \zeta \right) \quad (37)$$

where  $\lambda$  is the total number of available transformer capacities,  $q_n$  is the number of transformers, and  $p_n$  is the cost per unit.  $\varsigma$  is the total number of conductor sizes,  $l_n$  is the total length, and  $\varrho_n$  is the cost per meter of the conductor.  $\mu$  is the total number of utility poles, and  $\zeta$  is the cost of LV ceramic insulators per utility pole.

For the case of a DN using photovoltaic distributed generation the objective function for the investment cost can be expressed as

$$\text{minimize } f_2^{DG}(c) = \text{minimize } \left( \sum_{n=1}^{\mathcal{F}} \mathcal{I}_n \iota_n + \sum_{n=1}^{\mathcal{B}} \mathcal{B}_n \nu_n + \sum_{n=1}^{\varsigma} l_n \varrho_n + \mathcal{P} \vartheta \right) \quad (38)$$

where  $\mathcal{F}$  is the total number of inverter types,  $\mathcal{I}_n$  is the number of inverters for each type, and  $\iota_n$  is its cost.  $\mathcal{B}$  is the total number of battery types,  $\mathcal{B}_n$  is the number of batteries for each type, and  $\nu_n$  is its cost. Finally,  $\mathcal{P}$  is the total number of photovoltaic panels and  $\vartheta$  is the cost of each one.



Power losses and quality issues of the distribution network can be minimized by improving the network infrastructure and equipment capacity. This implies high investment costs; therefore, (37) or (38) are crucial to balance the optimization of the problem.

#### 4.1.3. Constraints

The equality constraints of the problem are represented by the power-flow equations (39), since the generated power must be equal to the total load plus power losses.  $(P_{g_i}, Q_{g_i})$  are the active and reactive generation outputs, and  $(P_{l_i}, Q_{l_i})$  are the active and reactive loads at node  $i$ .  $G_{ij}$  and  $B_{ij}$  are the conductance and susceptance of the admittance matrix, respectively.

$$\begin{aligned} P_{g_i} - P_{l_i} &= V_i \sum_{j=1}^{\mu} V_j (G_{ij} \cos \theta_{ij} + B_{ij} \sin \theta_{ij}) \\ Q_{g_i} - Q_{l_i} &= V_i \sum_{j=1}^{\mu} V_j (G_{ij} \sin \theta_{ij} + B_{ij} \cos \theta_{ij}). \end{aligned} \quad (39)$$

The inequality constraints include: a) DTs/DGs capacity (40), where  $(S^{max}, S^{min})$  are the apparent power limits and  $\tau$  is the total number of DTs/DGs in the system; b) capacity of batteries (41), where  $(SB^{max}, SB^{min})$  are the permissible limits to store energy; c) voltage magnitude (42), where  $V^{min}$  and  $V^{max}$  are established limits; and d) thermal limits (43), where  $I_{ij}$  is the magnitude of the current between the nodes  $(i, j)$ ,  $I^{max}$  is the conductor ampacity,  $(\bar{V}_i, \bar{V}_j)$  are voltages in phasor representation, and  $y_{ij}$  is the branch admittance.

$$S^{min} \leq S_{T_i} \leq S^{max}; \quad i = 1, 2, \dots, \tau \quad (40)$$

$$SB^{min} \leq SB_{T_i} \leq SB^{max}; \quad i = 1, 2, \dots, \tau \quad (41)$$

$$V^{min} \leq V_i \leq V^{max}; \quad i = 1, 2, \dots, \mu \quad (42)$$

$$I_{ij} = |(\bar{V}_i - \bar{V}_j) \cdot y_{ij}| \leq I^{max} \quad (43)$$

For the distribution network planning we also need geographical constraints to avoid using: d) restricted branches (44), where  $U_{ij}$  is the branch between the nodes  $(i, j)$  and  $\Gamma$  is the set of branches with restriction ( $U_{ij}^{rst}$ ); and e) restricted nodes (45), where the DTs/DGs cannot be located, for this,  $\Psi$  is the set of nodes with restriction ( $u_n^{rst}$ ) and  $u_{T_i}$  is a node where a DT or DG is installed.

$$U_{ij} \neq \forall U_{ij}^{rst} \in \Gamma; U_{ij} := [u_i u_j] \quad (44)$$

$$u_{T_i} \neq \forall u_n^{rst} \in \Psi; i = 1, 2, \dots, \tau. \quad (45)$$

#### 4.1.4. Reformulation of the Objective Function in Terms of Constraints

For the first stage of TS-MOEAP only it is considered the power loss of the system (36). Therefore, the equality constraints (39) can be satisfied during the power-flow calculation and the inequality constraint (44) can be satisfied during the network construction. The inequality constraints (42), (43) and (45) can be satisfied through penalizing  $f_1$  (36). Finally, the objective function for the first stage can be reformulated as

$$\text{minimize } f'_1(c) = \text{minimize}(f_1(c) + f_{p1} + f_{p2} + f_{p3}) \quad (46)$$

$$f_{p1} = w_1 \sum_{i=1}^{\mu} |\min(V_i - V^{min}, 0, V^{max} - V_i)| \quad (47)$$

$$f_{p2} = w_2 \sum_{i=1}^{\eta} \max(I_{ij} - I^{max}, 0) \quad (48)$$

$$f_{p3} = w_3 \sum_{i=1}^{\tau} \max([u_{T_i} = u_n^{rst}] \Rightarrow [1], 0) \quad (49)$$

where equations (47), (48), and (49) are penalty functions applied when voltage magnitudes are out of limits, when there are overcurrents in the branches, and when transformers are located at restricted utility poles, respectively. Parameters  $w_1$ ,  $w_2$ , and  $w_3$  are penalty factors to delimit in a lesser (or greater way) the search space, and to ensure the desired operation regarding standard concerns.

## 4.2. Implementation of Stage-1 (IPSO – PRIM)

For the optimal placement of DTs/DGs, an IPSO algorithm is proposed based on a regular PSO [42, 43], which is a meta-heuristic method inspired by social behavior of bird flocking or fish schooling. The algorithm works with a population where each particle is a candidate solution, in our case a possible DT/DG location. As illustrated in Figure 4.1, each particle is influenced by its inertia, individual best position, and the global best position found among all particles. Unlike the PSO, the IPSO does not initiate the particles randomly, and it has an accumulative memory to reduce the computational time, due to the complexity of evaluating a DN by means of a power flow analysis. The equation that governs the movement of each particle was represented in (2), and the equation that updates their position is illustrated in (1) (please see section 2.3.1 for more details).

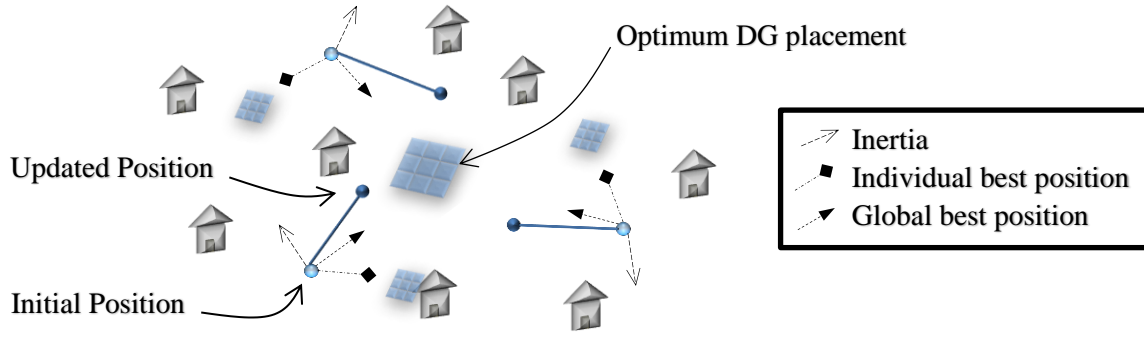


Figure 4.1. Optimal placement of DTs/DGs by the IPSO.

### 4.2.1. Initialization

The IPSO algorithm begins assigning a  $\varepsilon_k$  number of particles to each  $G_k$  set within a chromosome  $c_i$ , according to its size  $\psi_k$ , i.e.

$$\varepsilon_k = \max[\text{round}(\psi_k \cdot \mathcal{O}), 2]; \quad k = 1, 2, \dots, \tau \quad (50)$$

where  $\mathcal{O}$  is a constant value assigned by the user. Considering that the set  $G_k$  represents a real network, the particles can be linearly distributed, excluding the extremes for practical reasons, e.g.

$$G_1 = [u_1 \underbrace{u_2}_{x_1} u_3 \underbrace{u_4}_{x_2} u_7]. \quad (51)$$

Figure 4.2 shows a graphical illustration of this process, where two particles (represented as photovoltaic panels,  $\chi_1$  and  $\chi_2$ ) are located in each group.

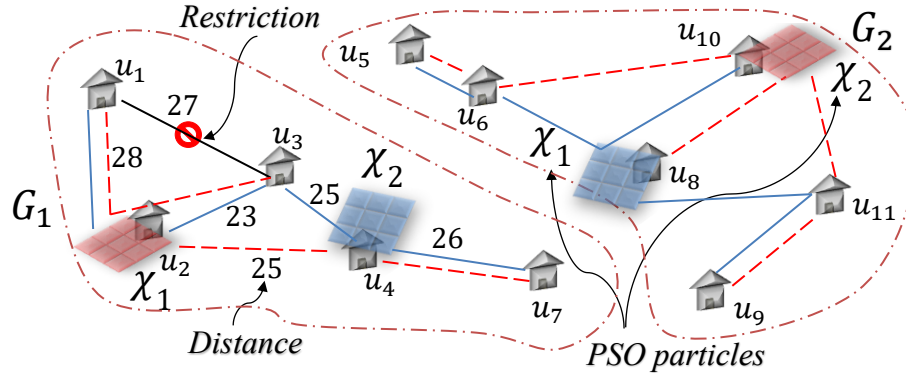


Figure 4.2. IPSO-PRIM operation.

#### 4.2.2. Particle Evaluation

The fitness  $f_1'(\chi_i)$  of each particle is calculated through (46), performing the following steps:

- Network Construction:** As explained in section 3.1, a radial distribution network can be found by considering it as a weighted undirected graph, from which we can obtain a minimum spanning tree by using a traditional *Prim's algorithm*. From a starting node, this algorithm adds at each step the shortest possible branch to make a new link to another node. An example of this process is shown in Figure 4.2, for the group  $G_1$ . The construction starts at the generation center  $\chi_1$ , then the following nodes to add based on the *Euclidean distance* are  $u_3$ ,  $u_4$ ,  $u_7$ , and  $u_1$  through the branches  $\overrightarrow{u_2u_3}$ ,  $\overrightarrow{u_2u_4}$ ,  $\overrightarrow{u_4u_7}$ , and  $\overrightarrow{u_2u_1}$  (dotted red lines). To avoid selecting a restricted branch (e.g.  $\overrightarrow{u_3u_1}$ ) a penalty is added to its distance, therefore another alternative must be taken. With this penalty, we satisfy the inequality constraint (44).
- Power Flow Computation:** Using the  $y_{ij}$  admittance of the branches found in the previous step, an admittance matrix  $Y_{bus}$  can be calculated, as explained in section 3.2.1. Considering the location of each particle  $\chi_1$  as the slack bus of the system, and the remaining nodes as *PQ* type, the power-flow equations (39) can be solved using an iterative method such as Gauss-Seidel, as explained in sections 3.2.2 and 3.2.3. From the power flow analysis, we can get voltage nodes, branch currents, power losses, and therefore  $f_1'(\chi_i)$  through (46). As the power flow analysis is a process that consumes valuable computational time, the IPSO records all the solutions found so far

by the particles, this avoids repeating the power-flow computation if another particle falls in the same place.

- c) **Conductor Optimization:** For the DT/DG optimal placement, the algorithm builds the network with the thickest conductor available, this way we are sure to apply a penalty to the fitness value  $f_1'(\chi_i)$  if a voltage node or a branch current is out of limits. When the DT/DG placement is found, and the current network of  $G_k$  does not have any technical problem, the algorithm reduces the wire size of the branches and recalculates the power-flow. If the network still does not present any problem, the wire size is reduced again; otherwise, the algorithm stops and keeps the last wire. i.e.

$$\forall U_{ij} \in G_k \mid 3/0, 2/0, 1/0, 2AWG \quad (52)$$

where 3/0, 2/0, 1/0 and 2 AWG are available ACSR wire sizes.

- d) **DG/DT sizing and Cost Calculation:** The last step in the evaluation of each particle is the cost calculation of each group  $G_k$ , through (37) or (38). This process is required for the second stage of TS-MOEAP which implements both objective functions,  $f_1(c)$  and  $f_2(c)$ . The investment cost of each group, named as  $f_2(G_k)$ , can be calculated in this stage after find the size of the DT or DG, the conductor size, and the topology of the network, please see section 3.3 for more details. We must note that the IPSO does not require this value to find the optimal placement of DTs/DGs and this information is only collected for Stage-2.

#### 4.2.3. Saving Results and Updating Data

After the evaluation, if  $f_1'(\chi_i)$  is the lowest personal fitness found so far by the particle  $\chi_i$ , its current position is saved in  $\vartheta_i$ . At the same time, if  $\vartheta_i$  is the best position among all the particles this result is saved in  $\sigma$ , and the fitness of the group is established by

$$f_1'(G_k) = f'(\sigma). \quad (53)$$

Using the memories  $\vartheta_i$  and  $\sigma$ , each particle updates its velocity and direction through (1) and (2), as explained in section 2.3.1. Finally, the DG or DT for each group will be placed in  $\sigma$ , as shown in Figure 4.3. Please note that Figure 4.3 also shows the optimal trajectory for the conductors of each group. Stage-1 is repeated for each group within a chromosome, and these results are sent to the second stage to optimize the topology of the network, as will be explained later in Chapter 5.

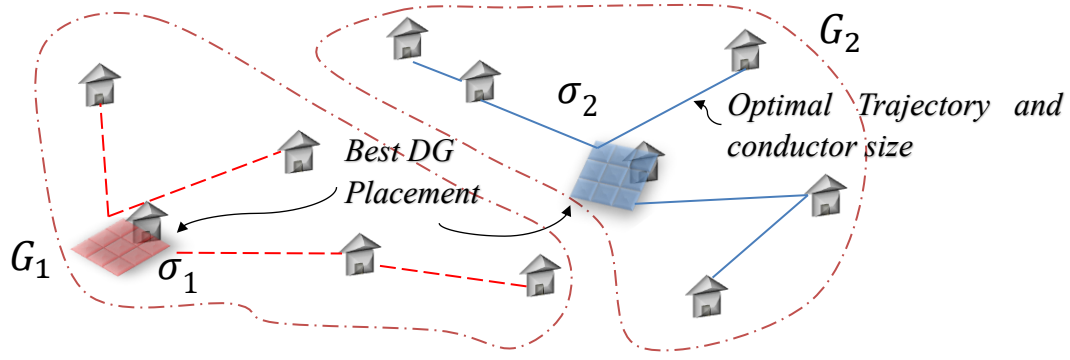


Figure 4.3. Optimal result after Stage-1 of TS-MOEA.

### 4.3. IPSO-PRIM Complete Algorithm

The general flowchart of the proposed IPSO-PRIM algorithm is shown in Figure 4.4.

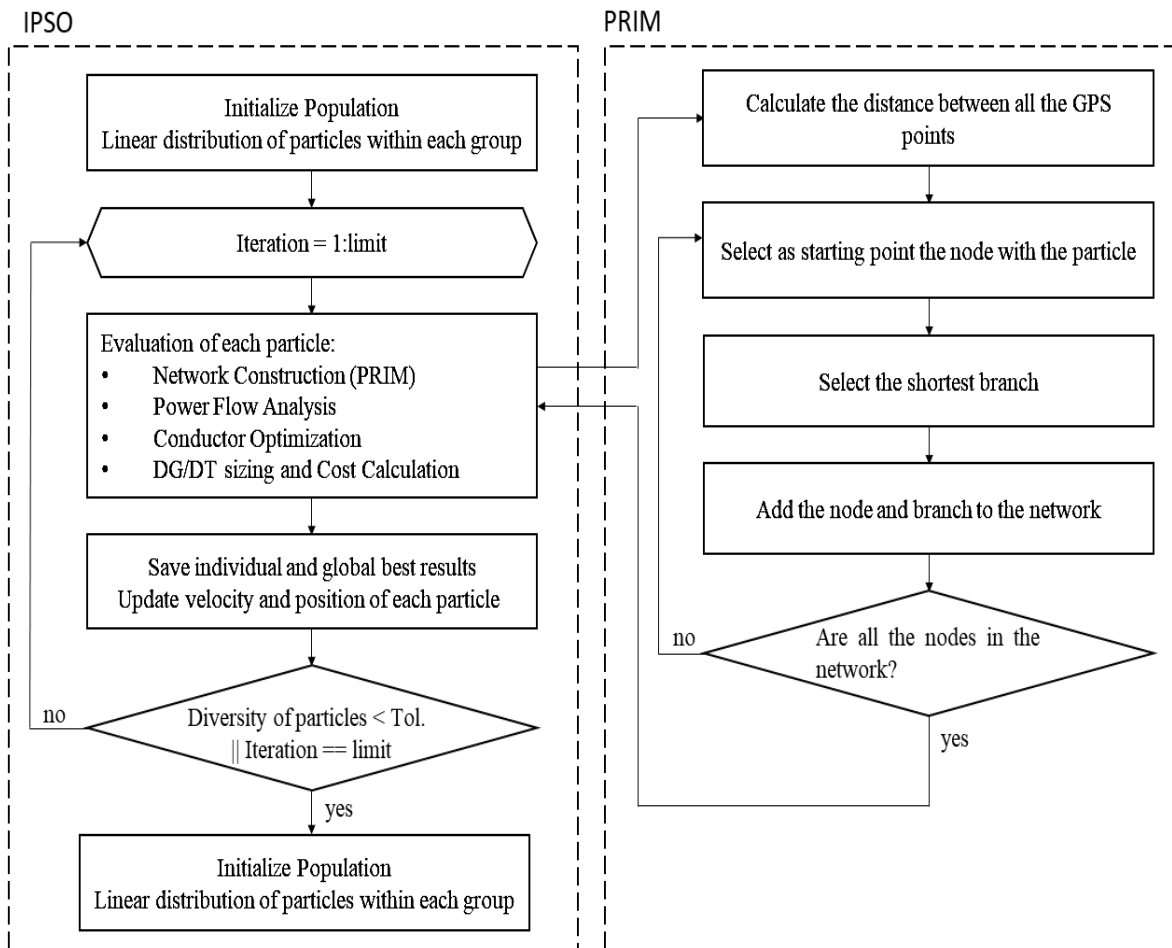


Figure 4.4. General flowchart of the IPSO-PRIM algorithm.

#### 4.4. Simulations and Results for the IPSO-PRIM Algorithm

To prove the effectiveness of the IPSO-PRIM algorithm, three test systems are considered which present different quality issues. For the design process the following data is used: three-phase systems; distribution voltage of 220 V; maximum voltage drop of 5 %; available transformers of 15, 30, 50, 75 and 100 kVA; and available ACSR conductors of 4, 2, 1/0, 2/0 and 3/0 AWG. Finally, the IPSO parameters chosen for these simulations are  $\mathcal{O} = 0.2$ ,  $\gamma = 0.6$ ,  $\alpha = 0.5$ , and  $\beta = 2$ .

##### 4.4.1. LVDN Design Minimizing Power Losses

In this case, the IPSO-PRIM algorithm must design an LVDN minimizing power losses when several options do not have quality issues. The parameters of the system are 167 users, 17 utility poles, and demand per user of 0.65 kVA.

The optimal design is shown in Figure 4.5, and as we can see the algorithm built the network radially. Furthermore, the transformer was located at  $p_{10}$ , where the total power loss is minimized as well as the fitness value. This is illustrated in Figure 4.6 (a). Note that  $p_8$  and  $p_{10}$  do not have quality issues.

If a restriction is imposed, e.g. on the utility pole  $p_{10}$ , the fitness value will be penalized for that node, and the IPSO will select another utility pole such as  $p_8$ . This is illustrated in Figure 4.6 (b). Note that the transformer is always located at the utility pole with the lowest fitness value.

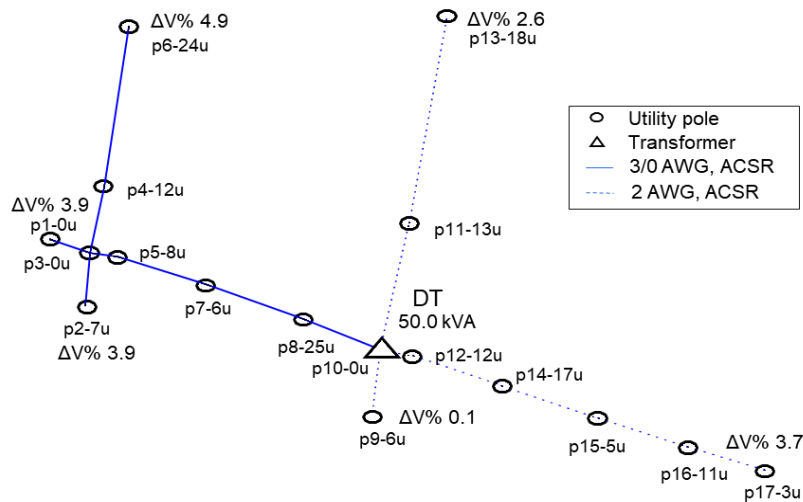


Figure 4.5. LVDN design with/without quality issues.

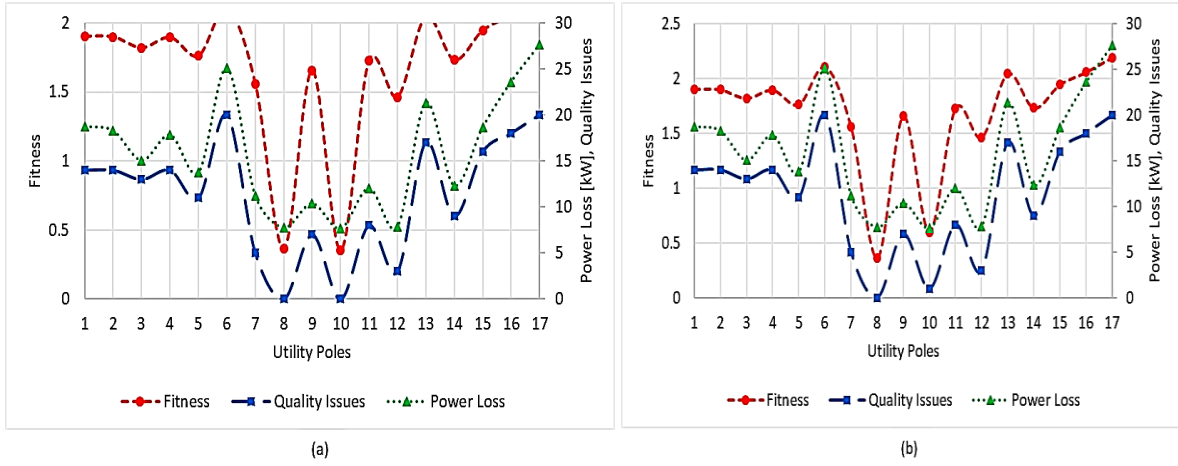


Figure 4.6. Curves for the fitness, power losses and quality issues. a) Considering only power losses. b) Considering a restriction on  $p_{10}$ .

#### 4.4.2. LVDN Design considering Branch Overcurrents

In this case, the IPSO-PRIM algorithm must design an LVDN with branch overcurrents. The parameters of the system are 85 users, 6 utility poles, and demand per user of 1.36 kVA. The optimal design is shown in Figure 4.7 (a), and as we can see, the transformer is placed at  $p_5$  where does not exist quality issues. The algorithm made this selection due to an overcurrent in the branch  $U_{3,5}$  (321 A, when the limit is 315 A). This is illustrated in Figure 4.7 (b).

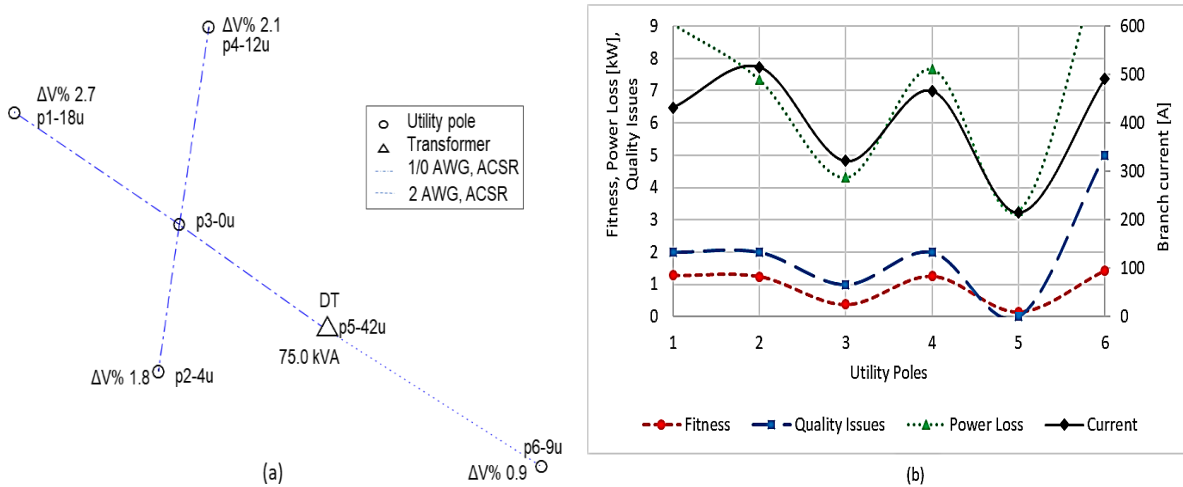


Figure 4.7. LVDN design considering branch overcurrents. a) LVDN optimal design. b) Fitness value, quality issues, power losses, and current per utility pole.



#### 4.4.3. LVDN design considering branch overcurrents and voltage drops

In this case, the proposed algorithm must design an LVDN which can present several quality issues. The parameters of the system are 112 users, 16 utility poles, and demand per user of 1.02 kVA. The optimal network design is shown in Figure 4.8 (a), and as we can see the network was built radially, the transformer was placed at  $p_8$ , and some branches have the maximum available conductor size (3/0 AWG). To prove that this is the optimal configuration, the transformer is moved to  $p_5$  and  $p_{11}$  (see Figure 4.8 (b) and Figure 4.8 (c), respectively), where several quality issues such as voltage drops and overcurrents appear.

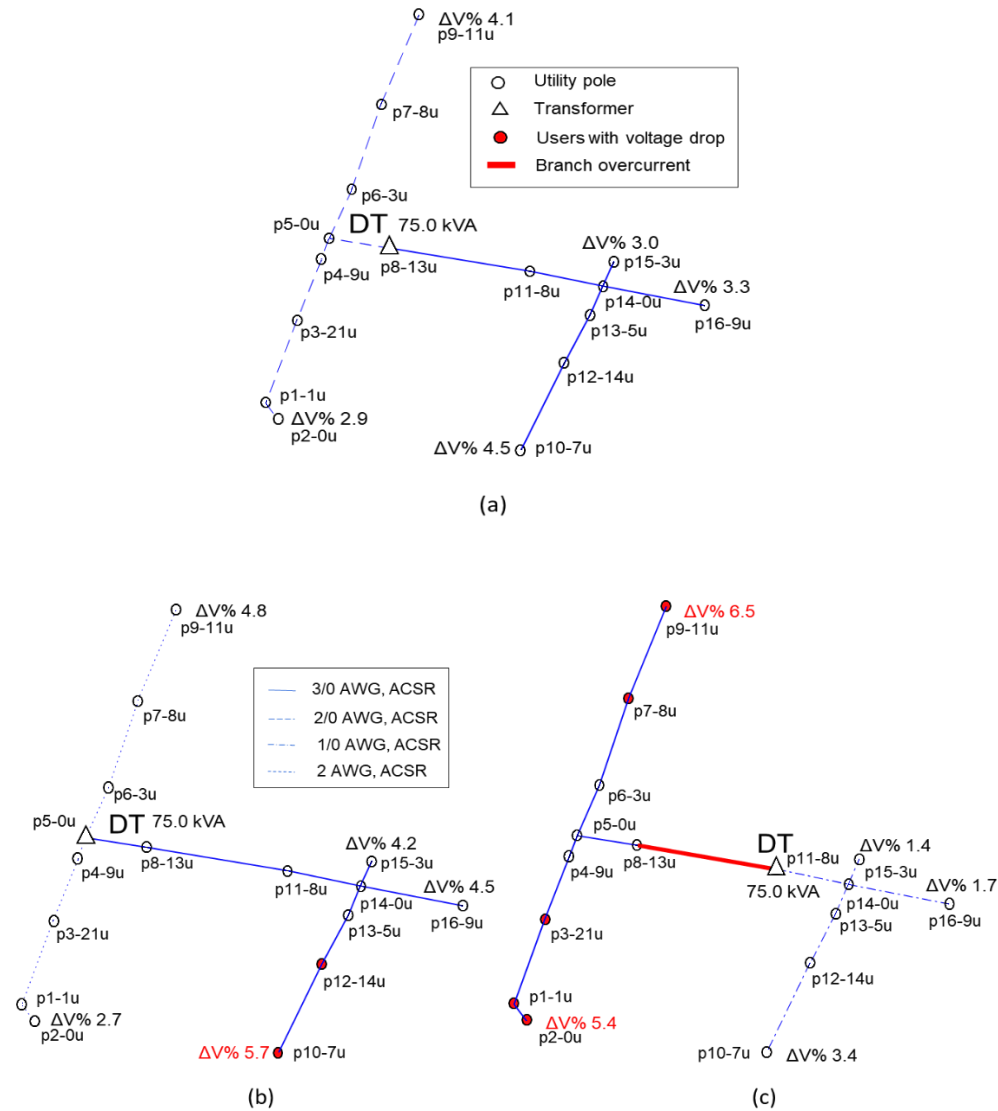


Figure 4.8. LVDN design regarding voltage drops and overcurrents. a) LVDN optimal design. b) Transformer located at  $p_5$ . c) Transformer located at  $p_{11}$ .

## **4.5. Summary**

We have described the implementation of the first stage of TS-MOEAP, composed of a greedy algorithm (PRIM) and an improved particle swarm optimization technique (IPSO). This chapter detailed the problem formulation, particularities of the algorithm and some simulations to prove the performance of Stage-1.

## Chapter 5

### Stage-2 of TS-MOEAP (INSGA – HO)

In this chapter we explain how the second stage of TS-MOEAP is applied to optimize the topology of distribution networks, at primary and secondary level, minimizing power losses and investment costs. Here is detailed the proposed INSGA-HO algorithm and each one of its operators such as the selection, the heuristic mutation, and the recombination. At the end of this chapter, a summary of the TS-MOEAP approach is presented along with a flowchart and a pseudocode of the entire proposed algorithm (INSGA-HO/IPSO).

#### 5.1. Reformulation of the Objective Functions in Terms of Constraints

For the second stage of TS-MOEAP, the optimization is performed by minimizing power losses and investment costs, considering quality issues as the constraints of the problem. We select these two objectives because they are related to the change of network topology. For example, to minimize power losses we can install more DTs or DGs, changing their location, or dividing users into smaller groups. These changes cause an increment of investment costs; therefore, this variable is also taken into account to avoid unnecessary costs due to oversizing. Finally, the objective functions for Stage-2 can be reformulated as

$$\text{minimize}_{c \in \Pi} [f'_1(c), f'_2(c)]; \quad \begin{cases} f'_1(c) = f_1(c) + f_{p1} + f_{p2} + f_{p3} \\ f'_2(c) = f_2(c) + f_{p4} + f_{p5} \end{cases} \quad (54)$$

$$f_{p4} = w_4 \sum_{i=1}^{\tau} |\min(S_{T_i} - S^{\min}, 0, S^{\max} - S_{T_i})| \quad (55)$$

$$f_{p5} = w_5 \sum_{i=1}^{\tau} |\min(SB_{T_i} - SB^{\min}, 0, SB^{\max} - SB_{T_i})| \quad (56)$$

where  $f'_1(c)$  is similar to (46), and (55) and (56) are penalty functions applied to the total investment cost when the capacity of DTs/DGs and battery banks are out of limits.  $w_4$  and

$w_5$  are penalty factors to delimit in a lesser or greater way the search space. These two objectives should be minimized using the proposed INSGA-HO explained below.

## 5.2. Implementation of Stage-2 (INSGA-HO)

The proposed INSGA-HO algorithm is based on the multi-objective evolutionary algorithm NSGA-II (please see section 2.4.2) that uses nondominated sorting and sharing. For a multi-objective problem as shown in (54), a solution  $c_i$  is said to dominate  $c_j$  (represented as  $c_i < c_j$ ) when

$$\forall n \in \{1, 2, \dots, m\}: c_i < c_j \Leftrightarrow f_n(c_i) \leq f_n(c_j). \quad (57)$$

Considering this concept, each solution can be assigned a *rank* equal to its nondominated level.  $c_i$  solutions not dominated by any other have rank 1 (they belong to the *pareto front*,  $\mathcal{F}_1$ ), the next best-solutions have rank 2 (front  $\mathcal{F}_2$ ) and so on. As we can see in Figure 5.1, the proposed INSGA-HO algorithm does not find all nondominated fronts at once, first, it finds  $\mathcal{F}_1$ ; if its size is smaller than  $N$  (size of the population), their members are chosen to form  $A^{(t+1)} = A^{(t)} \cup \mathcal{F}_1$ , and the next front can be found. If the size of  $|A^{(t)} \cup \mathcal{F}_2|$  is smaller than  $N$ , the members of  $\mathcal{F}_2$  are chosen to form  $A^{(t+1)} = A^{(t)} \cup \mathcal{F}_2$ , and the next front  $\mathcal{F}_3$  can be found, and so on.

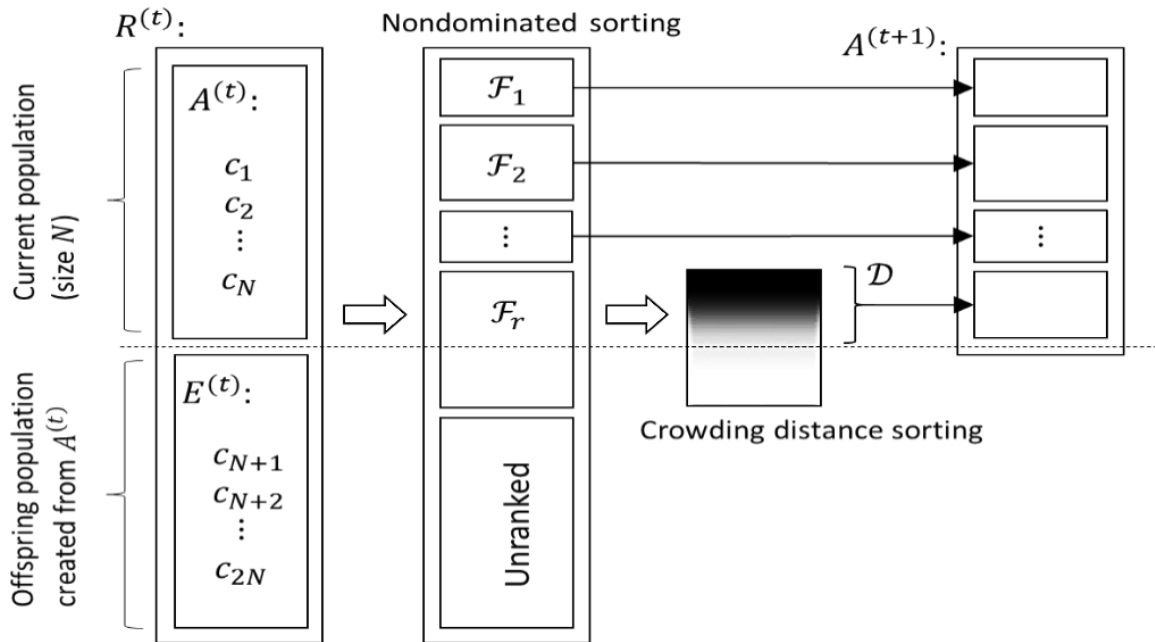


Figure 5.1. Nondominated sorting and crowding distance procedure.

This process is repeated until  $|A^{(t+1)} \cup \mathcal{F}_r| \geq N$ , in this case, the nondominated sorting is stopped, and the remaining members of the population  $A^{(t+1)}$  must be chosen from the last front  $\mathcal{F}_r$  by a crowding distance procedure ( $\mathcal{D}$ ).

Finally, in order to create an offspring population  $E^{(t)}$ , a binary tournament selection, recombination, and a mutation operator are used. In the tournament selection, two random individuals are compared by rank and crowding distance. The individual with the best rank is selected, but if both individuals belong to the same front, the individual with greater crowding distance is selected.

### 5.2.1. Nondominated Sorting Procedure

In order to find the rank of each solution  $c_i$  within a population  $R$  of size  $N$ , each solution can be compared with every other solution in the population to find if it is dominated. In this process for each solution we calculate two entities:

1. Domination count  $n_{c_i}$ , that means the number of solutions which dominate the solution  $c_i$ , and
2.  $S_{c_i}$ , a set of solutions that  $c_i$  dominates.

All solutions in the first nondominated front will have their domination count as zero. Now, for each solution  $c_i$  with  $n_{c_i} = 0$ , we visit each member  $c_j$  that belongs to its set  $S_{c_i}$  and reduce its domination count by one. If for any member  $c_j$  the domination count becomes zero, we put this solution in a separate set  $T$ , which will be the second nondominated front. The above procedure is repeated then for each member of  $T$  to identify the third front and so on. This process continues until all fronts are identified.

For each solution  $c_i$  in the second or higher level of nondomination, the domination count  $n_{c_i}$  can be at most  $N - 1$ . Thus, each solution  $c_i$  will be visited at most  $N - 1$  times before its domination count becomes zero. At this point, the solution is assigned a nondomination rank and will never be visited again. The pseudocode of the nondominated sorting is illustrated in Figure 5.2.

For the Stage-2, the fitness values used for nondominated sorting and crowding distance calculation can be obtained by adding the individual fitness values of each  $G_k$  group found in Stage-1, i.e.

$$\begin{aligned}
f'_1(c_i) &= \sum_{k=1}^{\tau} f'_1(G_k) \\
f'_2(c_i) &= \sum_{k=1}^{\tau} f'_2(G_k) \\
i &= 1, 2, \dots, 2N.
\end{aligned} \tag{58}$$

---

```

1  foreach  $c_i \in R^{(t)}$  do
2       $S_{c_i} = \emptyset$ 
3       $n_{c_i} = 0$ 
4      foreach  $c_j \in R^{(t)}$  do
5          if  $(c_i \prec c_j)$  then                If  $c_i$  dominates  $c_j$ 
6               $S_{c_i} = S_{c_i} \cup \{c_j\}$     Add  $c_j$  to the set of solutions dominated by  $c_i$ 
7              else if  $(c_j \prec c_i)$  then        If  $c_j$  dominates  $c_i$ 
8                   $n_{c_i} = n_{c_i} + 1$         Increment the domination counter of  $c_i$ 
8              end
8          end
8      end
8
9      if  $(n_{c_i} = 0)$  then
10          $rank_{c_i} = 1$                          $c_i$  belongs to the first front
11          $\mathcal{F}_1 = \mathcal{F}_1 \cup \{c_i\}$ 
11     end
11 end
11
12  $k = 1$                                         Initialize the front counter
13 while  $\mathcal{F}_k \neq \emptyset$  do
14      $T = \emptyset$                                 Used to store the members of the next front
15     foreach  $c_i \in \mathcal{F}_k$  do
16         foreach  $c_j \in S_{c_i}$  do
17              $n_{c_j} = n_{c_j} - 1$ 
18             if  $n_{c_j} = 0$  then
19                  $rank_{c_j} = k + 1$              $c_j$  belongs to the next front
20                  $T = T \cup \{c_j\}$ 
20             end
20         end
20     end
20
21      $k = k + 1$ 
22      $\mathcal{F}_k = T$ 
22 end

```

---

Figure 5.2. Pseudocode of the Nondominated Sorting.

### 5.2.2. Crowding Distance Calculation

Instead of the sharing function approach implemented by other multiobjective genetic algorithms, the NSGA-II proposes a crowded-comparison approach which does not require *any* user-defined parameter for maintaining diversity among population members and has a better computational complexity.

To get an estimate of the density of solutions surrounding a particular  $c_i$  solution in the population, the average distance of two points can be calculated on either side along each of the objectives. This quantity serves as an estimate of the perimeter of the cuboid formed by using the nearest neighbors as the vertices, calling this the *crowding distance* ( $\mathcal{D}$ ).

Figure 5.3 shows the crowding distance of the  $c_i$  solution as the average side length of the cuboid shown with a dashed box.

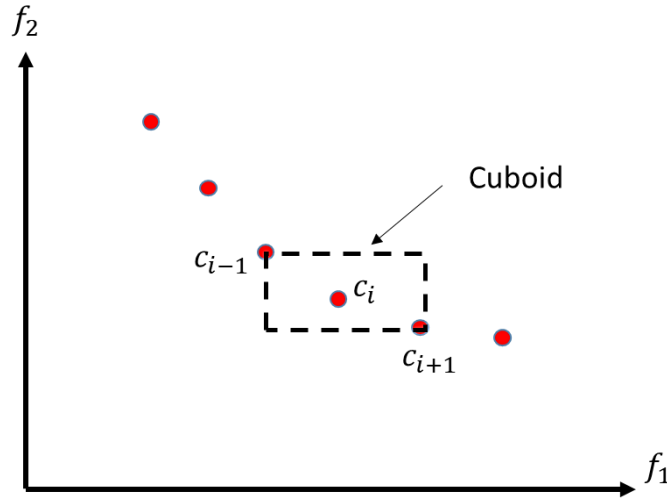


Figure 5.3. Crowding distance calculation.

Therefore, the operator  $\mathcal{D}$  estimates the density of solutions surrounding a particular  $i^{th}$  solution calculating the sum of individual distance values corresponding to each objective expressed as:

$$\mathcal{D}_i = \mathcal{D}_i + [f_n(c_{i+1}) - f_n(c_{i-1})] / [f_n^{max} - f_n^{min}]; n = 1, 2, \dots, m \quad (59)$$

where  $f_n^{max}$  and  $f_n^{min}$  represent the maximum and minimum fitness values of the  $n^{th}$  objective function. A solution with a smaller  $\mathcal{D}$  value is more crowded by other solutions, therefore to maintain diversity, the members with greater  $\mathcal{D}$  are selected.

### 5.2.3. Initialization

The INSGA-HO algorithm starts creating an initial random population  $R$  of size  $2N$ , on which each individual  $c_i$  is a possible configuration of the system, see Figure 5.1. This population can be represented by a matrix as explained in section 3.1. We must remember that the IPSO works with the sets  $G_k$  contained in  $c_i$ , while the INSGA-HO works with the entire integer vector  $c_i$ . Therefore, the initial population can be created by using the pseudocode shown in Figure 5.4, where  $(\tau^{min}, \tau^{max})$  are the limits for the number of DGs or DTs to install.

---

```

1 for  $i = 1 : 2N$  do
2    $gr = \text{randi}[\tau_{min} \ \tau_{max}]$ 
3   for  $j = 1 : \mu$  do
4      $R(i, j) = \text{randi}[1 \ gr]$ 
   end
end

```

---

Figure 5.4. Creation of a random population R.

### 5.2.4. Heuristic Mutation Operation

Considering the combinatorial complexity of DNs, the mutation operator has been modified to obtain better network topologies. Something well-known about DNs is that loads usually are connected to the nearest transformer group or generation center. Using this characteristic, the heuristic mutation operator ( $\mathcal{H}$ ) can find better solutions than a regular operator. For example, as shown in Figure 5.5, the heuristic operator first calculates the average center of each group (e.g.  $a$ ,  $b$ ,  $c$ ) and takes the farthest load to the respective center (e.g.  $u_1$ ,  $u_7$ ,  $u_8$ ). Later, the distances to the center of other groups are compared, e.g.  $u_7 - b$  is compared with  $u_7 - a$  and  $u_7 - c$ . If a shorter distance is found the load is switched, e.g.  $u_7$  is switched to  $G_3$ ,  $u_8$  is switched to  $G_1$  and  $u_1$  is maintained in  $G_1$ .

A configuration mutates if a random value between  $[0,1]$  is superior to a mutation rate  $\varpi$ , as shown in equation (60). Applying the heuristic operator  $\mathcal{H}$  to the configuration  $c_1 = [1 \ 1 \ 2 \ 2 \ 1 \ 2 \ 2 \ 3 \ 3 \ 3 \ 3]$  of Figure 5.5, the result is  $\mathcal{H}(c_1) = [1 \ 1 \ 2 \ 2 \ 1 \ 2 \ 3 \ 1 \ 3 \ 3 \ 3]$ .

$$c_{m_i} = \begin{cases} \mathcal{H}(c_i), & \text{if } \text{rand}[0, 1] \geq \varpi \\ c_i, & \text{if } \text{rand}[0, 1] < \varpi. \end{cases} \quad (60)$$



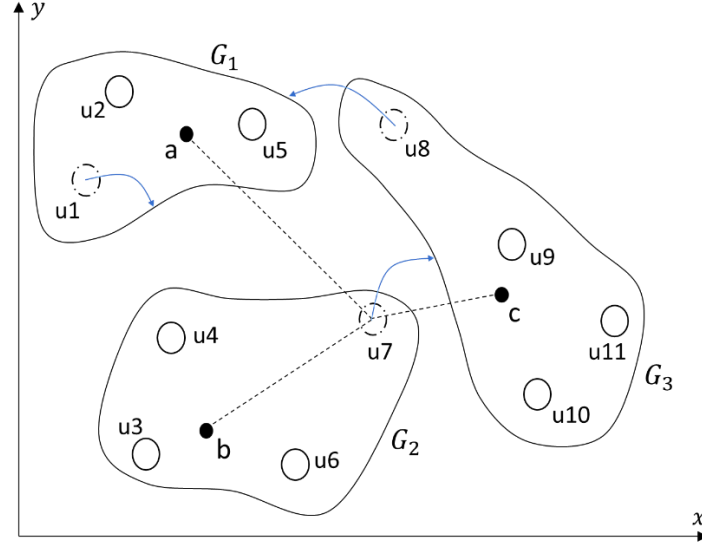


Figure 5.5. Heuristic mutation operation.

### 5.2.5. Recombination Operation

Due to the integer encoding, and the random order of  $G_k$  groups, a uniform crossover is used for recombination (see Sec. 4.2 of [42]). This operator takes two parents from the population  $A^{(t+1)}$  and creates two new individuals by selecting each gene from the first or second parent at random. For each position of the new chromosome, if a random value between  $[0,1]$  is below a crossover rate  $\delta$ , the gene is inherited from the first parent, otherwise from the second. The second chromosome is created using the inverse mapping of the first one. For example, assuming that the parents are  $c_i = [a_{i1} \ a_{i2} \ \dots \ a_{i\mu}]$ , and  $c_j = [b_{j1} \ b_{j2} \ \dots \ b_{j\mu}]$ , the offspring is created by

$$r_n = \begin{cases} a_{in}, & \text{if } \text{rand}[0, 1] \leq \delta \\ b_{jn}, & \text{if } \text{rand}[0, 1] > \delta. \end{cases} \quad n = 1, 2, \dots, \mu \quad (61)$$

$$c_{ij} = [r_1 \ r_2 \ \dots \ r_\mu].$$

A graphic representation of the recombination and heuristic mutation is shown in Figure 5.6 (a) and the result of both operators is illustrated in Figure 5.6 (b). Finally, we can conclude that a system can be improved by means of network reconfiguration, obtaining a new topology in each evolution, where power losses and investment costs can be minimized.

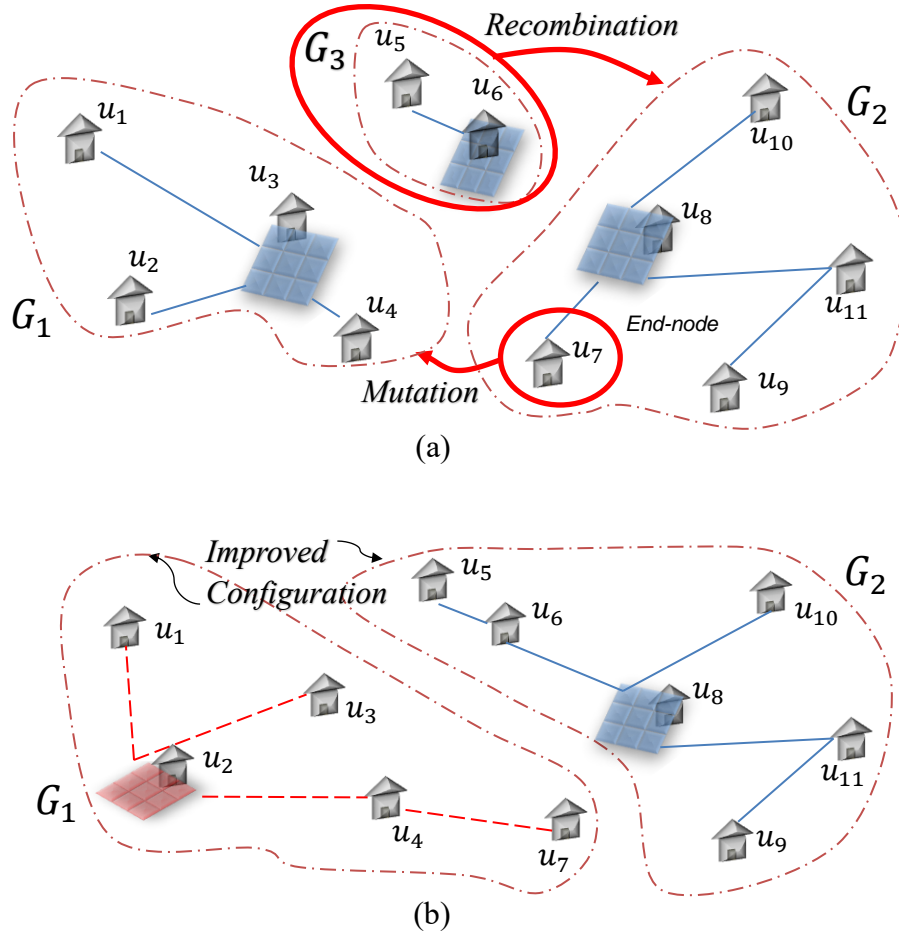


Figure 5.6. INSGA-HO process. a) Recombination and heuristic mutation. b) Configuration result.

### 5.2.6. Termination Condition

As EAs are stochastic and mostly there are no guarantees of reaching an optimum, a termination condition based on the fitness level might never get satisfied, and the algorithm may never stop. Therefore, we must extend this condition with one that certainly stops the algorithm. The following options are commonly used for this purpose:

- The maximally allowed CPU time elapses.
- A maximum number of iterations or evolutions.
- The fitness improvement remains under a threshold value for a given period of time.
- The population diversity drops under a given threshold.

In our particular case, for the INSGA-HO we are going to use a maximum number of iterations, and for the IPSO the diversity of the population.

### 5.3. Summary of TS-MOEAP

TS-MOEAP can be defined as an algorithm composed of two stages of optimization, each implementing an EA, in order to design or improve a distribution network. The operation of each stage can be summarized as follows:

- Stage-1. Optimal placement and sizing of DTs/DGs, as well as optimal branch routing and conductor sizing, please see Figure 5.7 (a).
- Stage-2. Optimal network reconfiguration, that implies changing the topology of the network and the number of DTs/DGs (or user groups), please see Figure 5.7 (b).

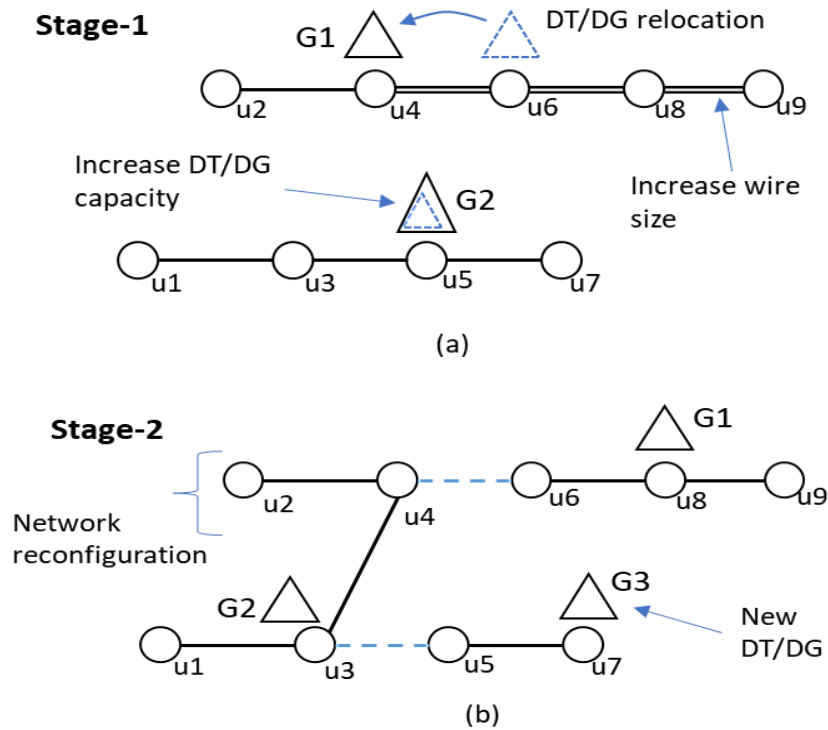


Figure 5.7. TS-MOEAP operation. a) Stage-1. Optimal size and placement of DTs/DGs and conductors. b) Stage-2. Network reconfiguration.

For the first stage, an IPSO algorithm is proposed for its simplicity and outstanding performance being ideal as a subroutine. For the second stage, an INSGA-HO is proposed for its ability to solve complex multiobjective problems without the need to calibrate several parameters, furthermore, its heuristic mutation operator has the advantage to find better solutions by performing specific changes on the chromosomes.

In order to develop TS-MOEAP, the following assumptions were made:

- i. a projected unit demand ( $P_{UD}$ ) is used for the network design and transformer sizing;
- ii. primary lines can be extended to any utility pole to feed DTs or DGs;
- iii. the quantity and location of utility poles do not change, something common in practice;
- iv. the loads connected to one transformer or distributed generator will form a group, and
- v. each utility pole, interconnection point, or load will have a  $(x_i, y_i)$  GPS coordinate.

In the following section, the complete algorithm of TS-MOEAP (combining both the IPSO and the INSGA-HO) is presented, with a general flowchart and a detailed pseudocode.

#### **5.4. Complete Algorithm of TS-MOEAP (INSGA-HO/IPSO)**

The proposed algorithm of TS-MOEAP is developed in MATLAB and its pseudocode is shown in Figure 5.8. The general flowchart of the proposal is shown in Figure 5.9.

#### **5.5. Main Contributions of the Proposal**

Among the most important contributions of TS-MOEAP we have:

- i. The proposal can optimize primary and secondary DNs, unlike other works that can only optimize MVDNs.
- ii. The optimization of both levels is possible thanks to the type of representation. Instead of using binary vectors to represent switches, we use integer vectors to represent groups of loads. This permits the algorithm to face the complicated topology of LVDNs and use the same code for optimizing MVDNs.
- iii. The approach can find the optimal network topology and the optimal location of DTs or DGs, at the same time. This is possible thanks to the implementation of two stages.
- iv. The INSGA-HO is proposed specially for DN design. It overcomes a conventional NSGA-II by finding the nondominated fronts one at a time and incorporates a heuristic mutation operator for a better search of solutions.
- v. The IPSO is proposed to overcome the computational time of a conventional PSO through an accumulative memory and a linear distribution of the particles. This helps reduce excessive repetitions of the power flow analysis.

- vi. The approach uses a greedy algorithm to build the network -always in radial form- using the GPS coordinates of the loads.
- vii. Finally, the proposed approach is able to design a distribution network from scratch or redesign an existing network to improve it.

---

**Data:** System parameters, GPS coordinates, users and loads, geographical and technical constraints, available equipment and costs.

**STAGE-2: NSGA-HO**

```

1 Create a random population  $R^{(t)}$  of size  $2N$   $c_i \in R^{(t)}$ ,  $i = 1, 2, \dots, 2N$ 
2 for  $t = 1 : t^{limit}$  do
3   for  $i = 1 : 2N$  do
4     Identify  $T_k$  groups inside  $c_i$ ,  $T_k \in c_i$ .
5      $f'_{1_i}(c_i) \leftarrow 0$ ;  $f'_{2_i}(c_i) \leftarrow 0$ ;
6     for  $k = 1 : \tau$  do
7       STAGE-1: IPSO
8       Initialize  $\chi_j$  particles within  $T_k$ 
9       Network construction using PRIM
10      while Population diversity > Tol. do
11        Power-flow computation
12        Calculate objective function  $f'_{1_j}(\chi_j)$ 
13        Save the global best result,  $f'_{1_k}(T_k)$ 
14        Update  $v_j$  velocity and  $\chi_j$  position
15      end
16      Optimize conductor size
17      Calculate transformer capacity
18      Calculate objective function  $f'_{2_k}(T_k)$ 
19       $f'_{1_i}(c_i) \leftarrow f'_{1_i}(c_i) + f'_{1_k}(T_k)$ 
20       $f'_{2_i}(c_i) \leftarrow f'_{2_i}(c_i) + f'_{2_k}(T_k)$ 
21    end
22  end
23  Sort  $R^{(t)}$  by nondominated fronts and crowding distance
24  Truncate  $R^{(t)}$  to form  $A^{(t)}$  (size  $N$ )
25  Make selection, recombination, and mutation operations on  $A^{(t)}$  to form an
    offspring  $E^{(t)}$ 
26  Combine current population and offspring,  $R^{(t+1)} \leftarrow A^{(t)} \cup E^{(t)}$ 
27 end

```

---

**Result:** The most economical  $c_i$  configuration from the pareto set.

---

Figure 5.8. Pseudocode of TS-MOEAP.

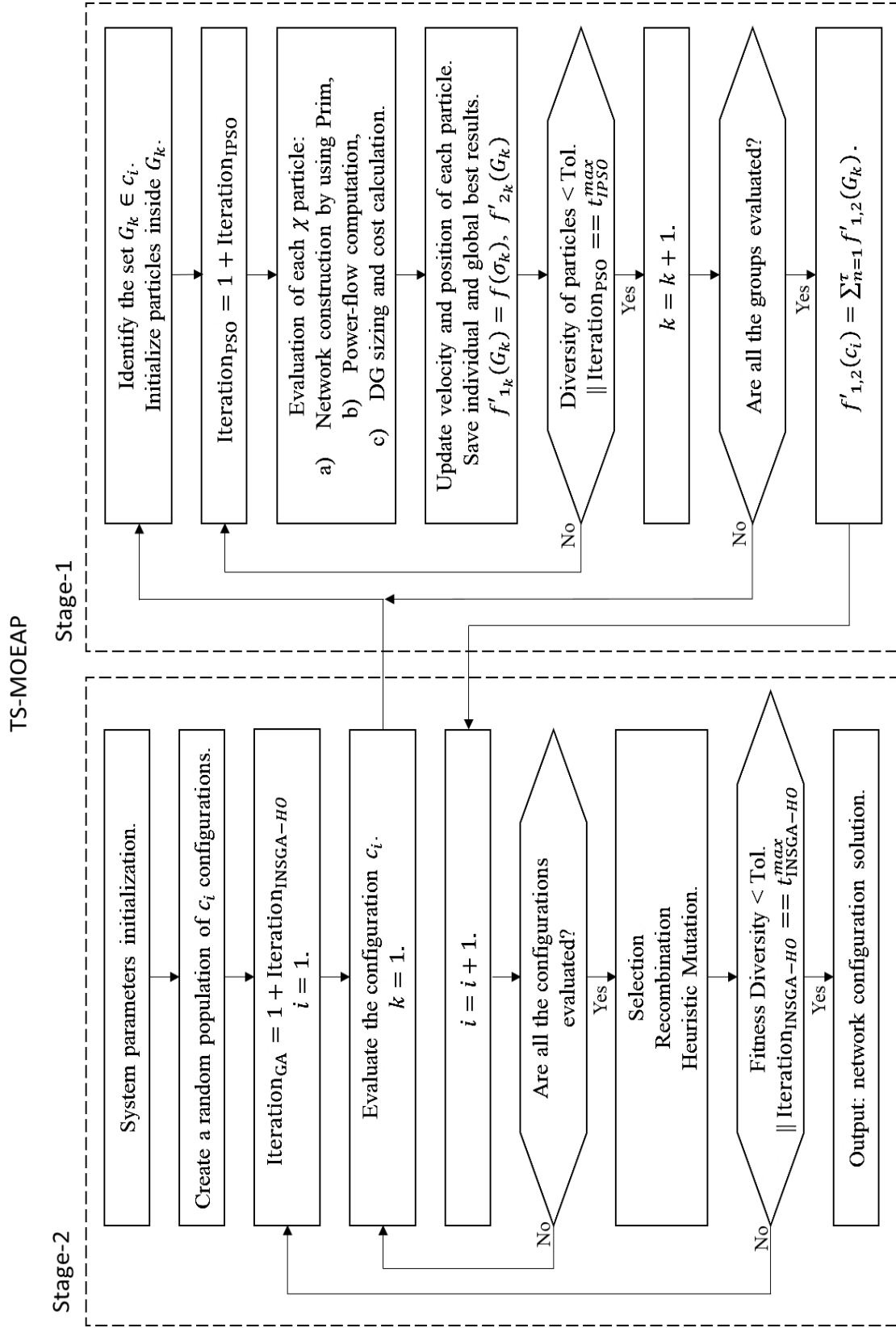


Figure 5.9. Flowchart of TS-MOEAP.

## Chapter 6

### Implementation of TS - MOEAP

In this chapter, we present different case studies solved by TS-MOEAP such as the design of off-grid electrification projects, optimal condition restoration of low voltage distribution networks, and optimal reconfiguration of medium voltage networks. For each case different scenarios will be presented, and the results will be compared against other algorithms. A practical tool developed on Android will also be presented at the end of this chapter.

#### 6.1. Optimal Design of Off-Grid Electrification Projects with DG

The TS-MOEAP approach is proposed to design two off-grid electrification projects that require distributed generation (DG). The design of this type of systems can be considered as an NP-Hard combinatorial optimization problem; therefore, due to its complexity, the approach tackles the problem from two fronts: optimal network configuration, and optimal placement of DGs. As the first attempt of TS-MOEA, the approach will be based on a particle swarm optimization technique (PSO) and a genetic algorithm (GA), improved with the heuristic mutation operator explained in section 5.2.4. In this particular case, the multiobjective problem is transformed into a single-objective problem using scalarization, i.e.

$$\min f = w_a f'_1(c) + w_b f'_2(c) \quad (62)$$

TS-MOEAP will permit to find the optimal network topology, the optimal number and capacity of the generation units, as well as their best location. Furthermore, the algorithm must design the system under power quality requirements, network radiality, and geographical constraints. The approach uses GPS coordinates as input data and develops a network topology from scratch, driven by overall costs and power losses minimization.

The main challenge about the design of *Off-Grid Electrification Projects* is to know how many DGs we should install to feed all users, satisfying power quality constraints, while minimizing investment costs. If a fully centralized system (only one DG for all users) is chosen, the total investment cost will decrease, but the power losses and quality issues may increase as well. On the other hand, if a fully decentralized system (a DG per user) is chosen, the total

power losses will be reduced but the total investment cost may increase. This hinders the network design; therefore, an optimization approach must be used to establish the optimal number of DGs and the optimal topology of the network. Considering these particularities, we illustrate the general idea to design an off-grid electrification project in Figure 6.1.

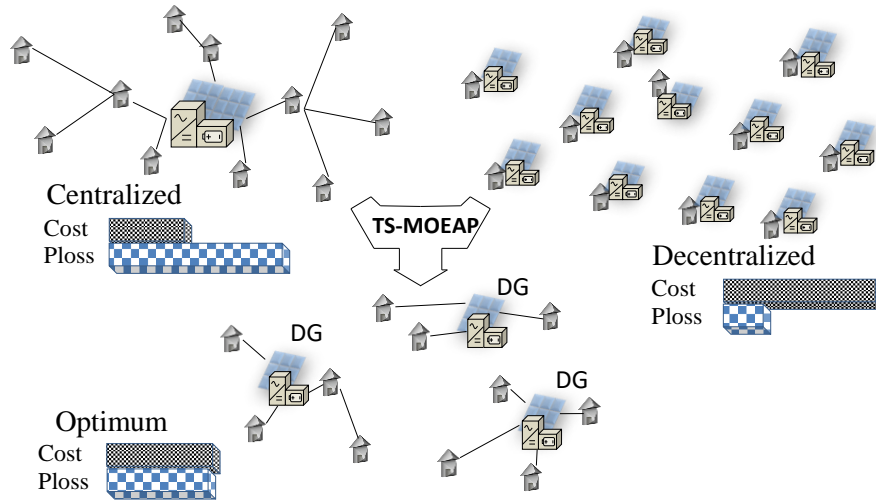


Figure 6.1. Application of TS-MOEAP to design an off-grid electrification project.

### 6.1.1 The Case Study

TS-MOEAP will be applied to design off-grid electrification projects for two rural communities, in the Ecuadorian Andes, which lack electric power. Each community will be denoted as CM1 and CM2, hosting 36 and 48 users respectively. Distributed photovoltaic generation was selected because the area of study is located at 2500 m above sea level, at 0° latitude, allowing an average solar radiation of 4.4 kWh/m<sup>2</sup>, and an average temperature of 18 °C as shown in Appendix A. These data were obtained from RETScreen [49]. The geographical coordinates for each community were obtained in situ, see Figure 6.2 (a) and (b). Each GPS point can either represent a load, a cluster of loads, or a waypoint.

Due to the lack of an existing distribution system, battery banks are implemented. The entire system is designed at 240 V, with a voltage drop limit ( $\Delta V$ ) of 5.5%, a peak load per user of 2.23 kVA, and an average energy consumption of 200 kWh/month. The impedance of the different conductors was obtained from libraries available in ETAP™.



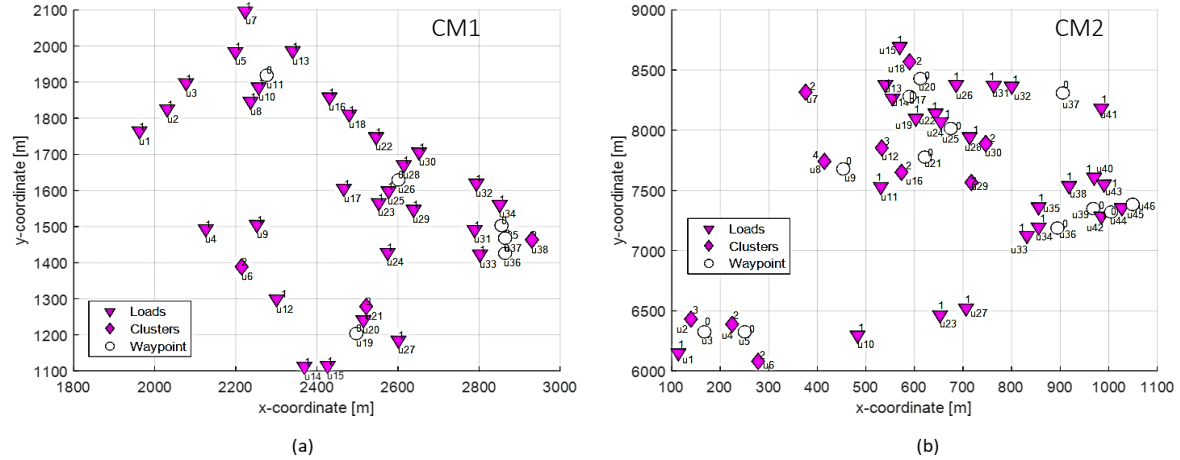


Figure 6.2. Geographical coordinates of the case studies. a) Community CM1. b) Community CM2.

The main characteristics and reference prices (\$/US) of the considered equipment are listed in Table 3.2 and Table 3.4, of section 3.3. We must note that the considered inverters can control the power supply at a given voltage-frequency and charge/use the battery bank according to the amount of generation.

Finally, the effectiveness of the proposed GA-PSO algorithm is tested under two scenarios: 1) simulating a centralized and decentralized system by blocking the number of DGs to be installed, and 2) using a single objective fitness function and standard variation operators (crossover and mutation).

### 6.1.2. TS-MOEAP Optimal Results

The evolution process -for the GA-PSO scheme applied to CM1- is shown in Figure 6.3. Each capture shows the best configuration found until the  $n$ th-evolution with their respective fitness, power losses, and total costs. For each  $G_n$  group, the required photovoltaic capacity and the size of the battery bank are detailed. The description of each element used in the graphic is shown in Table 6.1.

Table 6.1. Nomenclature.

○	Waypoint	——	2 AWG conductor
▽	One Load	----	1/0 AWG conductor
◇	Load Group	-. - . - .	2/0 AWG conductor
□	Distributed Generation	-----	3/0 AWG conductor

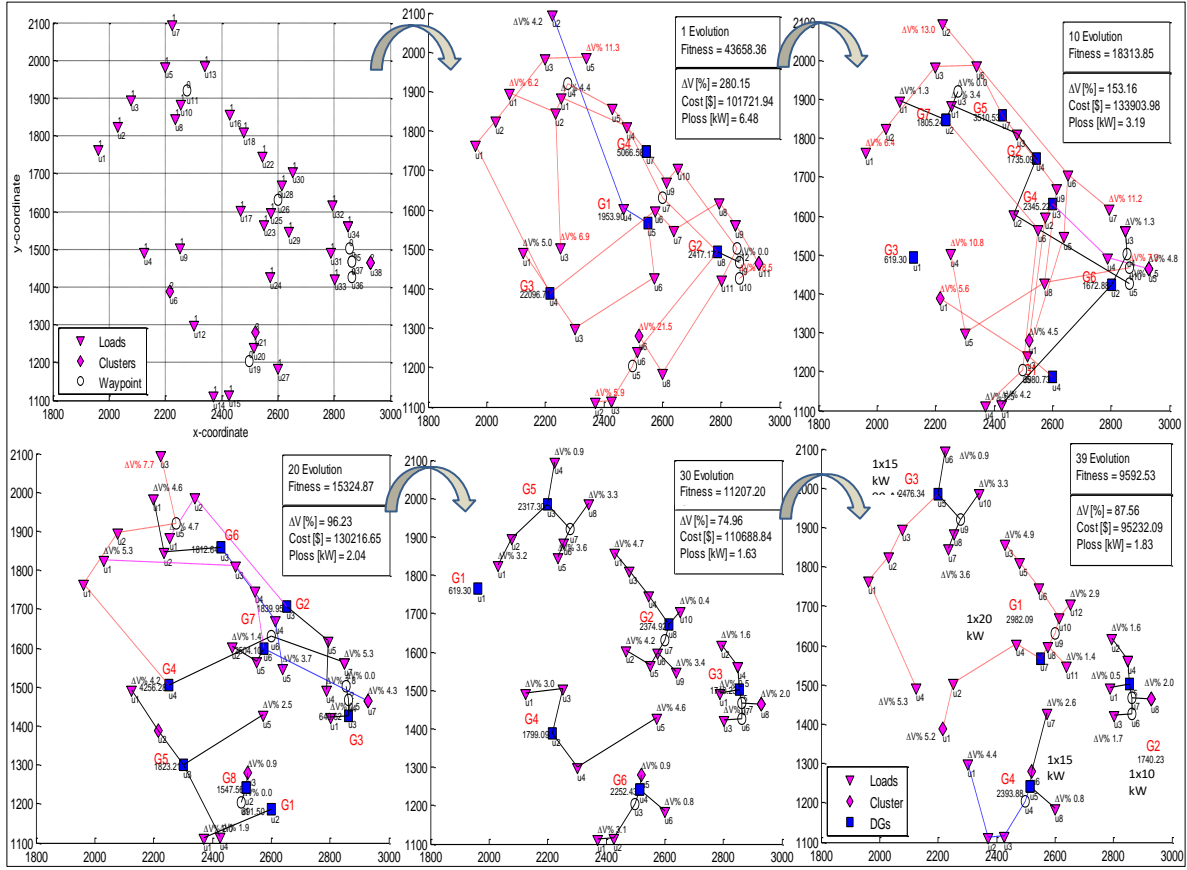


Figure 6.3. TS-MOEAP evolution process and results for CM1.

As we can see in Figure 6.3 the algorithm starts from *scratch*, taking the GPS points from CM1 to propose, initially, random configurations. In the following generations, the GA algorithm learns and proposes better configurations due to the selection, crossover, and mutation. At the same time, the PSO searches the best location for the DGs and evaluates the proposed configurations. In the first evolutions, the results are naturally *primitive*, since the number of groups can vary drastically, the configurations present no logic, and some points of the network violate the imposed constraints. However, after several evolutions, the system develops a defined structure and its fitness decreases as well as power losses and costs. For CM1, after 39 evolutions, the main result is the electrification of the entire community, installing 4 DGs with a configuration with minimal power losses and investment costs.

To reach acceptable results some parameters must be tuned. For example, the constant weights  $w_a$  and  $w_b$  are the most difficult to establish because the balance of the system, between *efficiency* and *investment costs*, depends on these two values. In order to select these components, several simulations were carried out, concluding that  $f'_1$  must have more

weight than  $f'_2$ . Moreover, it is important to calibrate the penalty values  $w_1, w_2, w_3, w_4$  and  $w_5$  of equations (47), (48), (49), (55) and (56) for the proper delimitation of the search space, and to prevent the selection of unfeasible solutions within the evolutionary process. Therefore, it was found (by try and error) that satisfactory results can be obtained with  $w_a = 1$ ,  $w_b = 0.1$ ,  $w_1 = 300$ ,  $w_2 = 1500$  and  $w_{3,4,5} = 10000$ . Other established parameters are: GA population 70; the max-iteration number  $t_{GA}^{max} = 300$ ,  $t_{PSO}^{max} = 100$ ; crossover factor  $\delta = 0.5$ ; and mutation rate  $\varpi = 0.6$ .

Applying the aforementioned parameters, the most recurrent results for CM1 and CM2 - after 100 simulations- are summarized in Table 6.2, and the network design for CM2 is shown in Figure 6.4. From these results, we can notice that for each community the algorithm found well-balanced configurations since DGs' capacities were better used. This is verified by observing that the algorithm grouped as many users as possible to a DG until reaching the maximum voltage drop limit (5.5 %), see e.g. Figure 6.4, nodes  $G_4 - u_{12}$  and  $G_5 - u_2$ . In addition, we must note that the PSO located the DGs at nodes where power losses, voltage deviations, and quality issues may be reduced; e.g. see Figure 6.4 (a),  $G_1 - u_5$ ,  $G_5 - u_5$ . This is demonstrated in Table 6.3, where other DG locations (for  $G_5$ ) are evaluated.

Table 6.2. TS-MOEAP results for CM1 and CM2.

	CM1	CM2
Users	36	48
Best Fitness	9593	13089
Total Power Loss [kW]	1.83	3.53
Total Cost [\$]	95232	130050
DG units	4	5
Installed Capacity [kW]	60	85
Bat. Bank [Ah]	330	420
Max $\Delta V$ per node [%]	5.3	5.4
Total Evolutions	39	54
Iteration Time [24]	3	9

Table 6.3. Results for different DG placement in CM2- $G_5$ .

Node	Power Loss [kW]	Max $\Delta V$ [%]	Quality Issues
$u_3$	1.14	7.7	1
$u_4$	0.84	6.8	2
$u_5$	0.98	5.4	0
$u_7$	1.99	12.9	2

Finally, although the possible configurations can be millions, the GA-PSO algorithm could find satisfactory results analyzing only a few cases (e.g. 1400 for CM1), from which it took the best *genes* to create better designs. This is validated with the convergence curve shown in Figure 6.5.

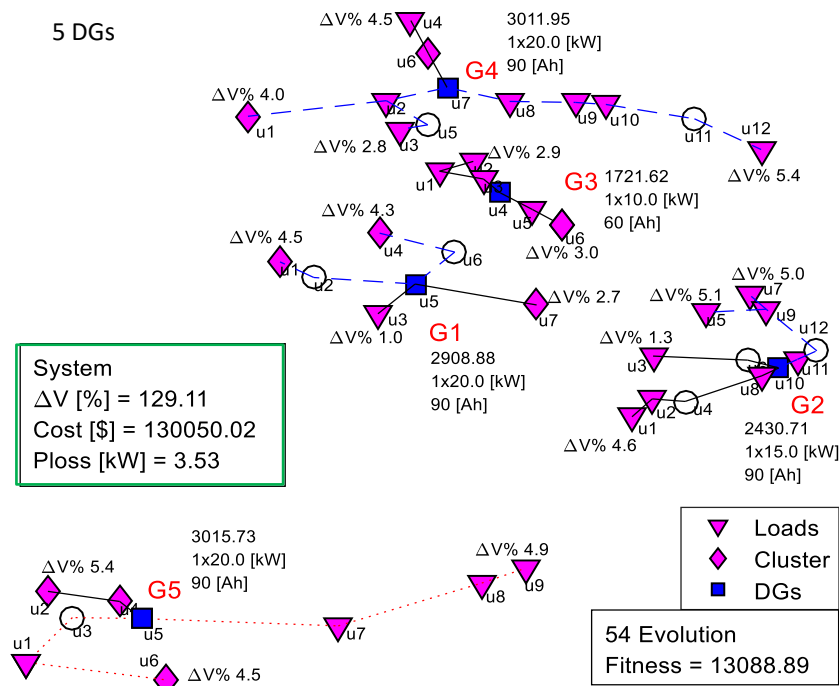


Figure 6.4. Optimal configuration for CM2 by TS-MOEAP.

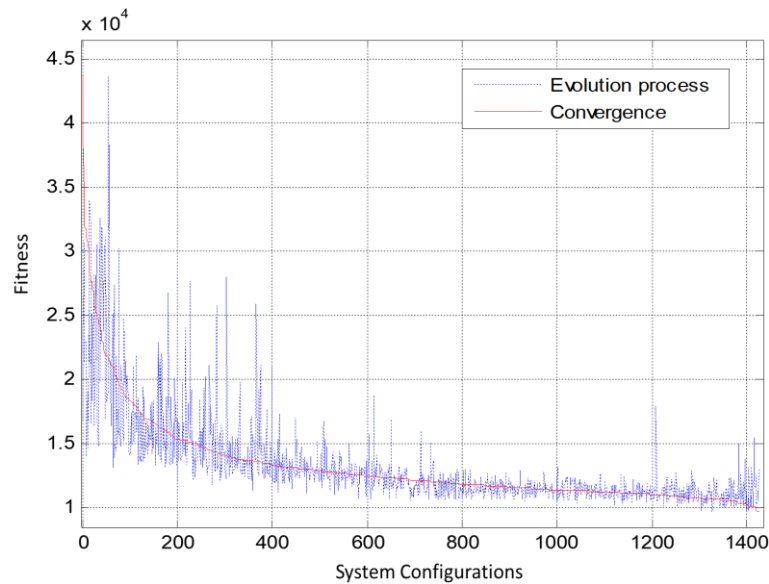


Figure 6.5. TS-MOEAP convergence curve.

### 6.1.3. TS-MOEAP versus Centralized/Decentralized Systems

In this scenario, we want to prove the effectiveness of the TS-MOEAP approach to finding a balanced design between costs and power losses. In order to do this, the number of DGs is increased and decreased by one (respect to the optimal result) to obtain a *centralized* and *decentralized* reference model. This was done by blocking the number of DGs that the algorithm can install. As we can see in Figure 6.6 (a) and Table 6.4, with one less DG the total cost of the system is reduced, but there are quality issues for some users, e.g. see Figure 6.6 (a) -  $G_4$ , nodes  $u_6$ ,  $u_{12}$ ,  $u_{14}$ . On the other hand, with an extra DG, the total power loss is reduced but the total cost is increased, as shown in Figure 6.6 (b). This demonstrates that the configurations found by the GA-PSO algorithm have the optimal number of DGs to minimize costs and satisfy the demand and power quality constraints.

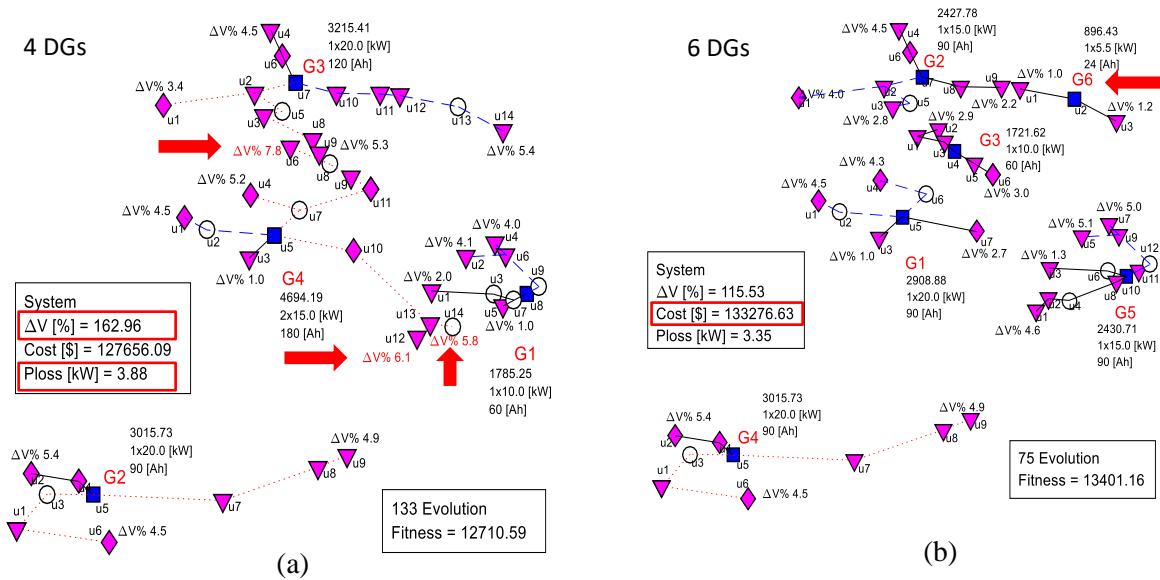


Figure 6.6. Non-optimal results for CM2 a) Centralized System. b) Decentralized System.

Table 6.4. TS-MOEAP vs centralized/decentralized models.

	CM1			CM2		
	Centralized	TS-MOEAP	Decentralized	Centralized	TS-MOEAP	Decentralized
DG units	3	4	5	4	5	6
Ploss [kW]	2.30	1.83	1.55	3.88	3.53	3.35
Total Cost [\$]	91759	95232	100157	127656	130050	133277
Quality Issues	4	0	0	3	0	0

#### 6.1.4. TS-MOEAP versus a Single Objective Model with Standard Operators

In this scenario, the importance of a multi-objective fitness function, and the need for improved variation operators are demonstrated. In order to do this,  $f'_2(c)$  is disabled to have a single objective fitness function, and a 2-point crossover along with a common swap mutation operator [42] is used.

The results are shown in Table 6.5, and as we can see, the single-objective model has resulted in minor power losses and higher costs than the optimal model. The reason is that the algorithm evenly distributed the users between the DGs, wasting installed capacity in the process. Furthermore, without the counterbalance of  $f'_2(c)$ , the algorithm tends to install a DG per user, therefore for the simulation, the number of DGs was pre-established in 4 and 5 for CM1 and CM2 respectively. On the other hand, the model with standard variation operators reports the worst results, being 20% more expensive and 25% more inefficient than the optimal model. This result is mainly due to the random changes of the loads from one group to another by the swap mutation operator. Therefore, we conclude that improved variation operators (specially the mutation one) are extremely necessary to achieve satisfactory results in this type of optimization problems.

Table 6.5. TS-MOEAP vs Single Objective/Standard Operators.

	Single Objective	TS-MOEAP	Std. Operators
<b>CM1</b>			
Ploss [kW]	1.81	1.83	2.20
Total Cost [\$]	106693	95232	113651
Installed Capacity [kW]	70	60	65
<b>CM2</b>			
Ploss [kW]	3.51	3.53	9.21
Total Cost [\$]	142656	130050	160483
Installed Capacity [kW]	95	85	85

The TS-MOEAP approach was successfully applied to design off-grid systems with distributed photovoltaic generation. Although the problem is multi-objective, the GA-PSO approach provided satisfactory configurations to feed all users with energy under power quality requirements. We can say that the results belong to a space of solutions that is bounded from above by a totally centralized system and from below by a totally decentralized one, where the desired balance between cost and efficiency is kept.

## 6.2. Optimal Condition Restoration of Secondary Distribution Networks

Since the secondary side of distribution networks (low voltage distribution lines) is continuously subject to changes through time due to the increase of load demand, its optimal operation falls inevitably in degradation. Consequently, in order to avoid repercussions such as faults, congestions and other issues that are detrimental to energy quality, we are prompted to redesign the network. To do so, we can implement TS-MOEAP, which is able to solve this kind of problems.

As explained before, the approach is composed of two stages due to the complexity to redesign an entire network, therefore the optimization process is divided as follows: 1) optimal placement and sizing of distribution transformers (DTs), as well as conductor sizing and branch routing, and 2) optimal network reconfiguration (NR). For the first stage the improved particle swarm optimization technique (IPSO) -explained in section 4.2- will be used, and for the second stage the improved nondominated sorting genetic algorithm with a heuristic mutation operator (INSGA-HO) -explained in section 5.2- will be implemented. TS-MOEAP is able to find a new network configuration where all the quality issues are solved, taking as main objectives the minimization of power loss and total investment cost of the system.

### 6.2.1. Background of the Problem

In the last few years, Ecuador has built several hydroelectric plants causing an excess of generation capacity. Due to this particularity, the government is motivating residential users to change gas stoves by induction stoves. The new electric loads, with an average power of 4 kW, have caused an increment of demand of almost twice, as shown in Figure 6.7. Here we can see three defined peaks due to the use of the induction stove. The current LVDNs are not prepared to support this increased demand; therefore, an optimal planning to reconfigure them is needed.

In order to prove the effectiveness of TS-MOEAP two real SDNs -with critical quality issues and technical problems- are considered to be improved, to then compare results with other algorithms. The case studies -denoted as LVDN1 and LVDN2- were obtained from an urban area as shown in Appendix B, and these present different characteristics such as topology, installed capacity, number of users, load demand, and quality issues. The data, which can be found in [50], is shared by the utility company E.E.R.C.S in collaboration with the Ecuadorian government.

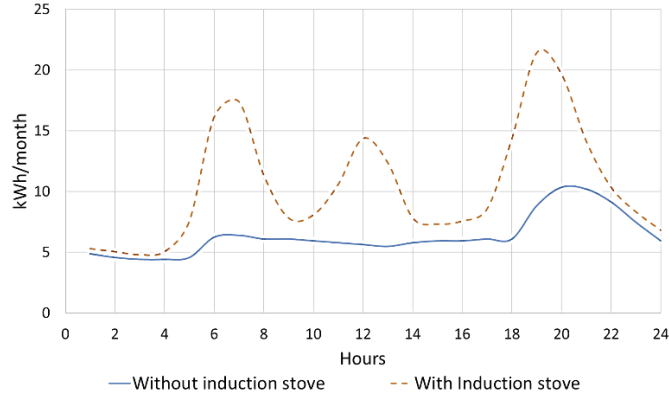


Figure 6.7. Demand profile of a residential user.

### 6.2.2. Case Study LVDN1

The LVDN considered for this case study is shown in Figure 6.8 and has the following characteristics: 3-phase system, primary voltage of 22 kV, secondary voltage of 220/127 V, 400 residential users, 88 utility poles, and 6 DTs with an installed capacity of 335 kVA. Active and reactive loads, at each utility pole, are shown in Appendix C.

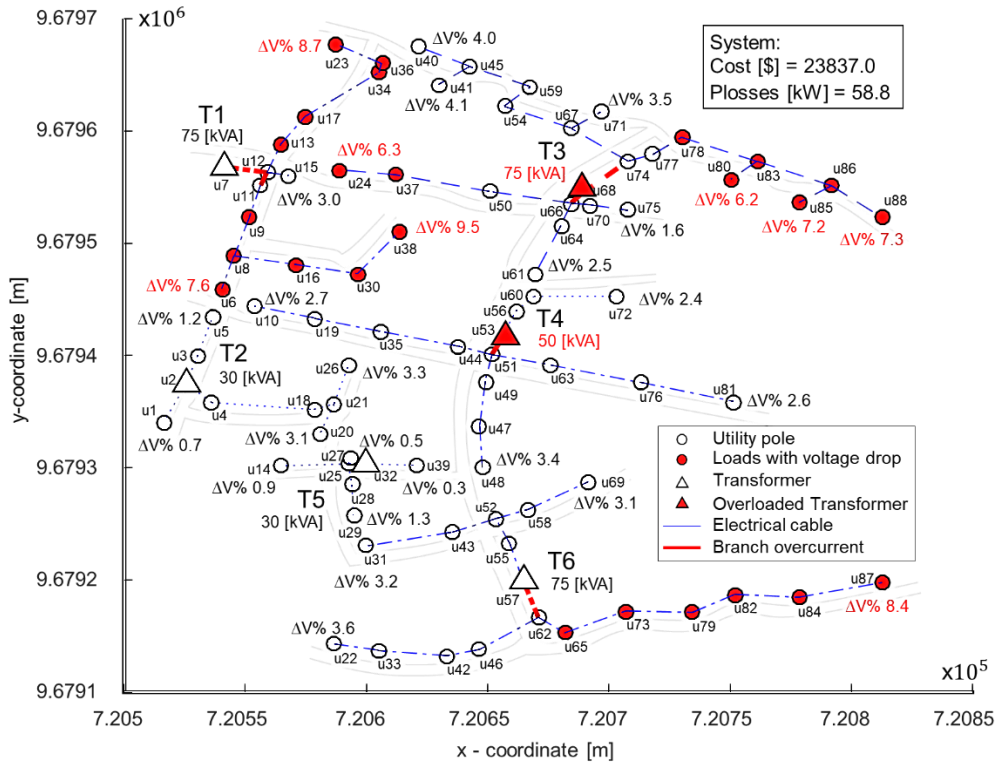


Figure 6.8. Test system LVDN1.



The problems that affect the system are also shown in Figure 6.8 and summarized in Table 6.6, accounting for a total of 33 quality issues, including nodes with low voltage magnitude, branches with overcurrent, and overloaded transformers. The system has a total power loss of 58.8 kW with a total investment cost of \$ 23837, reference values that must be minimized.

Table 6.6. Quality issues of the test system LVDN1.

	Qty.	Specification
Overloaded DTs	2	$T3, T4$
Nodes with a low voltage magnitude	25	$u_6, u_8, u_9, u_{13}, u_{16}, u_{17}, u_{23}, u_{24}, u_{30}, u_{34},$ $u_{36} - u_{38}, u_{65}, u_{73}, u_{78} - u_{88}$
Branches with overcurrent	6	$U_{7,12}, U_{11,12}, U_{51,53}, U_{57,62}, U_{66,68}, U_{68,74}$

The main input data for the algorithm are:

- GPS coordinates, and loads per utility pole, see Figure 6.8 and Appendix B,
- Geographical and technical constraints, see Table 6.7,
- Available main equipment and their average costs, see Table 3.2 and Table 3.3.
- Projected unit demand  $P_{UD} = 1.36$  kVA and overload factor  $\xi = 0.8$ ,
- Iteration limits for the IPSO and NSGA-HO, 100 and 200 respectively,
- Penalty factors  $w_{1,2,3} = 1000$ , and  $w_4 = 300$ ,
- NSGA-HO mutation rate  $\varpi = 0.8$ , crossover rate  $\delta = 0.5$ , and population size 100,
- IPSO factors  $\gamma = 0.4$ ,  $\alpha = 1$ ,  $\beta = 2$  and  $\mathcal{O} = 0.3$ .

Table 6.7. Geographical and technical constraints of LVDN1.

	Constraints
Restricted branches	$U_{1,4}, U_{18,20}, U_{37,38}, U_{59,71}, U_{80,85}$
Restricted utility poles for transformers	$u_8, u_{30}, u_{39}, u_{52}, u_{60}, u_{79}$
Conductor ampacity for ACSR 3/0 AWG	315 A
Voltage magnitude limits	$\pm 4.5$ %
Maximum available transformer capacity	100 kVA

### 6.2.3. Results for LVDN1

Applying TS-MOEAP to solve the test system, the following result is the best obtained after 100 simulations. Figure 6.9 shows a random LVDN when the optimization process starts, and Figure 6.10 shows an optimal LVDN when the optimization process ends.

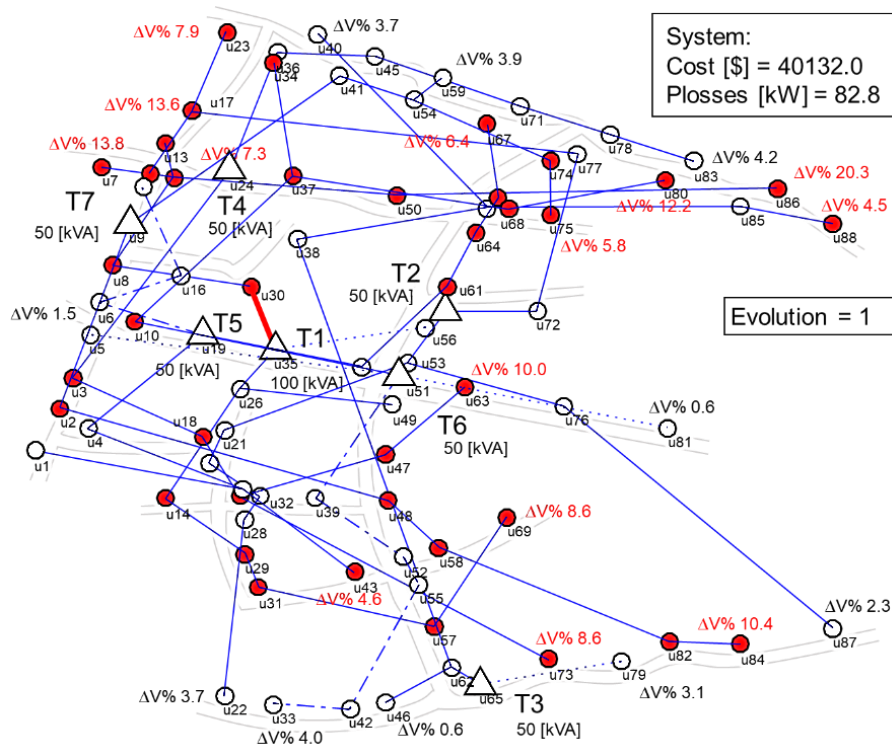


Figure 6.9. Random configuration from the first generation.

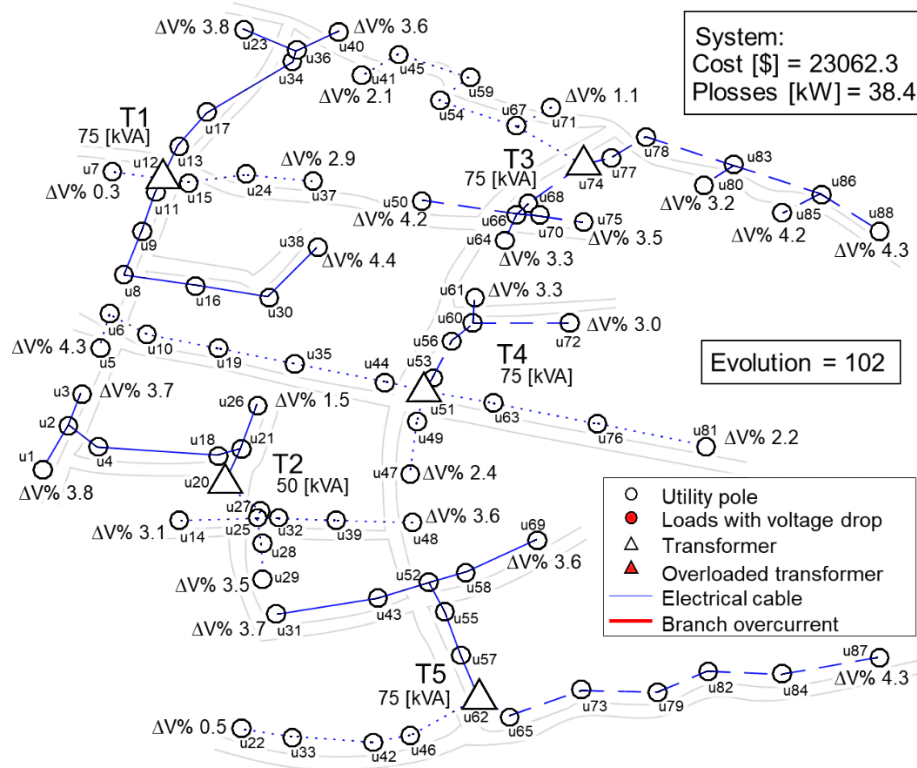


Figure 6.10. Best result for LVDN1 found by TS-MOEAP.

In the first generations, the configurations have poor quality because the initial population is generated at random, but as this population evolves better results are found. As we can see in Figure 6.10, TS-MOEAP converges to a solution where all the quality issues are solved, minimizing power losses and investment costs, therefore we can say that the optimal condition of this distribution network is restored.

Figure 6.11 (a) shows a comparison between voltage magnitudes (in descending order), before and after the optimization. Voltage drop is the most common problem in SDNs, however, TS-MOEAP found a network configuration where voltage magnitudes are above the limit. Figure 6.11 (b), shows branch currents for both, the original and the optimized system. As we can see, the original system exceeds the ampacity limit, even when the thickest conductor (3/0 AWG) has been used. In contrast, the optimized system corrected this problem and still has room to add more loads. Similarly, Figure 6.11 (c) shows a comparison between branch power losses. The optimized system has less power loss per branch even when it has one transformer less. This is possible thanks to the optimal network reconfiguration.

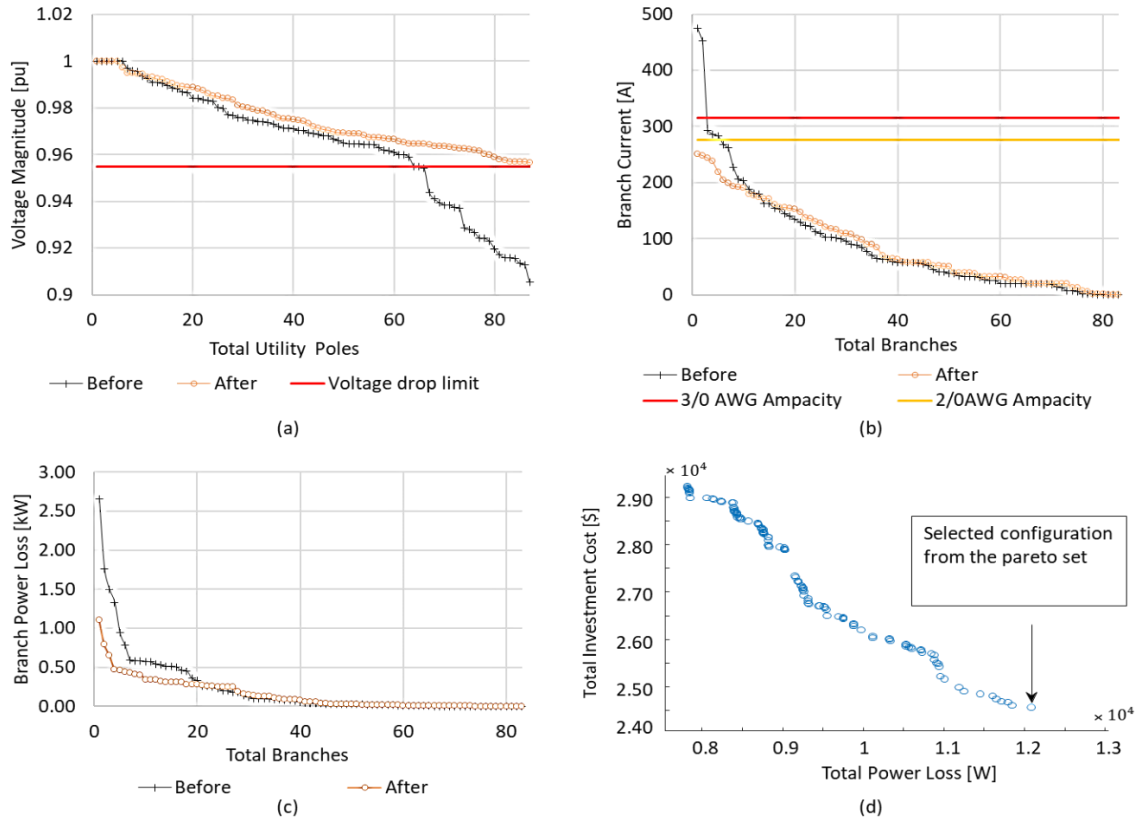


Figure 6.11. Different results before and after the optimization for LVDN1. a) Magnitude of voltages. b) Magnitude of currents. c) Branch power losses. d) Pareto front obtained by TS-MOEAP.

TS-MOEAP can find several nondominated configurations that will form a pareto set, from which the most economical is chosen, as shown in Figure 6.11 (d). A summary of results, before and after the optimization, is shown in Table 6.8, where voltage deviation ( $VD$ ) and installed capacity ( $IC$ ) are defined as follows

$$VD = \sum_{i=1}^{\mu} |V^{ref} - V_i| / V^{ref} \quad (63)$$

$$IC = \sum_{i=1}^{\tau} S_{T_i}. \quad (64)$$

$V^{ref}$  is the reference voltage of the SDN,  $V_i$  is the voltage at each node, and  $S_{T_i}$  is the capacity of each transformer. We should note that the optimized system obtained a lower investment cost than the original one. This is quite impressive, considering that to solve all quality issues the network usually must be oversized; therefore, investment costs also increase.

Table 6.8. Results for the test system LVDN1, before and after the optimization.

	Before	After	Difference
Total investment cost [\$]	23837	23062	-3.3 %
Total power loss [kW]	19.6	12.8	-34.7 %
Voltage deviation [p.u.]	1.45	0.99	-31.7 %
Installed capacity [kVA]	335	350	+4.3
Max. $\Delta V$ per node [%]	9.5	4.4	--
Total transformers	6	5	--
Quality Issues	33	0	--

#### 6.2.4. Comparison with other approaches

To validate the performance of TS-MOEAP, a comparison is made against the algorithms: NSGA-II, a multiobjective evolutionary algorithm based on decomposition (MOEA/D), a conventional GA and an analytic method (ANMT), for the Stage-2; and a traditional PSO for the Stage-1. The analytical method represents a procedure used by the utility company to make corrective maintenance as follows:

- i. For each  $T_k$  network with voltage drop problems, try to relocate the transformer, if the problems persist, increase the conductor size.
- ii. For each  $T_k$  network with branch overcurrents, try to relocate the transformer, if the problems persist, increase the conductor size.

- iii. If i. and ii. do not fix up voltage drops and overcurrents, split the network on the branch with the highest current.
- iv. If a transformer is overloaded, select a transformer with greater capacity. If the maximum available transformer is installed and the problem persists, split the network on the branch with the highest current.

To test the effectiveness of the IPSO and the heuristic mutation operator (see sections 4.2 and 5.2.4) both will be implemented for the GA and MOEA/D to compare results against their basic models. For the GA, the multi-objective problem is transformed into a single-objective problem using the equation (62) with  $w_a = 10$  and  $w_b = 0.08$ . Finally, the input data for these algorithms are the same as explained in section 6.2.2, and the parameters of MOEA/D are Tchebycheff decomposition, maximum iterations 100, population size 200, and the number of weight vectors 15.

As shown in Figure 6.12, the combination of the INSGA-HO and IPSO (proposed for TS-MOEAP) found the most economical configuration, amending all the problems despite an acceptable increase in power losses (the lower the better). On the other hand, ANMT which does not implement optimal NR, nor optimal DTs placement, has the highest investment cost. Furthermore, we must note that the GA-HO and MOEA/D-HO found better configurations than their basic models, thanks to the implementation of the heuristic mutation and the IPSO. Additionally, the GA-HO obtained better results than the NSGA-II even though the first one is using scalarization for the objective function.

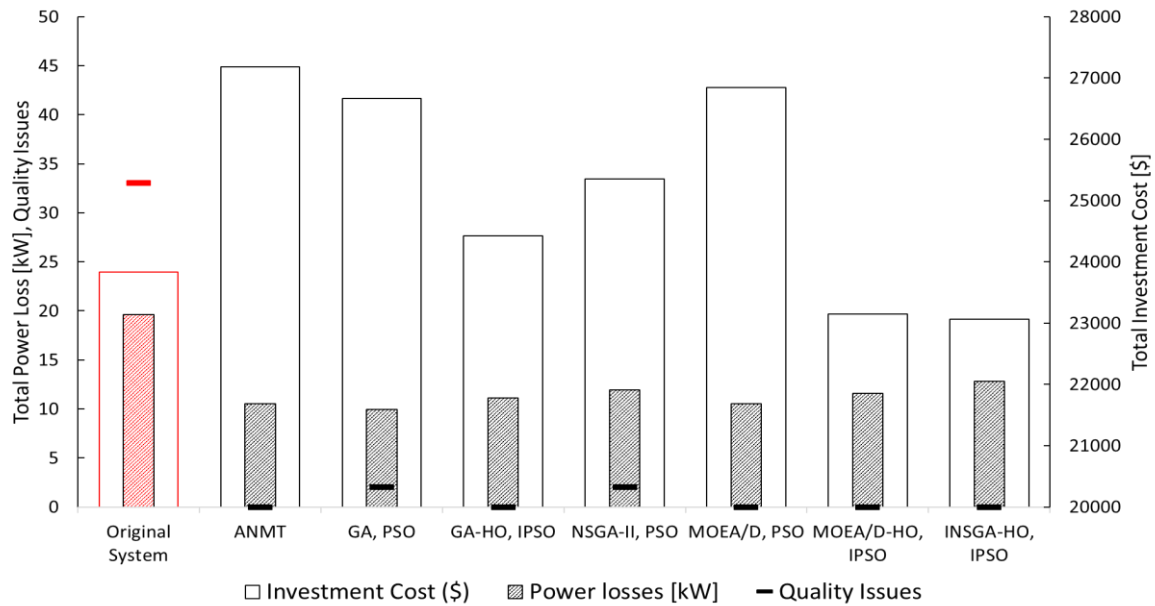


Figure 6.12. Algorithm comparisons for total investment cost, power loss, and quality issues.

With respect to MOEA/D, we found that this algorithm tends to install a greater number of transformers than other approaches. This causes an increase in the total investment cost as shown in Figure 6.12. After an analysis, we conclude that due to the discrete nature of the problem the solutions to neighboring subproblems are not very close in the decision space, causing a lack of ability to explore new areas, and therefore a lack of dominant solutions. This can be verified by observing the pareto front of MOEA/D and INSGA-HO in Figure 6.13. However, if the limits for the number of transformers to install is narrowed (e.g.  $\tau = 5:6$ ) and the heuristic mutation along with the IPSO are implemented, results as good as those of INSGA-HO can be found, with the advantage of less computational time.

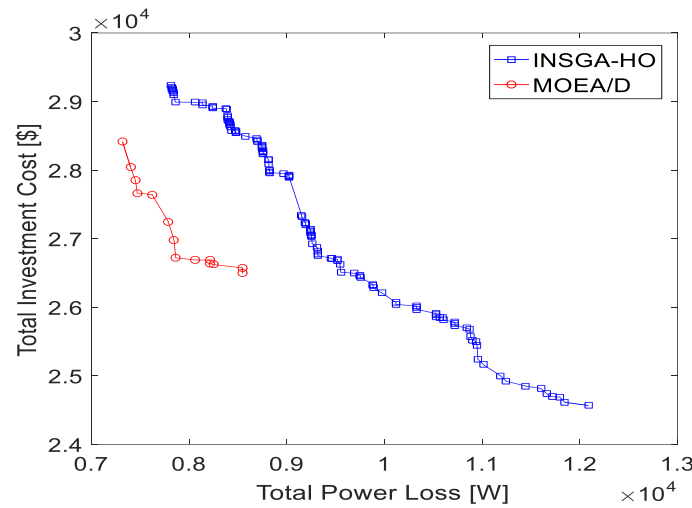


Figure 6.13. Pareto fronts of MOEA/D and INSGA-HO for the test system LVDN1.

Finally, Table 6.9 shows a comparison of different indexes. The most important is the ratio between total cost and installed capacity. This parameter shows us the algorithm's ability to find a cheap configuration which can feed all users under strict quality parameters. TS-MOEAP got the best value (65.9 \$/kVA) among the compared algorithms, proving that it can search and converge towards better configurations. Furthermore, we have the installed capacity and the index of oversizing, which are used to prove how well the loads are distributed among transformers. TS-MOEAP found a configuration that only needs an installed capacity of 350 kVA, that represents an oversizing of 10.4 % with respect to an average load of 317 kVA. As before, ANMT got the worst results, with an oversizing of 29.3 %. The algorithms that implemented the proposed heuristic mutation operator got better results in general. In summary, the aforementioned results provide evidence that TS-MOEAP can obtain better configurations using the proposed INSGA-HO and IPSO algorithms.

Table 6.9. Algorithm comparisons for LVDN1.

	ANMT	GA	GA-HO	NSGAI	MOEA/D	MOEA/D-HO	NSGA-HO
Investment cost [\$]	27185	26670	24421	25351	26844	23145	23062
Power loss [kW]	31.5	29.7	33.3	35.7	31.5	34.8	38.4
Voltage deviation [pu]	0.85	0.83	0.81	0.91	0.79	0.90	0.99
Total transformers	7	6	6	6	8	6	5
Installed cap. [kVA]	410	385	360	365	385	325	350
Oversizing [%]	29.3	21.5	13.6	15.1	21.4	2.5	10.4
Cost/Inst. cap. [\$/kVA]	66.3	69.3	67.8	69.5	69.7	71.2	65.9

### 6.2.5. Case Study LVDN2

The LVDN considered for the second case study is shown in Figure 6.14 and has the following characteristics: 3-phase system, primary voltage of 22 kV, secondary voltage of 220/127 V, 563 residential users, 58 utility poles, and 4 distribution transformers with an installed capacity of 375 kVA.

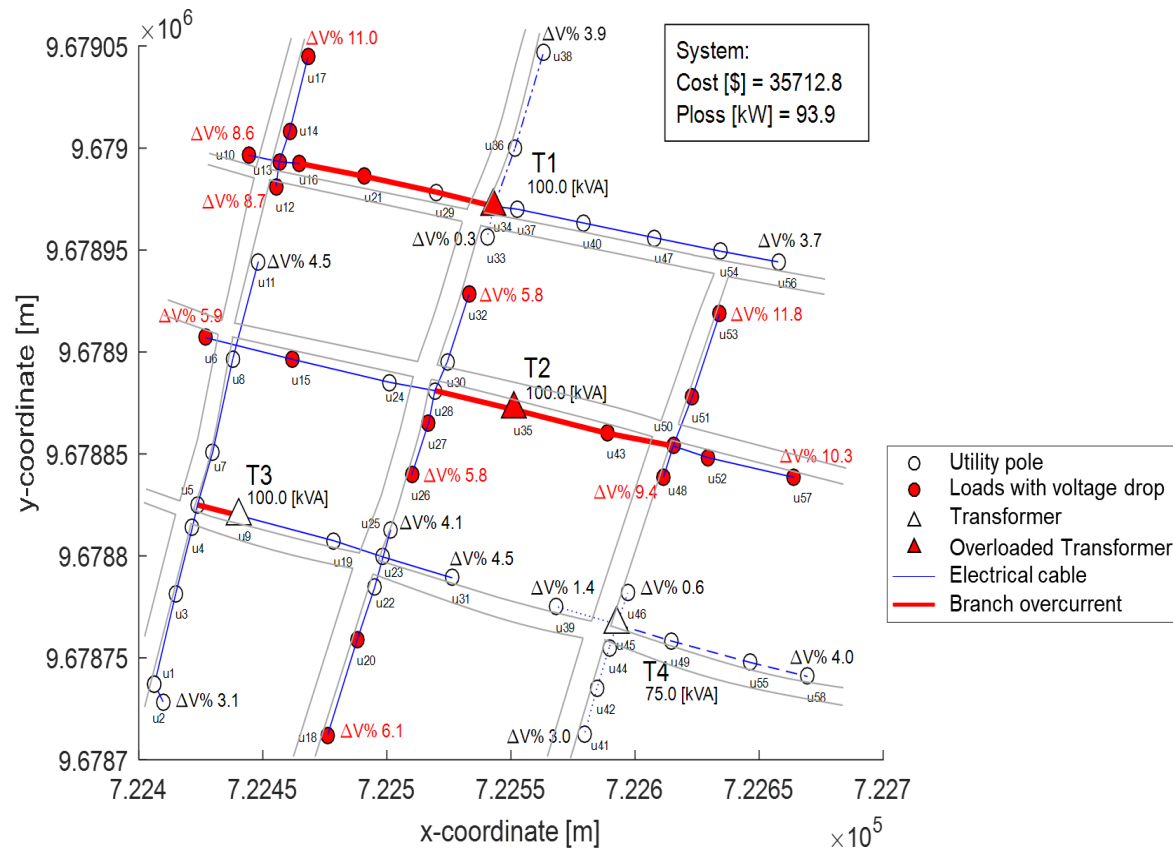


Figure 6.14. Test system LVDN2.

The problems that affect the system are shown in Figure 6.14 and summarized in Table 6.10, accounting for a total of 30 quality issues. The system has a total power loss of 93.9 kW with a total investment cost of \$ 35712.8, reference values that must be minimized.

The input data is similar to the LVDN1 case, changing only the GPS coordinates, the loads per utility pole, and the geographical constraints (see Table 6.11).

Table 6.10. Quality issues of the test system LVDN2.

	Qty.	Specification
Overloaded DTs	2	$T1, T2$
Nodes with a low voltage magnitude	21	$u_6, u_{10}, u_{12} - u_{18}, u_{20}, u_{21}, u_{26}, u_{27}, u_{32}, u_{34}, u_{35}, u_{38}, u_{43}, u_{48}, u_{50} - u_{53}, u_{57}$
Branches with overcurrent	7	$U_{5,9}, U_{16,21}, U_{21,29}, U_{29,34}, U_{28,35}, U_{35,43}, U_{43,50}$

Table 6.11. Geographical and technical constraints of LVDN2.

	Constraints
Restricted branches	$U_{4,9}, U_{10,12}, U_{2,18}, U_{25,31}$
Restricted utility poles for transformers	$u_5, u_{23}, u_{30}, u_{54}$
Conductor ampacity for ACSR 3/0 AWG	315 A
Voltage magnitude limits	$\pm 4.5 \%$
Maximum available transformer capacity	100 kVA

#### 6.2.6. Results for LVDN2

Figure 6.15 shows the cheapest configuration found by TS-MOEAP, which can solve all the quality issues presented in the test case. As illustrated in Figure 6.16, the new configuration is 36 % cheaper and has 50 % fewer power losses than the original design. In this particular case, the algorithm decided to install two new transformers to supply all the demand and regrouped the users in a different way. We should also note that the algorithm selected the most economic conductor for each branch, respecting voltage and current constraints.

To facilitate the analysis of the new network, the algorithm has been designed to display all the relevant information of each group. For example, for the transformer T4 of Figure 6.15, we get the results of Table 6.12. Here we can observe -in detail- which are the branches of the network with their distances and nodes; the number of users and lamps; the apparent power at each node; the size of the conductor with the impedance of each branch; the voltage at each node with its respective voltage drop; and the current through each line.



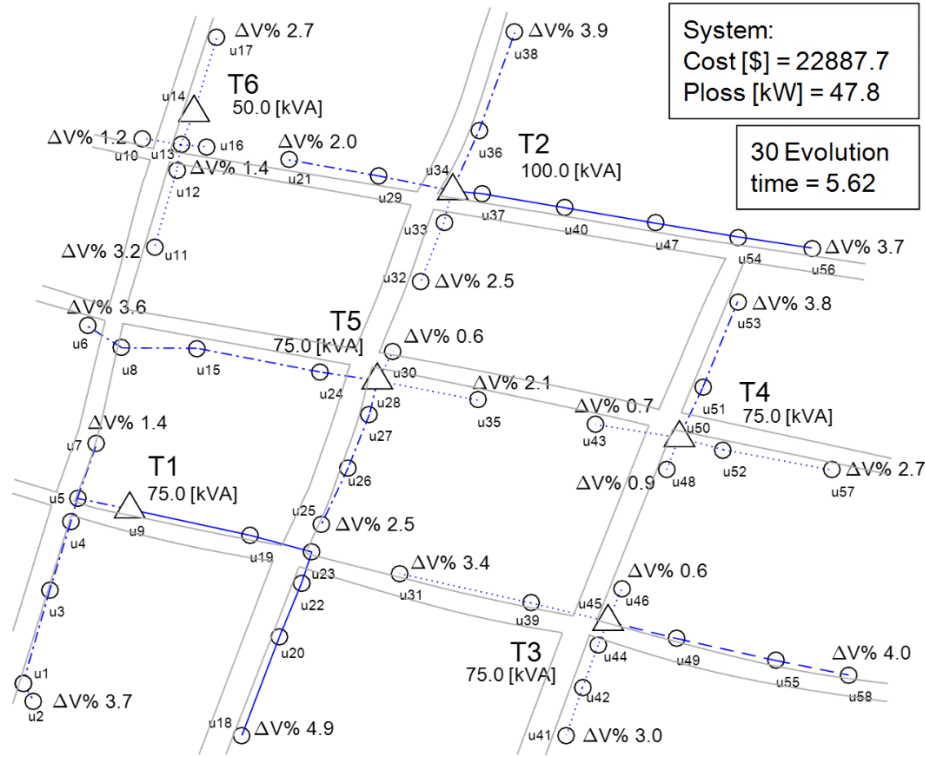


Figure 6.15. Best result for LVDN2 found by TS-MOEAP.

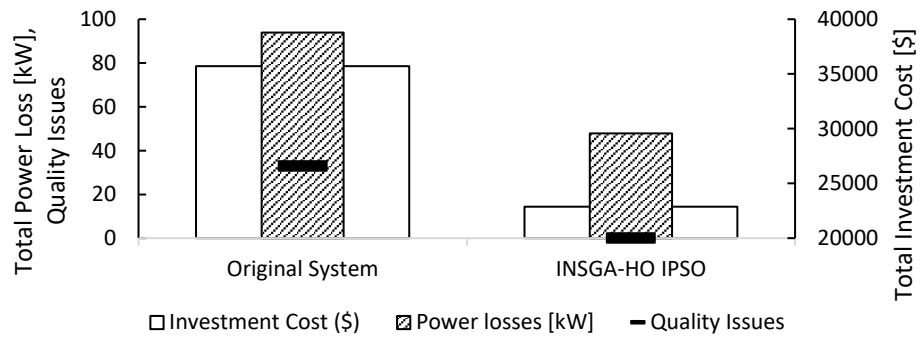


Figure 6.16. Results for LVDN2, before and after the optimization.

Table 6.12. Results for the network T4.

Br	Bi	Bj	D	Us	Lp	Cond	S	ZL	YL	VBus	VD	I <sub>max</sub>
			[m]			[AWG]	[kVA]	[ohm]	[s]	[V]	[%]	[A]
1	50	48	15	19	1	2	25.84	0.016 +0.006i	54.59 -21.11i	218.0 < 0.10°	0.91	118.9
2	50	43	27	8	1	2	10.88	0.028 +0.011i	31.49 -12.18i	218.5 < 0.07°	0.66	50.2
3	50	51	25	16	1	1/0	21.76	0.016 +0.009i	46.94 -26.04i	215.7 < 0.05°	1.94	229.8
4	51	53	42	20	1	1/0	27.20	0.027 +0.015i	28.01 -15.54i	211.7 < 0.10°	3.77	128.8
5	50	52	15	8	1	2	10.88	0.015 +0.006i	56.24 -21.74i	217.6 < 0.11°	1.08	146.1
6	52	57	35	15	1	2	20.40	0.036 +0.014i	4.1 -9.32i	213.9 < 0.29°	2.74	95.7

If we compare the results of Table 6.12 against the results of Table 6.13 (transformer T2, before the optimization) we found that indeed the algorithm solved all the quality issues listed in the Table 6.10.

Table 6.13. State information for network T2 before the optimization.

Br	Bi	Bj	D [m]	Us	Lp	Cond [AWG]	S [kVA]	ZL [ohm]	YL [s]	VBus [V]	VD [%]	I <sub>max</sub> [A]
1	35	43	39	8	1	3/0	10.88	0.016 +0.013i	36.91 -31.75i	208.0 < -0.47°	5.45	590.2
2	43	50	27	0	0	3/0	0	0.011 +0.009i	53.05 -45.63i	200.4 < -0.80°	8.90	537.8
3	50	51	25	16	1	3/0	21.76	0.010 +0.009i	57.60 -49.55i	197.2 < -0.95°	10.40	251.1
4	51	53	42	20	1	3/0	27.20	0.017 +0.014i	34.37 -29.56i	194.1 < -1.09°	11.78	140.6
5	50	52	15	8	1	3/0	10.88	0.006 +0.005i	94.74 -81.49i	199.2 < -0.86°	9.47	158.6
6	52	57	35	15	1	3/0	20.40	0.014 +0.012i	40.59 -34.92i	197.2 < -0.95°	10.34	103.9
7	50	48	16	19	1	3/0	25.84	0.006 +0.005i	91.96 -79.11i	199.35 < -0.85°	9.39	130.0

Figure 6.17 shows a comparison of voltage magnitudes, branch currents, and branch power losses, before and after the optimization. In general, TS-MOEAP improved each of these fields without exceeding established limits. Finally, Figure 6.18 shows the entire set of possible solutions found by TS-MOEAP before converging to the pareto front shown in Figure 6.17 (d).

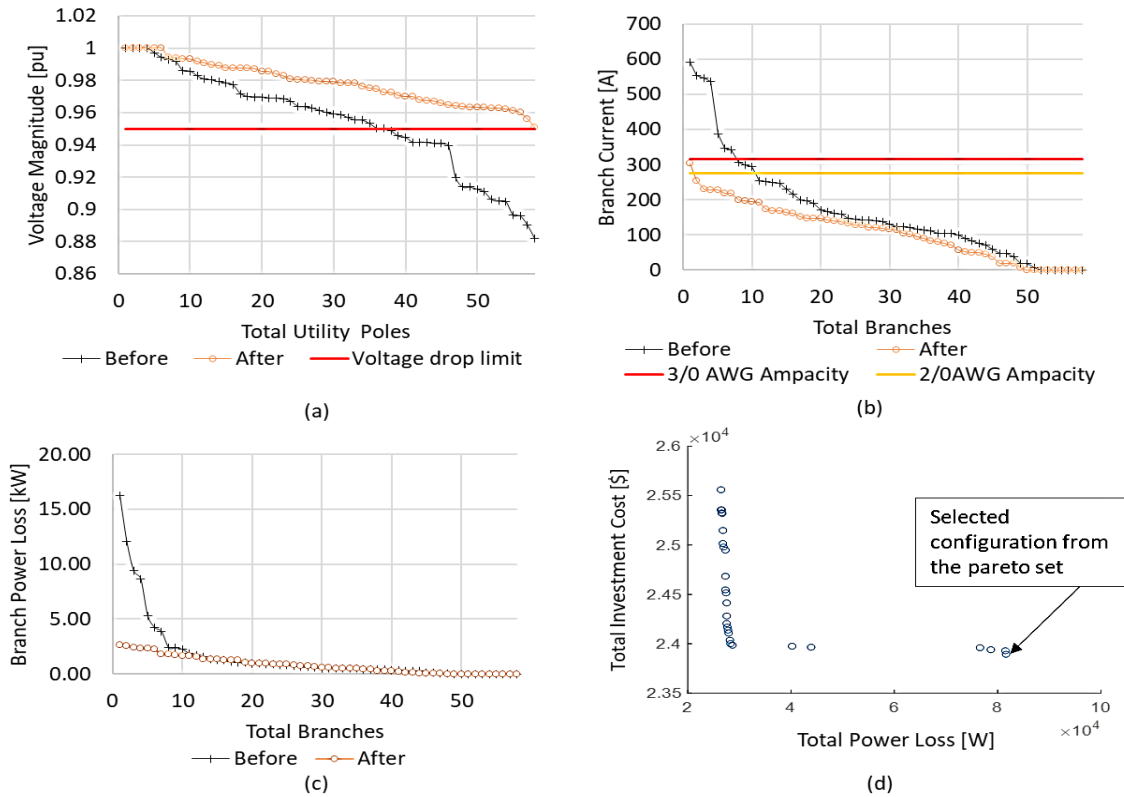


Figure 6.17. Different results before and after the optimization for LVDN2. a) Magnitude of voltages. b) Magnitude of currents. c) Branch power losses. d) Pareto front obtained by TS-MOEAP.

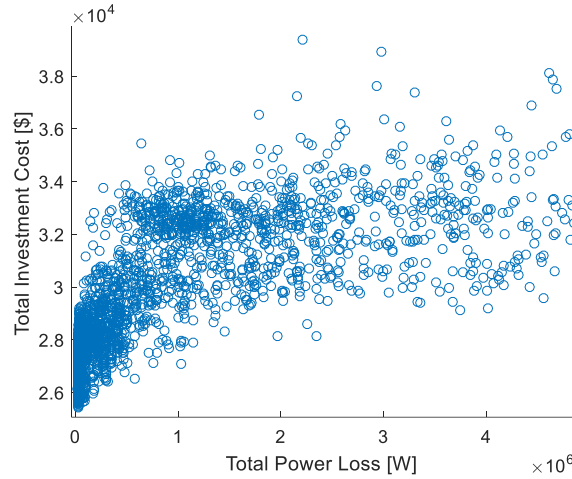


Figure 6.18. Entire set of possible solutions found by TS-MOEAP.

### 6.3. Optimal Reconfiguration of Primary Distribution Networks

The optimal reconfiguration of primary lines can improve the power system from different aspects such as power loss reduction, voltage profile enhancement, load balance improvement, and so forth. The regular process of reconfiguration is implemented by closing some tie switches (normally open switch) and opening some sectionalizing switches (normally closed switches) such that the network constraints are preserved, and the main targets are achieved at the same time.

Power losses minimization in distribution systems has become one of the most important challenges in this area, attracting a lot of attention to implementing different optimization techniques. The most effective strategy to decrease power losses in distribution systems is network reconfiguration that was introduced by Merlin and Back in 1975. The reconfiguration of the distribution network is the process of altering feeder topological structure without losing the radial topology or violating branch loading and voltage limits. Because of the huge number of switching combinations, as the candidates of the optimal configuration, network reconfiguration is known as a combinatorial, nonlinear, non-differentiable constrained optimization problem.

In our case, TS-MOEAP will be implemented to perform the optimal reconfiguration of primary distribution lines by changing the topology of groups (loads connected to different feeders) instead of opening or closing switches. This strategy allows us to use the same algorithm to optimize secondary networks in which switches are not implemented. Unlike low

voltage systems, in primary networks, the position of the feeder does not change therefore TS-MOEAP only implements the Stage-2 for the optimization (please see section 5.2).

### 6.3.1. Case Studies

Now, TS-MOEAP will be implemented to reconfigure the primary lines of the test systems LVDN1 and LVDN2 optimized in the previous sections. The primary networks to be reconfigured are denoted as MVDN1 and MVDN2 and have the following characteristics: 3-phase system, nominal voltage of 22 kV, 1 or 2 existing feeders, and maximum voltage drop limit of 3.5 %. The original diagrams of the test systems MVDN1 and MVDN2 are shown in Figure 6.19 and Figure 6.20 respectively. We should note that the reconfiguration will be done with the main objective of minimizing power losses and to support the new secondary networks of Figure 6.10 and Figure 6.15.

In general, the input data for the algorithm will be the same GPS coordinates as for LVDN1 and LVDN2, the location and size of the transformers, the number and location of the feeders, and the same geographical constraints shown in Tables Table 6.7 and Table 6.11.

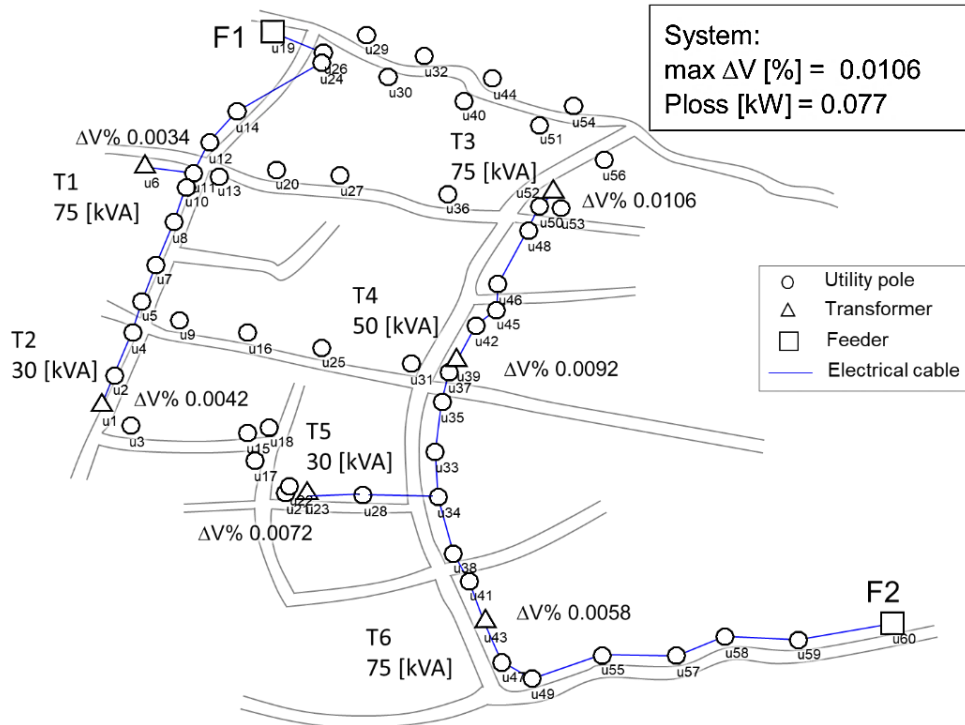


Figure 6.19. Test system MVDN1.

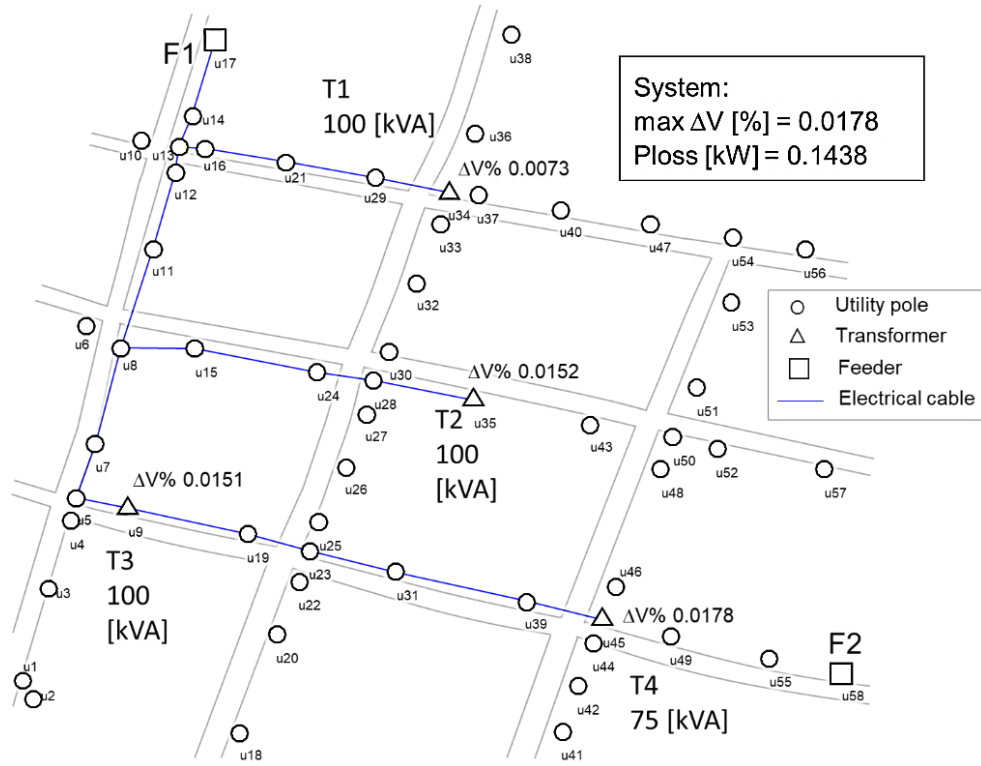


Figure 6.20. Test system MVDN2.

### 6.3.2. Results for MVDN1

For MVDN1 the feeders are located at nodes  $u_{19}$  and  $u_{60}$ , as shown in Figure 6.19, and the distribution transformers are located at nodes  $u_{12}$ ,  $u_{20}$ ,  $u_{51}$ ,  $u_{62}$ , and  $u_{74}$  as shown in Figure 6.10. Applying TS-MOEAP for the reconfiguration of this network, we obtain the model shown in Figure 6.21, and for illustrative purposes, Figure 6.22 shows how the network evolves until reach an optimal topology.

In this case, TS-MOEAP distributed three transformers to feeder F1, and two transformers to feeder F2, choosing the shortest path to interconnect them to each feeder. The new design of the primary network allows a better balance of loads, lower voltage drops, and lower power losses than the original system, supporting at the same time the new topology of LVDN1. A comparison of results before and after the optimization are shown in Table 6.14.

Table 6.14. Results for MVDN1, before and after the optimization.

	Feeder 1 [kVA]	Feeder 2 [kVA]	Ploss [kW]	$\Delta V [\%]$
Before	105	230	0.077	0.0106
After	200	150	0.042	0.0076

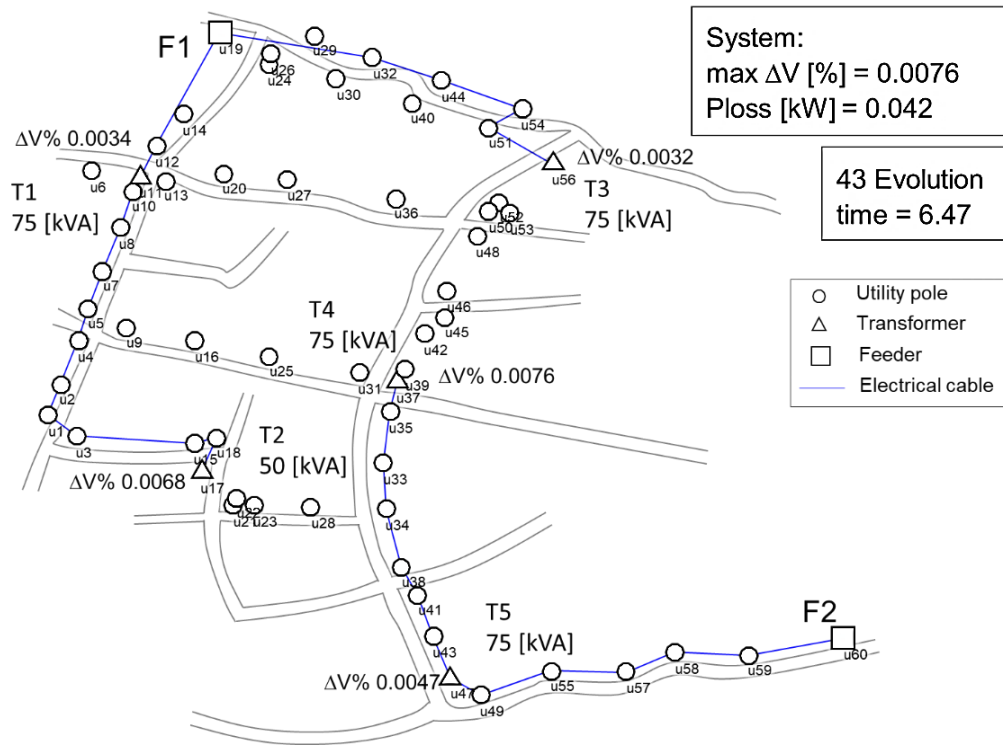


Figure 6.21. Best result for MVDN1 found by TS-MOEA.

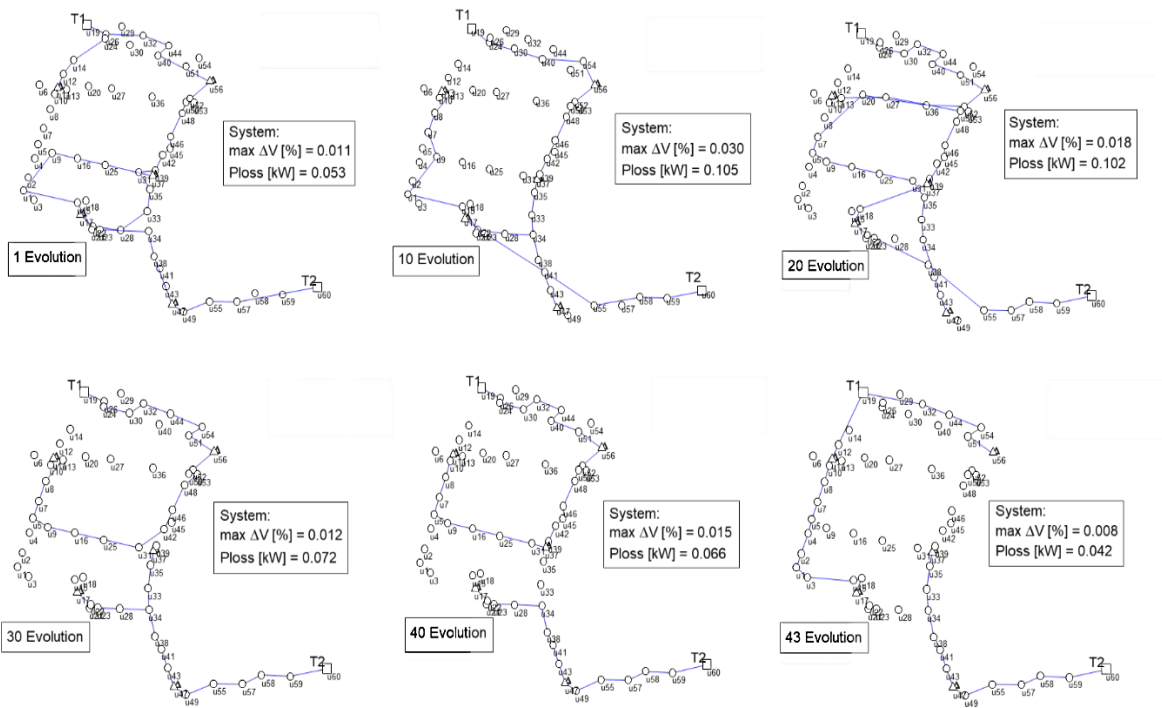


Figure 6.22. Evolutionary process for the reconfiguration of MVDN1.

Finally, Figure 6.23 shows the pareto front of MVDN1 obtained by TS-MOEAP, which presents an irregular shape due to the complexity and discrete characteristic of the combinatorial problem. We must note that from the pareto front the configuration with less power loss is selected, contrary to the optimization of secondary networks where the most economical configuration is preferred.

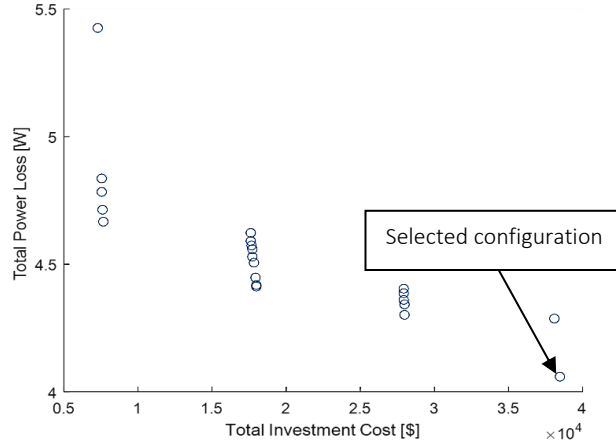


Figure 6.23. Pareto front of MVDN1 obtained by TS-MOEAP.

### 6.3.3. Results for MVDN2

For MVDN2 the feeders are located at nodes  $u_{17}$  and  $u_{58}$ , as shown in Figure 6.20, and the DTs are located at nodes  $u_9$ ,  $u_{14}$ ,  $u_{28}$ ,  $u_{34}$ ,  $u_{45}$  and  $u_{50}$  as shown in Figure 6.15. Applying TS-MOEAP we obtain the model shown in Figure 6.21, which is the best configuration to minimize power losses and to support the new network topology of LVDN2.

In this particular case, TS-MOEAP proposes a configuration using both feeders, F1 and F2, instead of one as in the original network. This causes a significant reduction in power losses, a better voltage profile, and a better balance of loads, as summarized in Table 6.15.

Finally, to verify these results a power flow analysis was performed using ETAP, for the original and optimized network. The simulation got similar results (bus voltages and power losses) to those of TS-MOEAP, which can be seen in Figure 6.25.

Table 6.15. Results for MVDN2, before and after the optimization.

	Feeder 1 [kVA]	Feeder 2 [kVA]	Ploss [kW]	$\Delta V$ [%]
Before	375	0	0.1438	0.0178
After	175	225	0.0596	0.0069

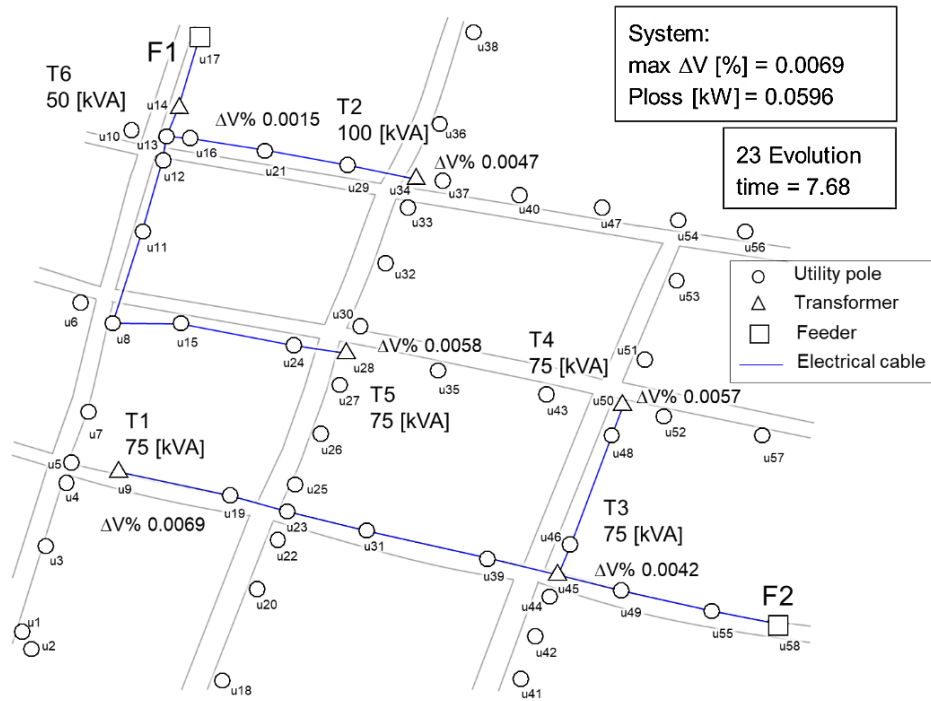


Figure 6.24. Best result for MVDN2 found by TS-MOEAP.

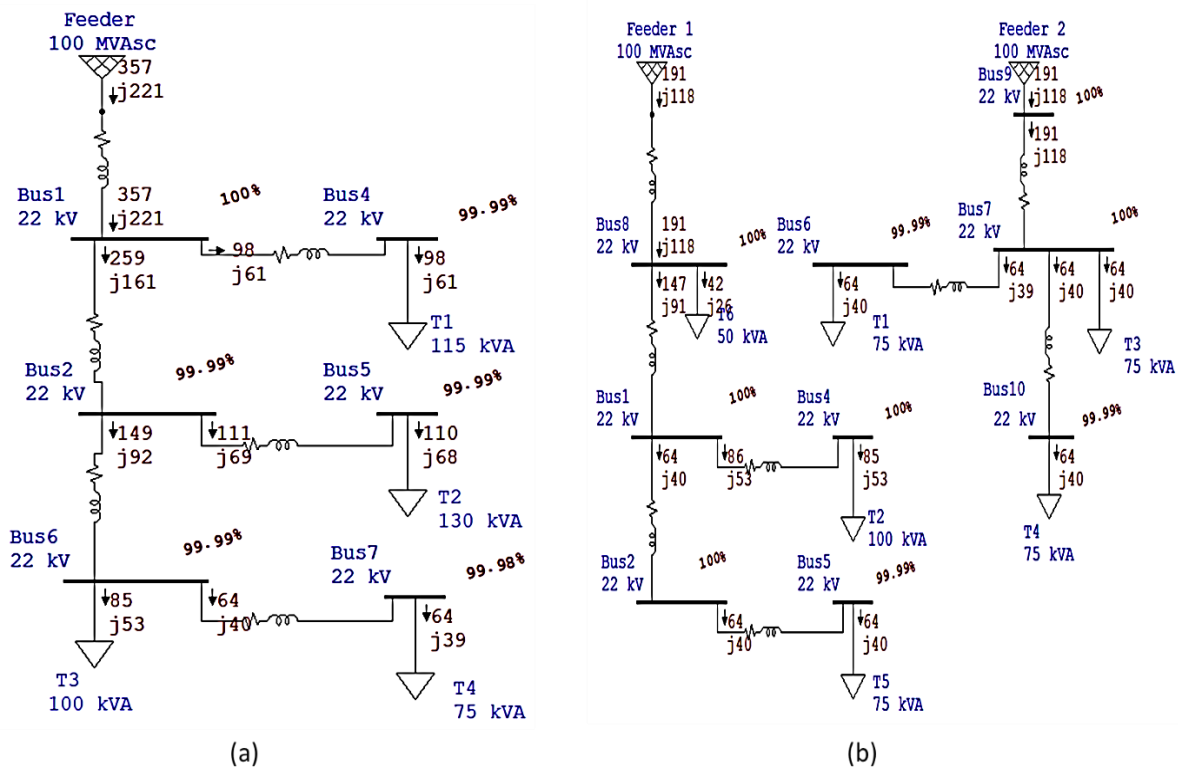


Figure 6.25. Optimal power flow for MVDN2. a) Original network. b) Optimized network.



## 6.4. Implementation of the IPSO-PRIM Algorithm in Android-Java

In order to have a friendlier interface for the network design, the IPSO-PRIM algorithm has been implemented in Android, giving the designer the capability to play with the topology and characteristics of the network. The application is intended to help with the design of a distribution network from scratch (using the proposed IPSO-PRIM algorithm) or to test the performance of an existing network by means of a power flow analysis. As mentioned in section 1.2.2, to begin the design of a DN we need a georeferenced topographic survey of the users and utility poles under the WGS84 UTM coordinate system. Therefore, the application in Android is ideal for network design since it can use the GPS of tablets or cellphones.

Among the advantages of this application, running on Android, we have:

- The code is written in Java; therefore, the application can run in small devices such as phones and tablets.
- With the GPS of the device, the network can be designed in situ.
- The graphics interface -which is touch- allows us to play with the topology of the network, e.g. changing the position of the transformer, the size of conductors, the number of phases, and the availability of branches.
- The application allows us to change some parameters for the network design such as voltage magnitude, projected unit demand, power factor, the power of public lamps, the maximum voltage drop limit, and the number of users/lamps per node.
- As the application is based on a power flow analysis, we can check if the proposed configuration or an existing network meets the required constraints. For this, the application will give us a visual warning of the elements that present problems.
- The application can show us in real time the final design of the network, greatly facilitating decision making by the designer.

### 6.4.1. Description of the Application

To start the network design, the first thing to do is to select the way in which the GPS coordinates will be obtained, i.e. in situ using the GPS of the device, or preloading an excel file, as shown in Figure 6.26. If we decide to load the coordinates using the device's GPS, we must specify the number of users and lamps for each point. The application gives us the option to delete the points by clicking on them to then use the delete button.

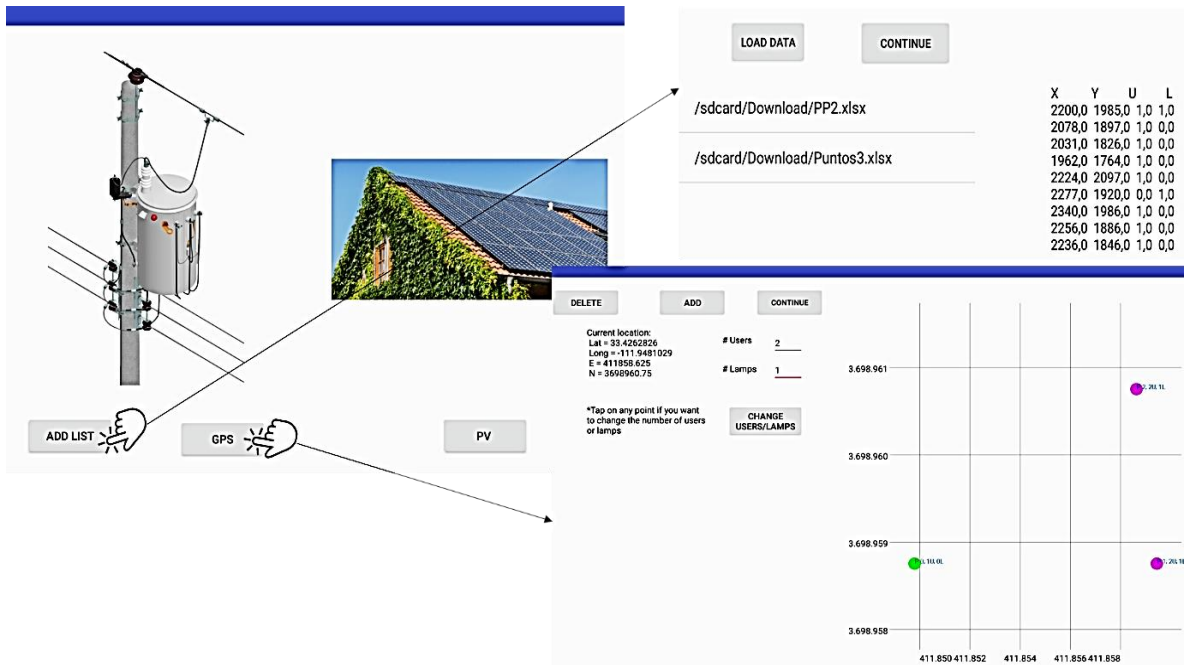


Figure 6.26. Obtaining GPS coordinates, using the device's GPS or an excel file.

Once the coordinates have been loaded, the application will give us a glimpse of the possible trajectory of the conductors, with the distance of each branch. At this point we can add a geographical constraint on each branch if there is something that blocks the cable route. For this, we must click on the branch and see if the status of the constraint changes from 0 to 1, as shown in Figure 6.27.

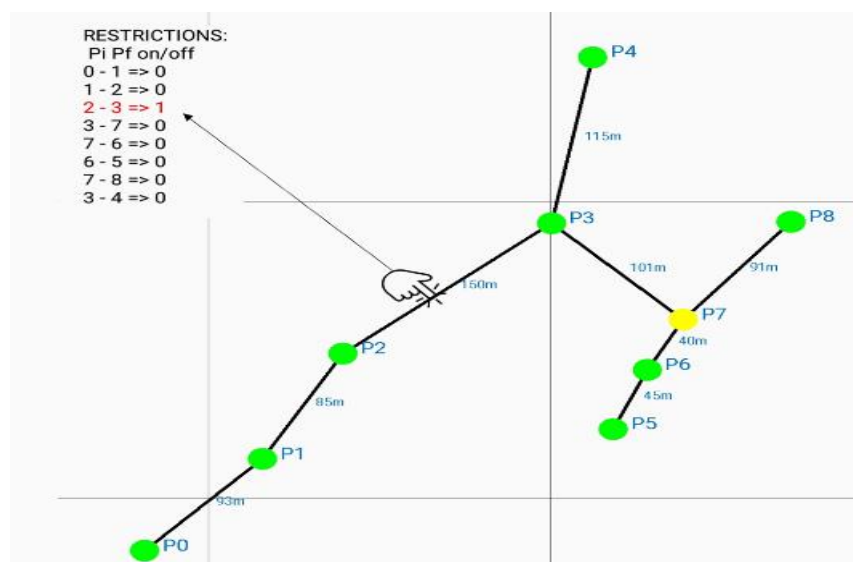


Figure 6.27. First glance of the network, with the activation of branch restrictions.

The next step is to modify and select the parameters with which we will design the network. Among these we have: nominal voltage, power factor, the power of public lamps, voltage drop limit, user category (projected unit demand [kVA]), and the number of phases (single phase or three phase). To change each value, we must click on the items as shown in Figure 6.28.

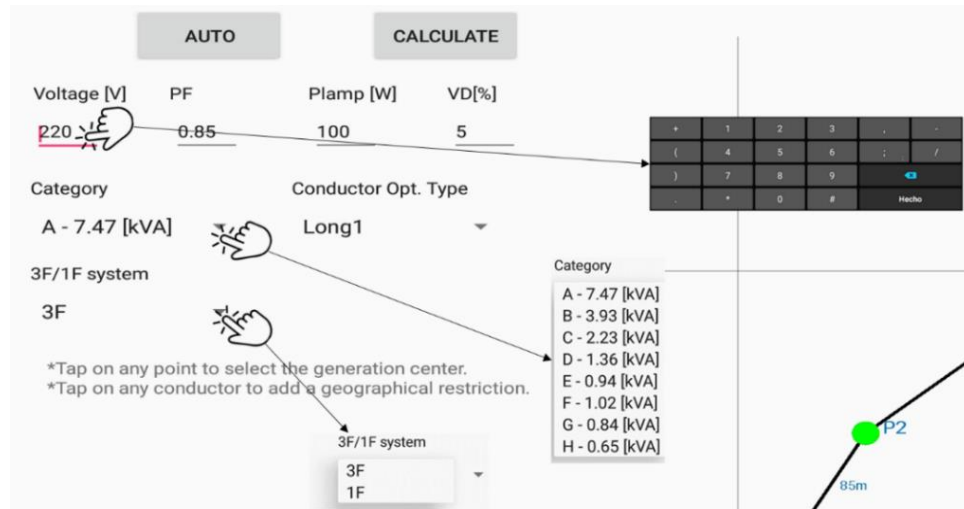


Figure 6.28. Changing parameters for the network design.

Once the design parameters are established we have two options: a) allow the algorithm to design the entire network, or b) test our own design. If we select the first option, we must click on the "AUTO" button to execute the IPSO-PRIM algorithm. On the other hand, if we select the second option we must first specify the position of the transformer and the size of the conductors (please see Figure 6.29), to then press the "CALCULATE" button which executes only a power flow analysis.

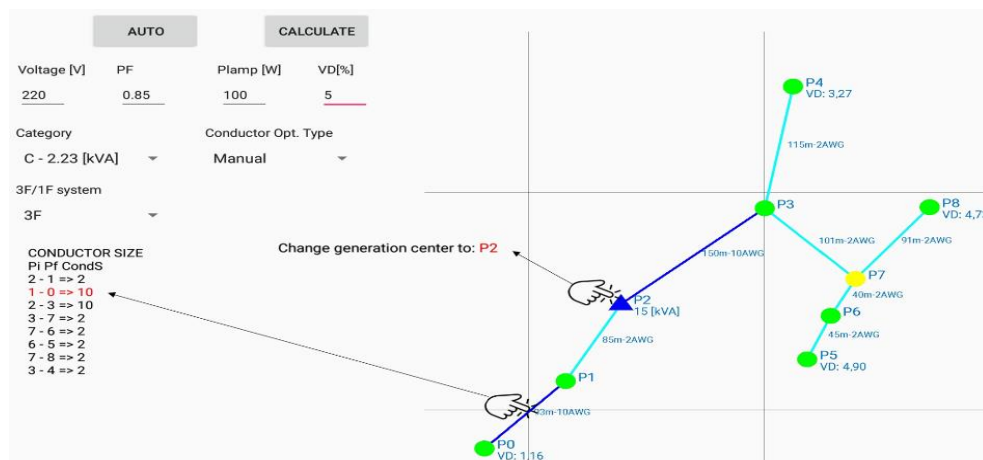


Figure 6.29. Setting the size of conductors and the location of transformer manually.

Figure 6.30 shows how the final result of the IPSO-PRIM algorithm looks like. In the diagram we can see the optimal location of the transformer with its size, and which is the optimal size of the conductors, as well as the voltage drop at the end-nodes. Additionally, the application summarizes the results of the power flow analysis such as line power losses, voltage magnitudes, number of loads, total power per node, currents through each branch, and so forth.

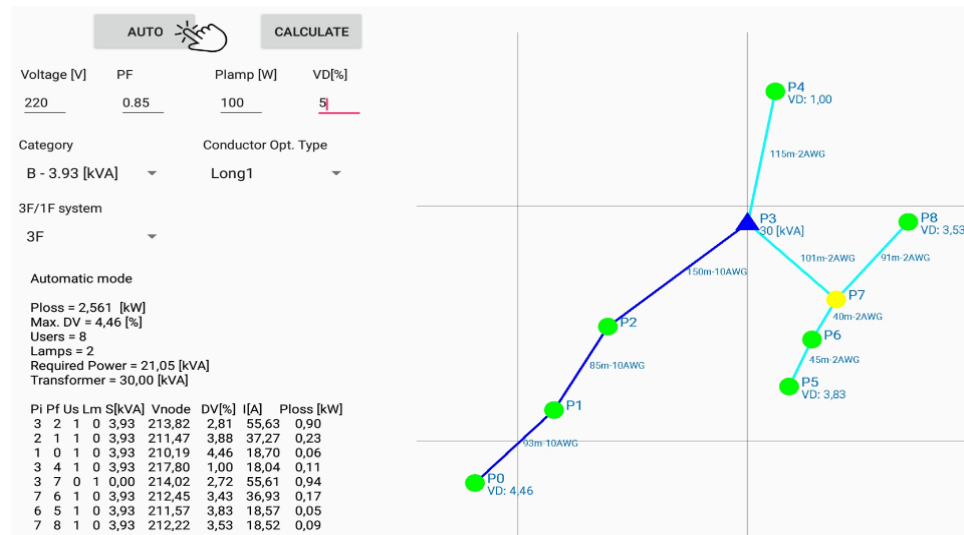


Figure 6.30. Network design by the IPSO-PRIM algorithm.

During the design, the application allows us to change any parameter as well as the topology of the network, with which we can compare different configurations to select the most adequate. In this process, the application will warn us -drawing the element in red- if any component in the network does not meet the established requirements such as minimum voltage magnitude, conductor's ampacity, or transformer's maximum capacity. An example of this case is illustrated in Figure 6.31.

In this way, we can conclude that this Android app can be a very useful tool for the design and control of distribution networks. For demonstration purposes only, the Java code for the IPSO algorithm is shown in Appendix D.

## 6.5. Summary

In this chapter TS-MOEAP was applied to design -from scratch- two off-grid electrification projects with PV systems, to optimize two existing secondary networks (with several quality issues), and to reconfigure two primary networks to support the new LVDN topologies.

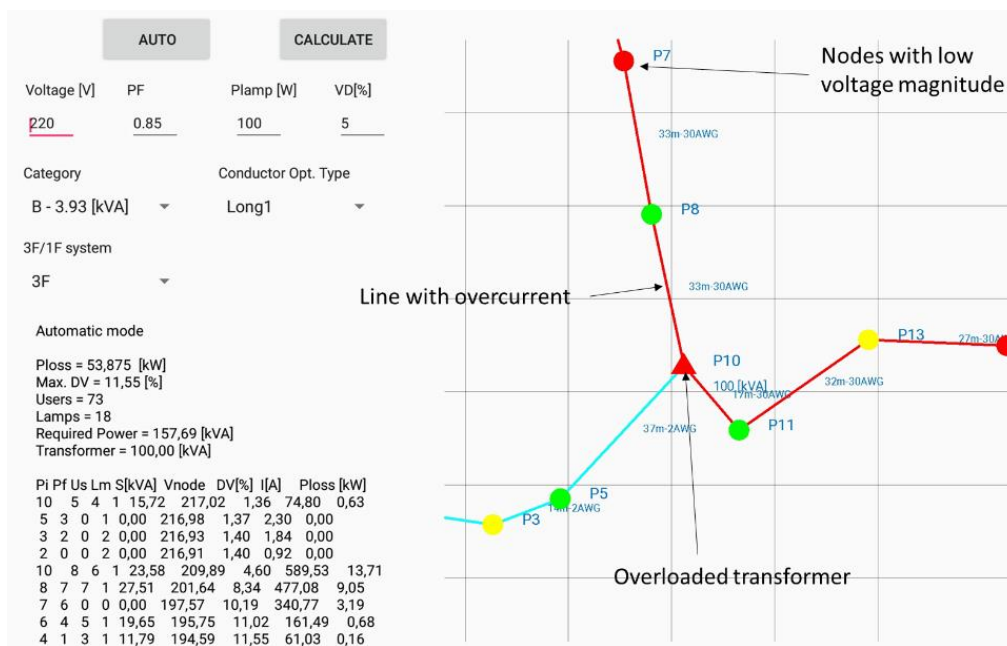


Figure 6.31. Example of a network presenting some problems.



## Chapter 7

# Network Optimization using DER-CAM

In this chapter, we will discuss how to optimize distribution networks through the installation of distributed energy resources (DERs) by means of a commercial software called DER-CAM. This program is specialized in finding the optimal investment solutions for a power system, with the main objective of minimizing total annual costs of energy supply. In our particular case, we will analyze the case study MVDN2, which is currently making a transition from the use of gas stoves to induction stoves. With DER-CAM we will see what the economic impact of this change is and how we can reduce the total investment cost by installing DERs.

### 7.1. DER-CAM

DER-CAM is a decision support tool intended to find optimal investment solutions of distributed energy resources (DER). The problem can be formulated as a mixed integer linear program (MILP) with the main objective of minimizing the total annual costs of energy supply (including investment costs) or to minimize carbon dioxide (CO<sub>2</sub>) emissions.

DER-CAM supports a wide range of DER technologies (between conventional and renewable) and can be used in multiple building and microgrid contexts such as grid-connected, islanded, off-grid microgrids, and systems based on either AC or DC infrastructure. The optimal DER investment solution found by DER-CAM includes the portfolio, sizing, placement, and dispatch of DERs [51].

The software consists of an optimization module, which includes an optimization algorithm and the supporting mathematical solvers, a graphical user interface, and a server application that enables remote access to the optimization component.

For the implementation of DER-CAM, the inputs of the model are:

- a. Load Data:* customer's end-use hourly load profiles, detailed for different uses such as space heat, hot water, natural gas only, (electric) cooling, (electric) refrigeration, and electricity only.

- b. *Electricity Tariff and Fuel Costs*: the structure and rates of the customer's electricity tariff, natural gas prices, and other relevant utility price data.
- c. *DER Technology Costs*: capital costs, operation and maintenance (O&M) costs, along with fuel costs associated with the operation of various available technologies.
- d. *Investment Parameters*: discount rate to be considered in the DER investment analysis and maximum allowed payback.
- e. *DER Technology Parameters*: basic technical performance indicators of generation and storage technologies.
- f. *Network Topology*: in case of multi-node microgrids, we must specify the topology of the network, including electricity cables and gas/heat pipes as well as their operational limits and characteristics, e.g. impedances, conductor ampacities, and voltage constraints.

Finally, the outputs provided by DER-CAM are

- a. A diagram of the network showing the *optimal capacity* and placement of all DER.
- b. Optimized strategic *dispatch* of all DER, considering energy management procedures.
- c. *Detailed economic results*, including costs of energy supply and all DER related costs.

An overall illustration of DER-CAM is shown in Figure 7.1.

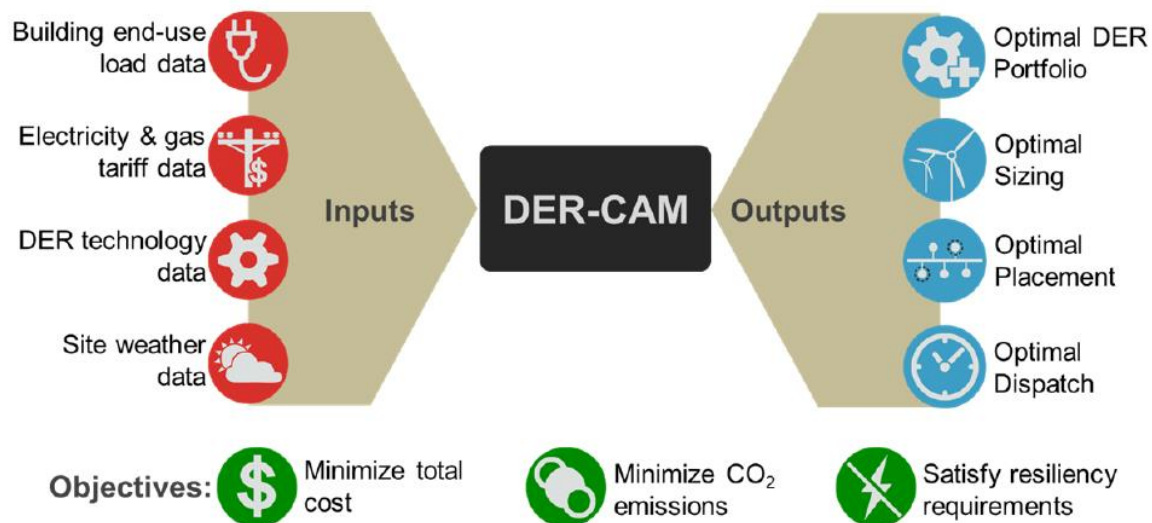


Figure 7.1. Overall input and output structure of DER-CAM [51].



## 7.2. Implementation of DER-CAM for the Case Study MVDN2

As mentioned in section 6.2.1, the background of the problem is the transition of gas stoves to induction stoves, which has caused a considerable increase in electricity demand, that cannot be supported by the current infrastructure. The case study that we are going to consider is MVDN2, detailed in section 6.3.1, and we will proceed as follows:

- i. First, we will analyze the original network topology (see Figure 6.20) -only with the use of gas stoves- by means of DER-CAM. This scenario will serve as a reference to verify the economic impact of improving the system.
- ii. As a second scenario, we will analyze the original network with the increase in demand, i.e. with the use of induction stoves, with and without the installation of DERs.
- iii. In the third scenario, we will analyze the network obtained by TS-MOEAP (see Figure 6.24), with and without the installation of DERs.
- iv. Finally, in the last scenario we analyze the impact of load shifting and peak shaving.

### 7.2.1. Scenario 1: Base Case

To start the analysis in DER-CAM we must first establish the topology of the network, as shown in Figure 7.2 (a), to then enter the load profile of each bus. The load profile can be obtained multiplying the curves of Figure 6.7 by a factor, based on the number of users connected to each bus, and the curve for the natural gas can be obtained taking only the peaks of the load profile with induction stoves and applying an efficiency factor of 47 % (efficiency of gas stoves). For example, Figure 7.2 (b) shows the load profile for bus 1.

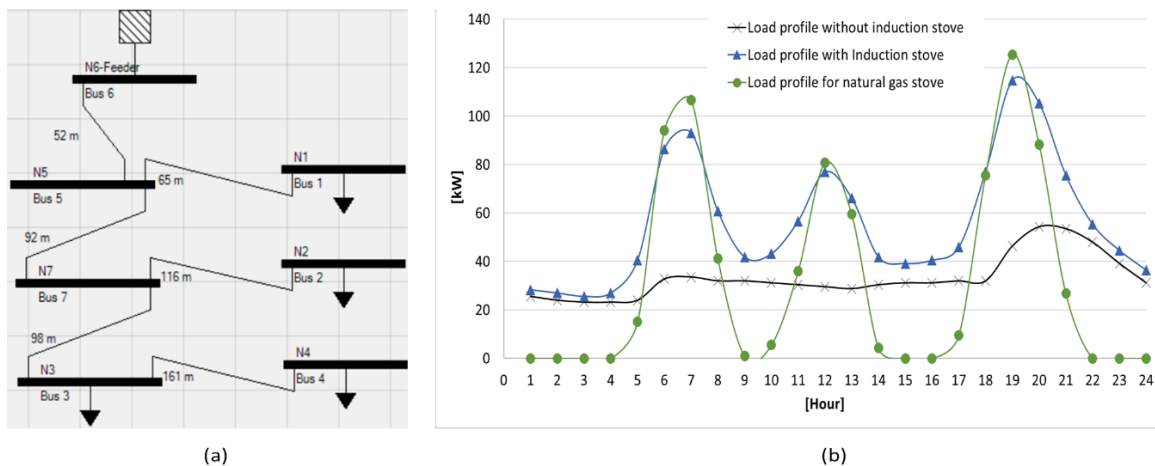


Figure 7.2. Scenario 1, base case. a) Topology of the network in DER-CAM. b) Load profile for Bus 1.

For all scenarios, the electricity tariffs will be established in 0.093 \$/kWh for regular hours and 0.12 \$/kWh for peak hours, with a tariff for natural gas of 0.016 \$/kWh. Finally, for the base case, the investment of renewable DERs will be disabled, and only the load profiles without induction stoves and those for natural gas will be considered.

Applying the aforementioned data, the summary of results for the base case is shown in Figure 7.3, detailing a total annual cost of \$ 302000 and a total annual CO2 emission of 588000 kg. The figure also shows that most of the cost is due to operating costs, and there are only small investments for gas supply (conventional source). We should note that for this case all the energy was purchased from the utility company.

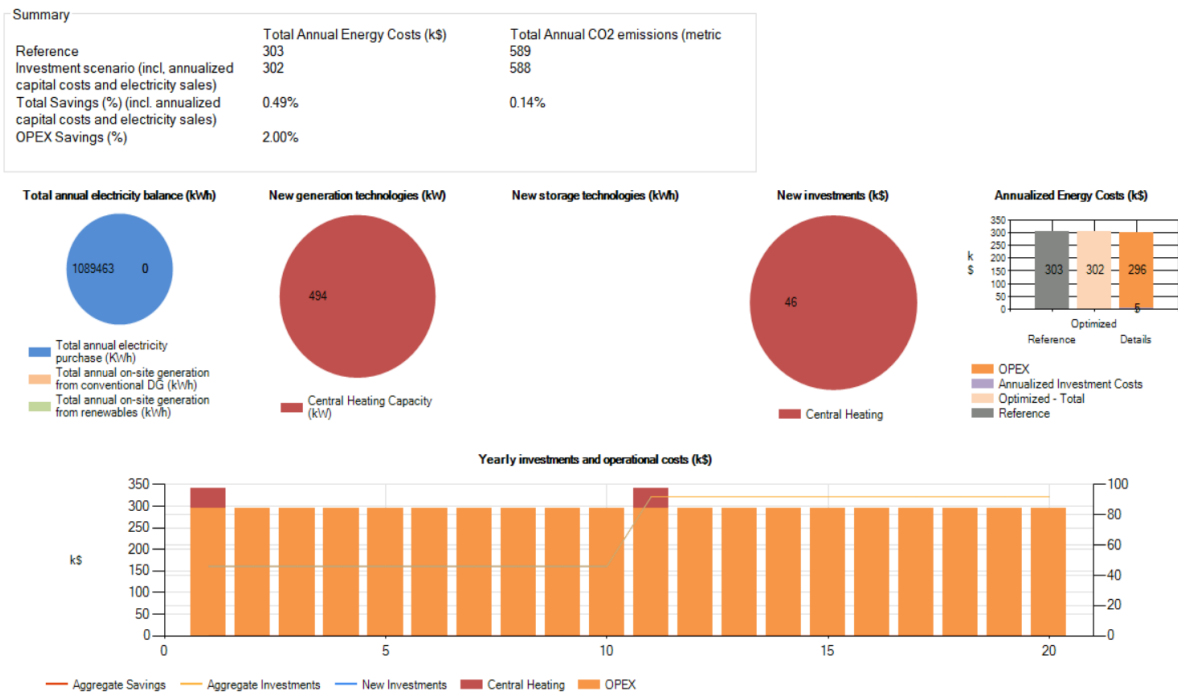


Figure 7.3. Summary of results for the base case.

### 7.2.2. Scenario 2: Original Network implementing Induction Stoves

Now, for this scenario, we will take the same topology of Figure 7.2 (a) using only the load profiles with induction stoves. For the first run the investment of renewable DERs will be disabled and for a second run it will be enabled (photovoltaic and electric storage). Between the parameters for investment, the interest rate will be established in 3 % and the maximum global payback period will be set to 10 years. Finally, the solar profile and the technical parameters of DERs will be taken from databases available in DER-CAM.

Figure 7.4 shows the summary of results for the base case implementing induction stoves, without the inversion of DERs. The total annual cost of energy increased to \$ 459000, somewhat expected due to the increase in electricity demand. On the other hand, if we run the same case enabling the investment of DERs, we obtain the results shown in Figure 7.5.

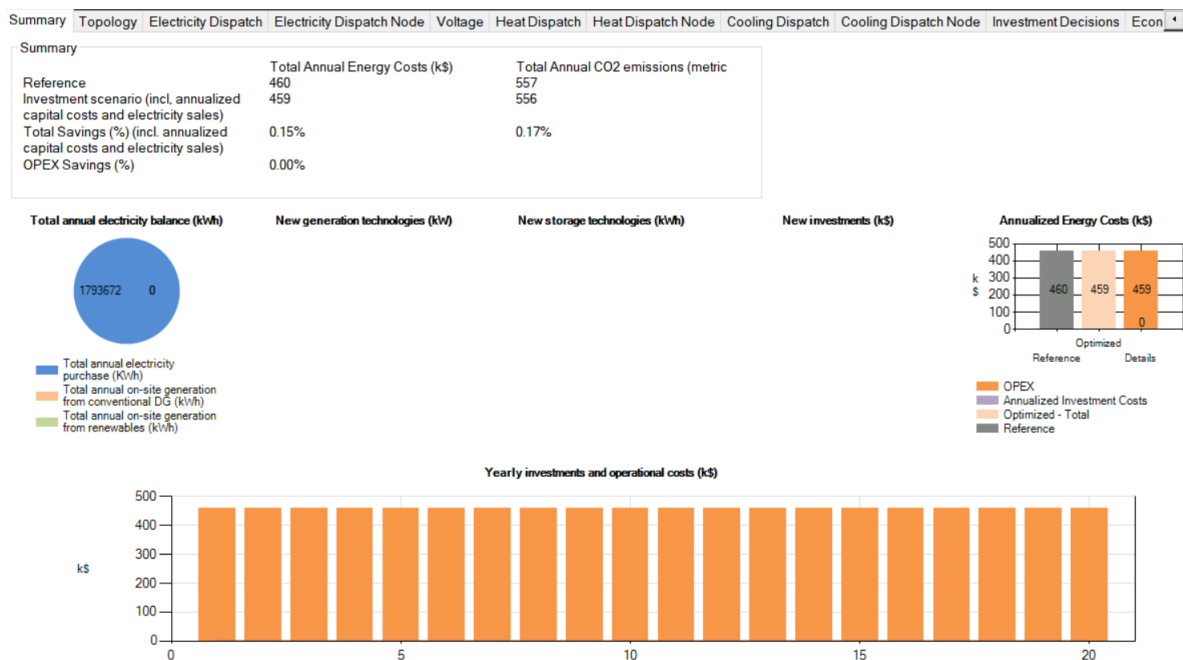


Figure 7.4. Summary of results for the base case with induction stoves and without DERs.

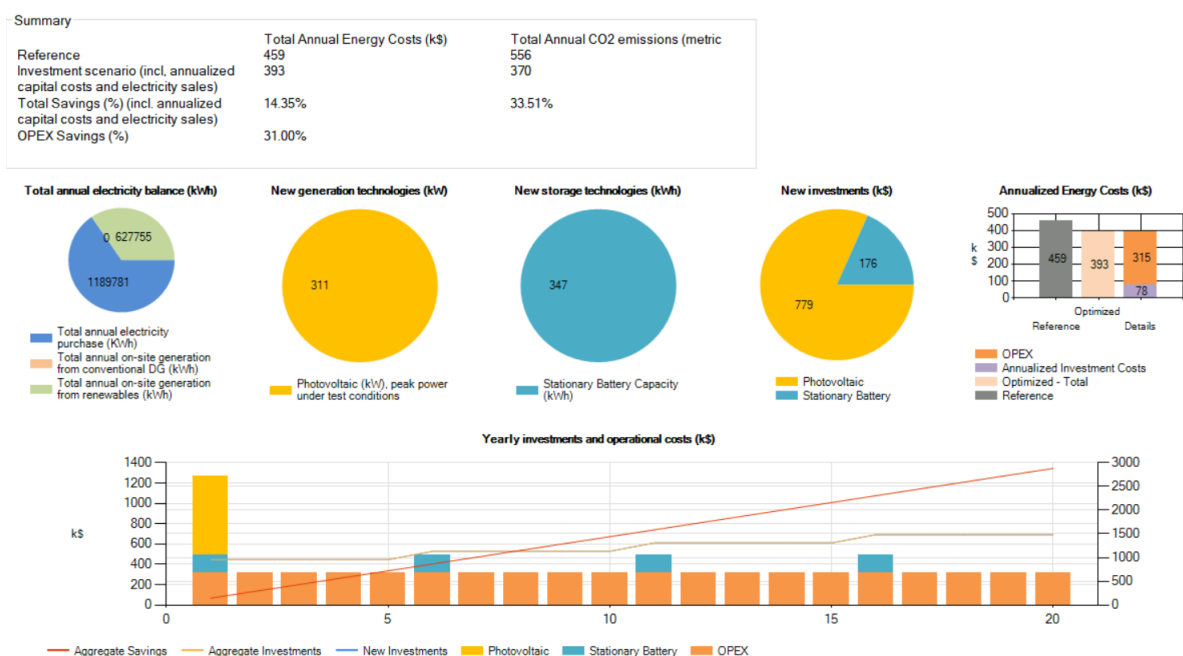


Figure 7.5. Summary of results for the base case with induction stoves and DERs.

As we can see, we have a total saving of 15% (including annualized capital costs and electricity sales) respect to the case without DERs, of which 31% are savings of operating expenses. This result is due in large part to the installation of a 311-kW photovoltaic system at bus 3 and the installation of 6 battery banks -with a capacity of 58 kWh each- in the remaining buses, please see Figure 7.6. The operating expenses are minimized due to the dispatch of the photovoltaic unit for self-consumption at noon, and by the use of batteries during peak hours. This is shown in the electricity dispatch of Figure 7.7.

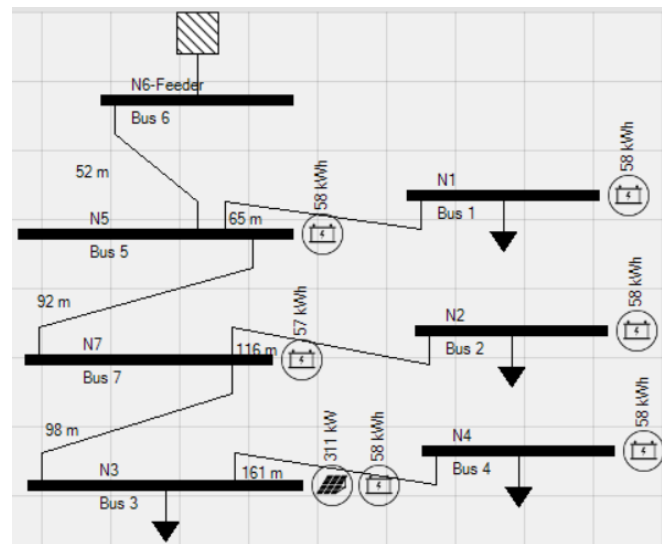


Figure 7.6. Installation of DERs for the base case with induction stoves.

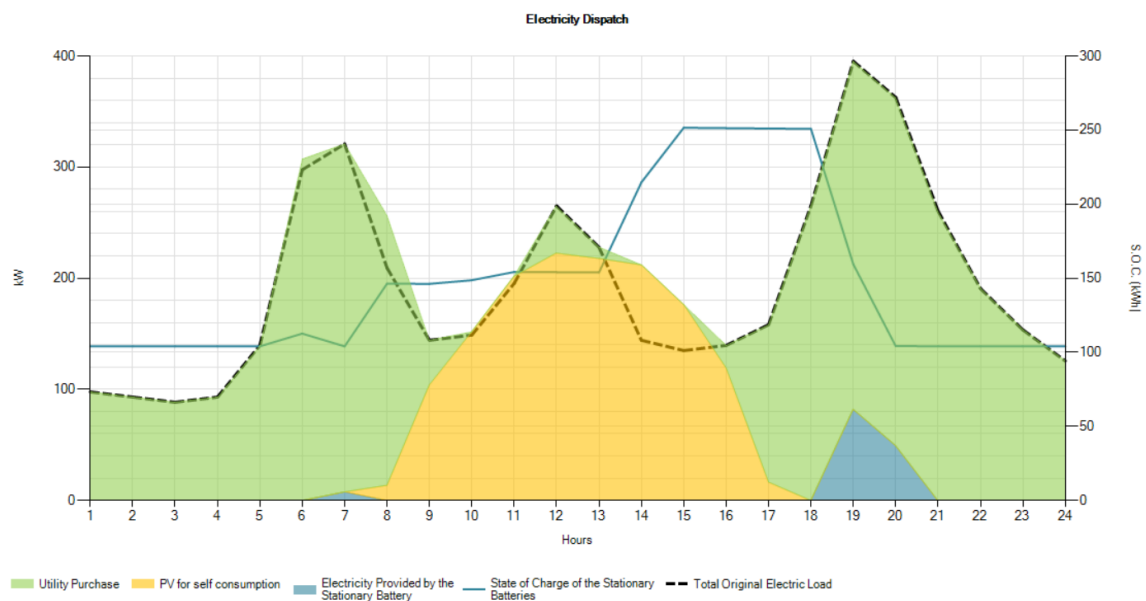


Figure 7.7. Electricity dispatch for the base case with induction stoves and DERs.

### 7.2.3. Scenario 3: Network optimized by TS-MOEAP, with/without DERs.

In this scenario, we analyze the network MVDN2 of Figure 6.24, which was previously optimized by TS-MOEAP. We must remember that this primary network supports the secondary network LVDN2, also optimized by TS-MOEAP (see Figure 6.15). If we do not implement DERs in this model, we obtain a total annual cost of \$475000 and a total annual CO2 emission of \$574000 kg. On the other hand, if we enable the installation of DERs, we obtain a total annual cost of \$ 406000 and a total annual CO2 emission of 381000 kg, as illustrated in Figure 7.8.

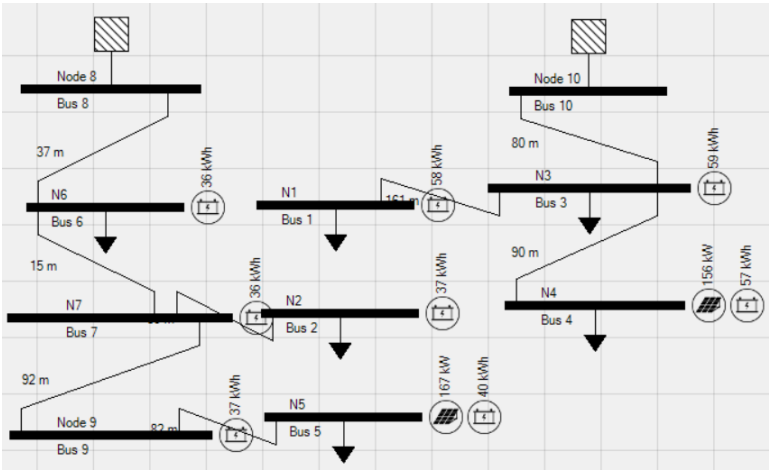
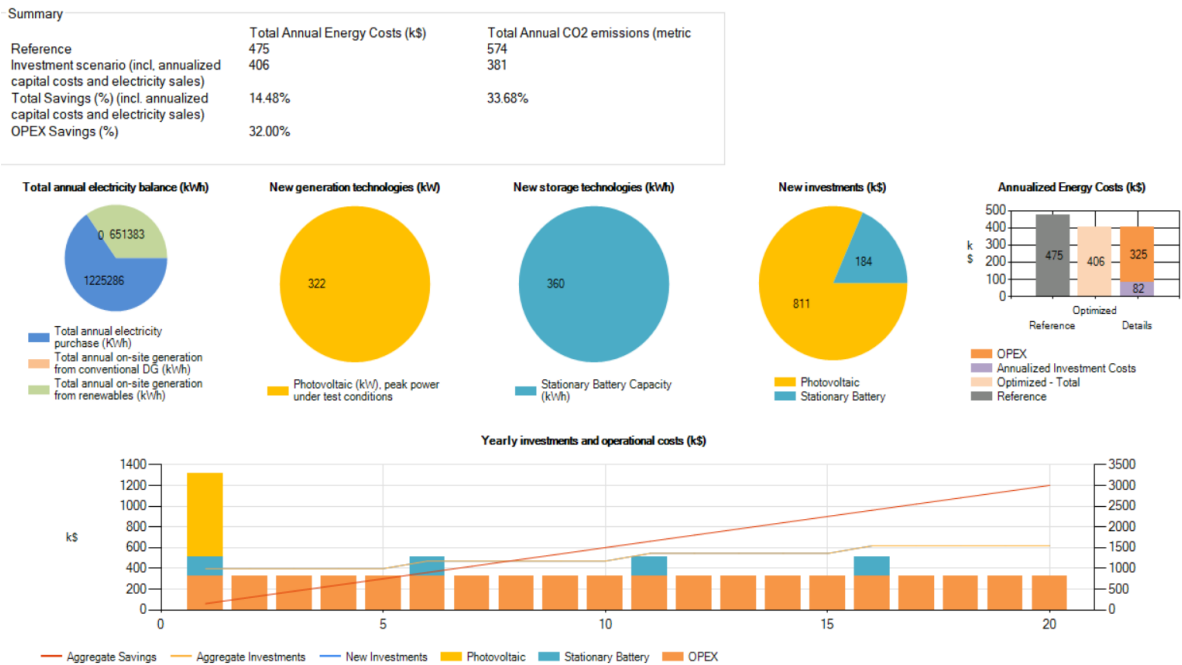


Figure 7.9. MVDN2 optimized by DER-CAM.

The total saving, which is around 15%, is mainly due to the installation of two photovoltaic systems and eight battery banks, as illustrated in Figure 7.9. This configuration allows to generate energy for self-consumption and to charge the batteries which will be used during peak hours (minimum state of charge 25% of the capacity). This can be seen in the electricity dispatch of Figure 7.10.

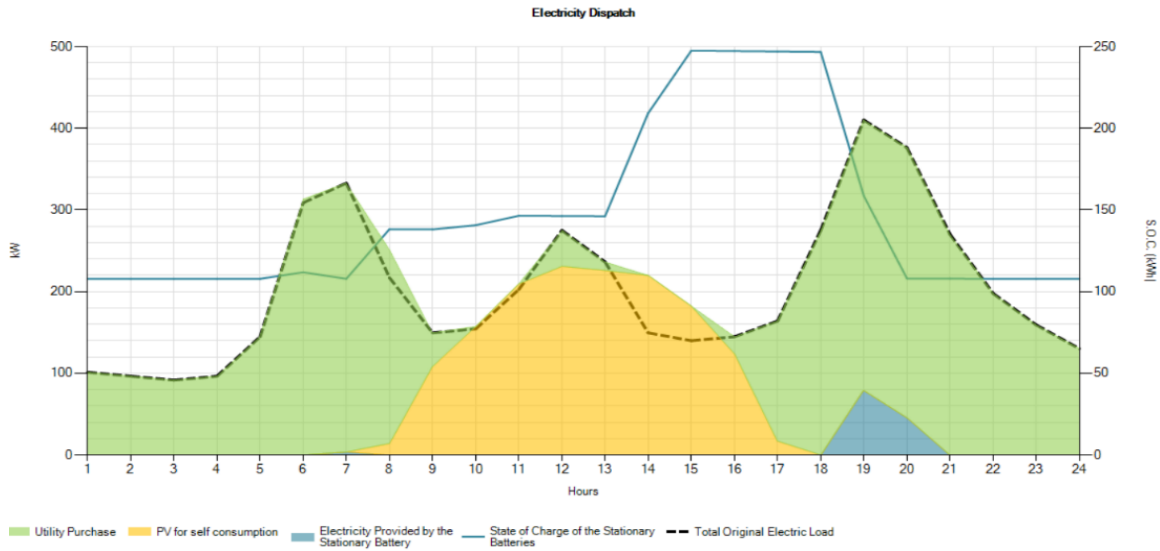


Figure 7.10. Electricity dispatch for the optimized network with induction stoves and DERs.

#### 7.2.4. Scenario 4: Impact of load shifting and peak shaving

If we calculate the load factor ( $f_{Load} = \text{Average Load} / \text{Peak Demand}$ ) of the utility when: DERs are not considered, when only PV systems are installed, and when PV systems along with batteries are mounted, we obtain the results shown in Figure 7.11.

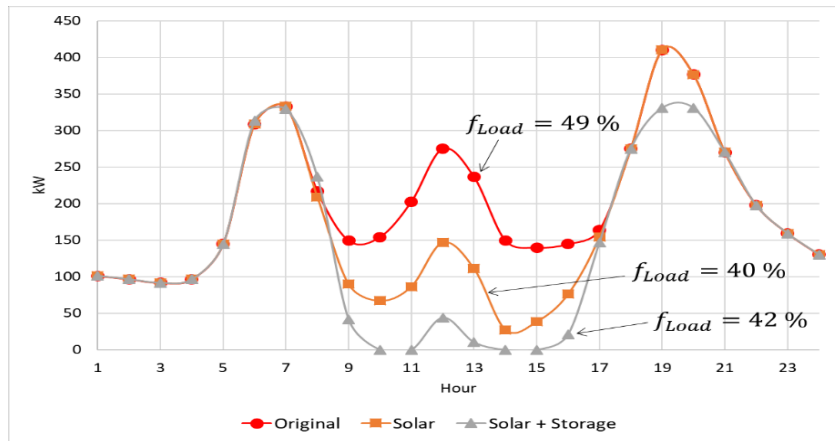


Figure 7.11. Load profiles of the utility and load factors.

As might be seen, the installation of photovoltaic systems causes the deterioration of the load factor (which is preferred close to 1). Therefore, to improve this parameter, peak shaving and load shifting can be used. In DER-CAM we can implement both methods, forcing the algorithm to install bigger batteries (e.g. 80 kWh per node) for peak shaving and enabling part of the load that may be subject to shifting (e.g. 3 % at each node). The result of this operation is shown in the electricity dispatch of Figure 7.12, and as we can see, DER-CAM dispatches the batteries to provide energy at peak hours (7 am and 7 pm). Also, it changes part of the load towards noon (red dotted line), where there is an excess of solar generation. We should note that this excess of generation is also used to charge the batteries. Finally, after this energy management procedures, the load factor is improved up to 53 %.

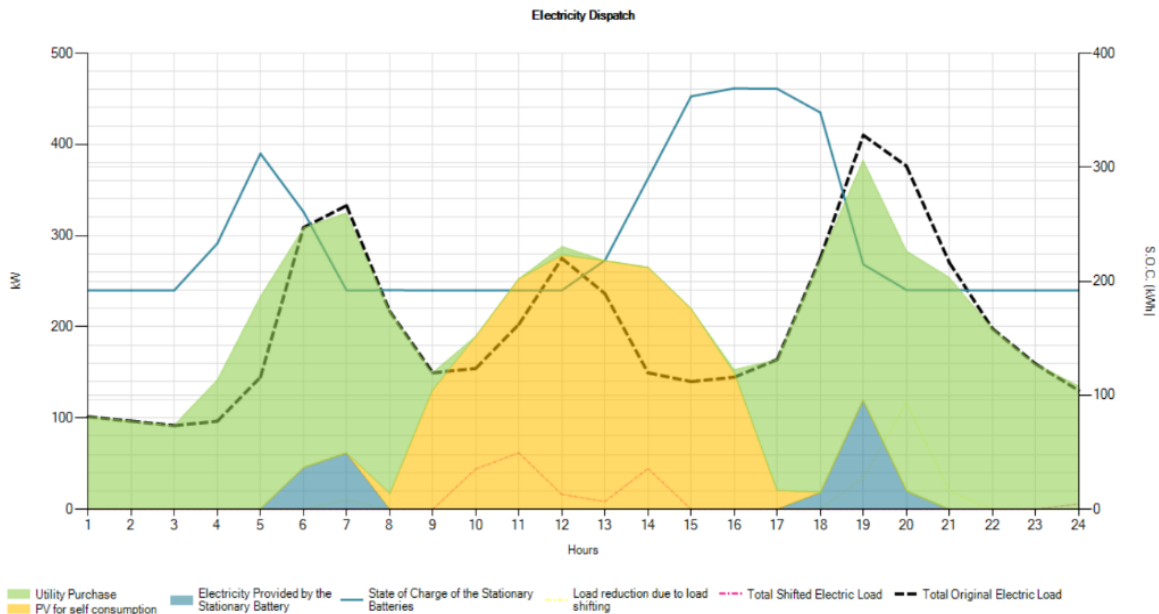


Figure 7.12. Electricity dispatch implementing load shifting and peak shaving.

### 7.2.5. Result combining TS-MOEAP and DER-CAM

Figure 7.13 shows a comparison of the results of the four scenarios. As we can see, the models that incorporate DERs present lower costs and emissions than those systems without them. This demonstrates that a system can still be improved, even when it has been reconfigured by TS-MOEAP. However, DER-CAM is intended only to find optimal investment solutions of DERs, at medium and high voltage levels, therefore secondary networks can still present technical problems.

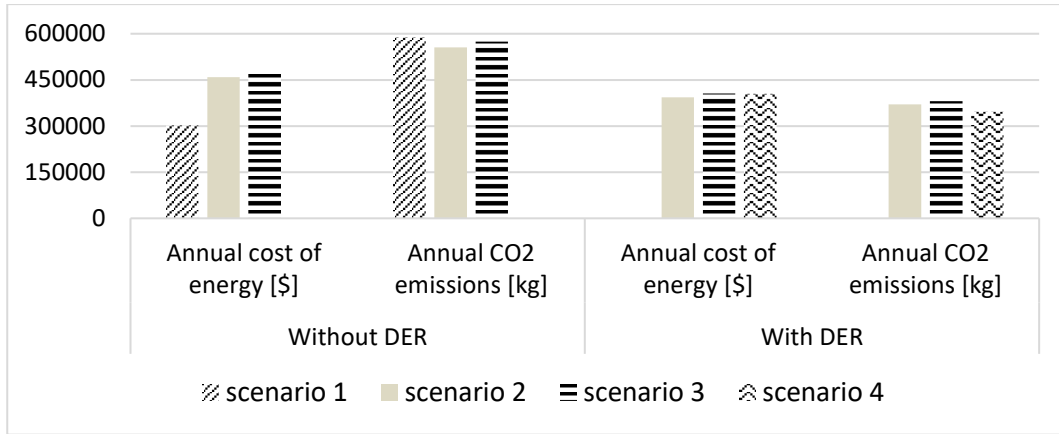


Figure 7.13. Comparison of scenarios, with/without DERs.

In this way, we can conclude that an entire system could be properly designed/improved if we combine both algorithms. First, we must use TS-MOEAP to find the optimal topology of the secondary and primary network, to later improve the operation of the primary network by installing DERs with the help of DER-CAM.

As a final result of this thesis, Figure 7.14 shows the optimal configuration for the MVDN2-LVDN2 system, obtained with the collaboration of TS-MOEAP and DER-CAM.

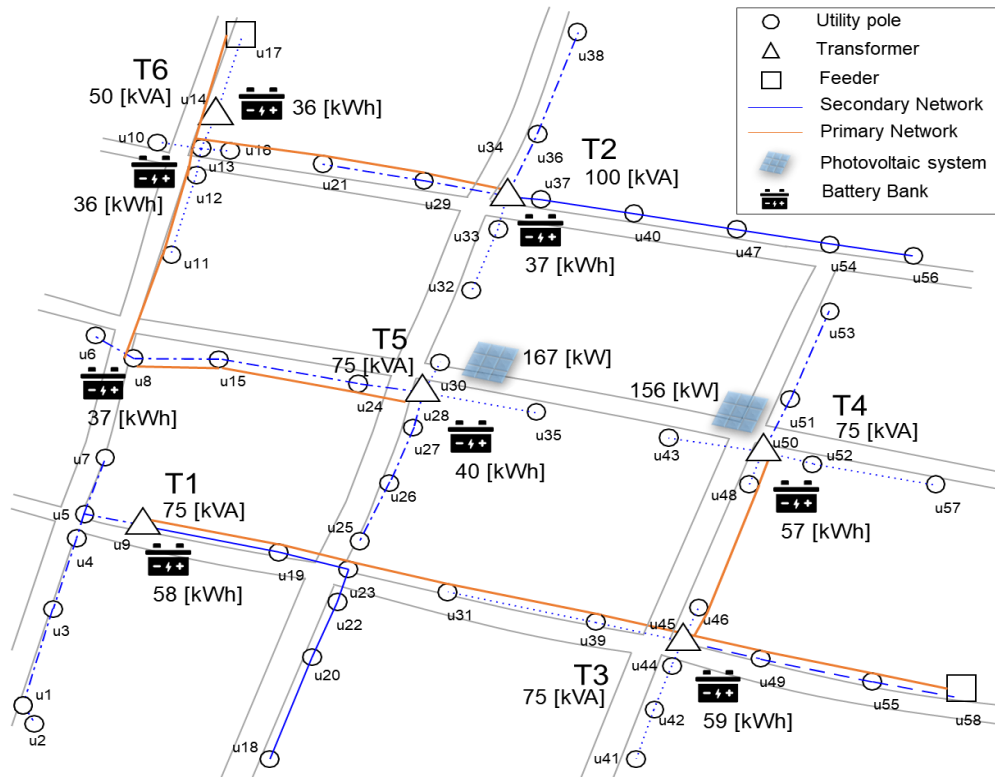


Figure 7.14. Test system MVDN2-LVDN1, improved by TS-MOEAP and DER-CAM.



### **7.3. Summary**

In this chapter we have complemented the proposal TS-MOEAP with the commercial software DER-CAM. This combination allows us to find the optimal topology of the network and the optimal investment solutions of DERs. As result we have a considerable reduction of investment and operational costs, as well as an optimum dispatch of generation along with peak shaving and load shifting.



## Chapter 8

### Conclusions and Future Work

In this thesis we proposed a *Two-Stage Multiobjective Evolutionary Approach* to design and optimize distribution networks at primary and secondary level. Due to the complexity of the optimization problem, the approach was implemented in two stages:

- Stage-1, for optimal placement and sizing of DTs/DGs, as well as optimal branch routing and conductor sizing, and
- Stage-2, for optimal network reconfiguration.

For the first stage, an IPSO algorithm was proposed for its simplicity and outstanding performance and for the second stage an INSGA-HO algorithm was introduced with the incorporation of a better mutation operator.

In the following, we summarize the main contributions developed in this thesis.

#### *Chapter 3:*

- We propose an integer vector representation for the genotype form of the distribution network. This new representation is better than the conventional binary representation, and it is based on groups of loads instead of individual switches. This allows us to use the same algorithm (INSGA-HO/IPSO) for LV and MV networks. The great disadvantage of other proposals is that they can only optimize MV networks.
- The proposed integer vector representation can be manipulated by both algorithms, the INSGA-HO and the IPSO. The genetic algorithm works with the complete chromosome, while the IPSO uses sub-vectors contained in the chromosome.
- For the construction of the network model, we consider the network as a weighted undirected graph from which we can obtain a minimum spanning tree using a greedy algorithm. For this, we use PRIM, which takes a graph as input and finds the subset of branches which will form the network with the minimum amount of wire length. The advantage of using PRIM is that the network is always built radially.

#### *Chapter 4:*

- The selected objective functions for the optimization problem are power losses and investment costs. We choose these two functions since they are directly related to the reinforcement of the network.
- Unlike a regular PSO, the IPSO does not initiate the particles randomly, because in practical cases a transformer is not located at the ends of the network. This helps improve computational time by not evaluating unnecessary nodes. Furthermore, as the power flow analysis is a process that consumes valuable computational time, the IPSO records all the solutions found so far by the particles, this avoids repeating the power-flow computation if another particle falls in the same place.
- During the evolutionary process the size of the conductors is not optimized, instead, the thickest available conductor is used. This helps to reduce computational time.
- The IPSO-PRIM algorithm can find the best position for a DG/DT by minimizing only power losses, applying penalties to the fitness value if there are voltage drops, branch overcurrents, or restricted nodes. The DT or DG is always located at the node with the lowest fitness value.

#### *Chapter 5:*

- The incorporation of the heuristic mutation operator significantly improved the performance of the INSGA-HO algorithm. This operator is one of the best contributions of this thesis since it was designed specifically to improve the topology of a network by changing the characteristics of chromosomes. This operator proved to be so efficient that even simpler algorithms (such as a GA) that incorporated it could find better results than other more complex algorithms such as an NSGA-II.
- The algorithm INSGA-HO presents better computational time than the NSGA-II since the first one was modified to not find all the nondominated fronts at once. Unlike Stage-1, Stage-2 uses both objective functions to balance the design of the network.
- Among the different recombination methods used for the INGA-HO, better results could be obtained with the uniform crossover since this operator applies a greater pressure of diversification.
- Compared to MOEA-D, the INSGA-HO algorithm is more complex and may take longer to converge to a solution. However, INSGA-HO can find better configurations in different scenarios, and MOEA-D has a poor performance when the number of DTs/DGs to be installed is high.

*Chapter 6*

- For the different scenarios in which TS-MOEAP was tested, using the INSGA-HO and IPSO algorithms, better results were obtained than other proposals. The algorithm was able to identify the optimal number, placement, and size of DTs/DGs; as well as the topology of the network and the size of the conductors.
- It was found that the algorithm can design a distribution network from scratch or reconfigure an existing network. In all cases, it was possible to minimize power losses, investment costs, and quality issues.
- The implementation of the IPSO-PRIM algorithm in Android proved to be very versatile since it considerably facilitated the design of a network.

*Chapter 7*

- DER-CAM is a decision support tool intended to find optimal investment solutions for distributed energy resources (DER), with the main objective of minimizing the total annual costs of energy supply or to minimize carbon dioxide (CO<sub>2</sub>) emissions.
- DER-CAM supports a wide range of DER technologies and can be used in multiple building and microgrid contexts. However, the software is not capable to optimize secondary distribution networks.
- The combination of DER-CAM with our proposal can further improve the configuration of the network through the implementation of DERs, helping to reduce especially operating expenses.

In the following we point out some future research directions:




- It is proposed to incorporate the installation of DERs into the optimization model, along with the optimal redesign of the network.
- We recommended expanding the android application for the design of primary networks and photovoltaic systems.
- It is proposed to test TS-MOEAP with different objective functions such as power losses, operative costs, and reliability indices.



# Appendix A

## Solar Radiation for the Case Studies CM1 y CM2

Table A.0.1. Solar radiation of the test area.

	<a href="#">NASA Surface meteorology and Solar Energy: RETScreen Data</a>		Month	Air temperature	Relative humidity	Daily solar radiation - horizontal	Atmospheric pressure	Wind speed	Earth temperature	Heating degree-days	Cooling degree-days
			°C	%	kWh/m <sup>2</sup> /d	kPa	m/s	°C	°C-d	°C-d	
	Responsible > Data: Paul W. Stackhouse, Jr., Ph.D.		January	17.8	76.7%	4.39	84.0	1.8	19.3	16	243
	Officials > Archive: John M. Kusterer		February	17.7	79.4%	4.25	84.0	1.8	18.9	17	218
	<a href="#">Site Administration/Help: NASA Langley ASDC User Services (support-asdc.nasa.gov)</a>		March	18.0	77.9%	4.45	84.0	1.8	19.4	13	248
	<a href="#">[Privacy Policy and Important Notices]</a>		April	17.6	77.3%	4.33	84.1	1.8	19.0	22	227
	Document generated on Tue Oct 28 14:14:42 EDT 2014		May	17.1	72.4%	4.19	84.1	2.0	18.5	31	222
			June	16.7	66.5%	4.15	84.2	2.5	18.1	40	202
	Latitude -3 / Longitude -78.8 was chosen		July	16.8	57.3%	4.19	84.2	2.5	18.7	39	213
			August	17.9	51.3%	4.49	84.2	2.5	20.4	19	243
			September	18.9	51.2%	4.55	84.1	2.2	21.8	5	266
			October	19.5	54.9%	4.54	84.0	2.0	22.7	3	293
			November	18.9	64.3%	4.73	84.0	1.9	21.7	5	266
			December	18.1	74.4%	4.57	84.0	1.9	19.9	12	252
	Unit	Climate data location									
Latitude	°N	-3									
Longitude	°E	-78.8									
Elevation	m	1625									
Heating design temperature	°C	11.83									
Cooling design temperature	°C	23.39									
Earth temperature amplitude	°C	11.07									
			Annual	17.9	67.0%	4.4	84.1	2.1	19.9	222	2893
Frost days at site	day	0	Measured at (m)					10.0	0.0		

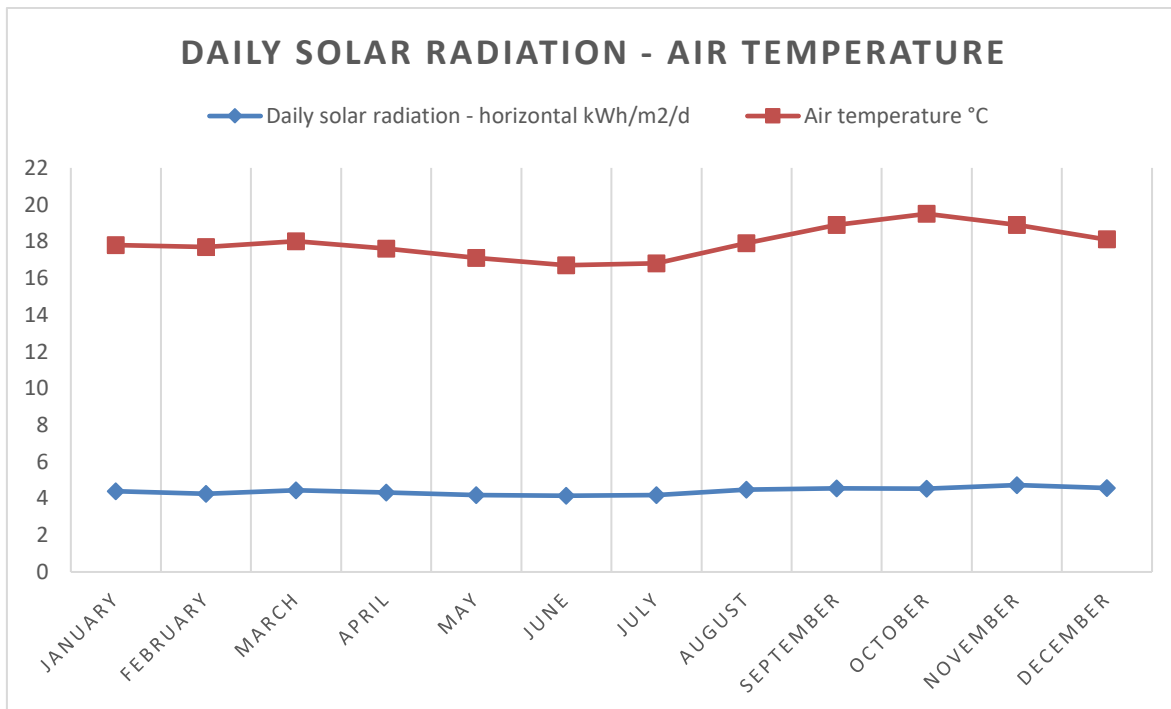


Figure A.0.1. Daily solar radiation and average temperature of the test area.





## Appendix B

### Diagram of the Urban Area for the Case Studies LVDN1 and LVDN2



Figure B.0.1. Diagram of the city, for the case studies LVDN1 and LVDN2.



## Appendix C

### Active and Reactive Loads for the Test System LVDN1

Table C.0.1. Active and reactive loads per node of the test system LVDN1.

$u_i$	P	Q	$u_i$	P	Q	$u_i$	P	Q	$u_i$	P	Q
	[kW]	[kVAr]		[kW]	[kVAr]		[kW]	[kVAr]		[kW]	[kVAr]
1	6.5	4.9	23	5.4	4.1	45	0.0	0.0	67	5.4	4.1
2	5.4	4.1	24	16.3	12.2	46	4.4	3.3	68	1.1	0.8
3	6.5	4.9	25	0.0	0.0	47	10.9	8.2	69	3.3	2.4
4	4.4	3.3	26	5.4	4.1	48	3.3	2.4	70	5.4	4.1
5	4.4	3.3	27	3.3	2.4	49	6.5	4.9	71	1.1	0.8
6	0.0	0.0	28	4.4	3.3	50	19.6	14.7	72	1.1	0.8
7	5.4	4.1	29	5.4	4.1	51	0.0	0.0	73	0.0	0.0
8	3.3	2.4	30	14.1	10.6	52	0.0	0.0	74	3.3	2.4
9	9.8	7.3	31	3.3	2.4	53	7.6	5.7	75	9.8	7.3
10	1.1	0.8	32	2.2	1.6	54	0.0	0.0	76	7.6	5.7
11	9.8	7.3	33	0.0	0.0	55	7.6	5.7	77	4.4	3.3
12	0.0	0.0	34	12.0	9.0	56	16.3	12.2	78	7.6	5.7
13	1.1	0.8	35	5.4	4.1	57	6.5	4.9	79	19.6	14.7
14	6.5	4.9	36	3.3	2.4	58	6.5	4.9	80	3.3	2.4
15	4.4	3.3	37	8.7	6.5	59	0.0	0.0	81	2.2	1.6
16	5.4	4.1	38	0.0	0.0	60	6.5	4.9	82	0.0	0.0
17	8.7	6.5	39	5.4	4.1	61	10.9	8.2	83	2.2	1.6
18	3.3	2.4	40	0.0	0.0	62	5.4	4.1	84	6.5	4.9
19	4.4	3.3	41	3.3	2.4	63	2.2	1.6	85	2.2	1.6
20	3.3	2.4	42	0.0	0.0	64	5.4	4.1	86	10.9	8.2
21	1.1	0.8	43	5.4	4.1	65	10.9	8.2	87	0.0	0.0
22	0.0	0.0	44	6.5	4.9	66	0.0	0.0	88	3.3	2.4



## Appendix D

### Java Code for the IPSO Algorithm

```
public void IPSO (View view){

    int nn = a.length;    //Number of particles
    int partc = Math.round(nn*35/100);
    if (partc <= 1){partc = 2;}
    double f;
    double [][] RECP = new double [nn][2];    //Accumulative memory
    int RP = partc;

    int [] xlim;
    if (nn<=3){xlim = new int []{0, nn-1};}
    else{xlim = new int []{1, nn-2};} //Search limits

    int iter = 100; //Iteration limits

    double [] vx = new double [partc];
    for(int i=0; i<partc; i++){vx[i]=0.1;} //Initial velocity

    double vmax_x = (xlim[1]-xlim[0])/5;    //Limits for velocity
    double vmin_x = -vmax_x;

    double wmax = 0.9;    //Inertial weight limits
    double wmin = 0.1;

    double C1 = 1;    //Cognitive and social variables
    double C2 = 2;

    double [] x = linspace(xlim[0],xlim[1],partc);
    double [] pBest = x.clone();
    double [] fpBest = new double [partc];

    for (int i=0; i<partc; i++){ //pBest

        Trafo=(int) x[i]; //position of transformer
        calculoDV();    //Power flow subroutine
        fpBest[i] = suma(D,16);
        RECP[i][0] = x[i]; RECP[i][1] = fpBest[i];}

    double gBest = Math.round((xlim[0]+xlim[1])/2); //Best result
    Trafo = (int) gBest; calculoDV();
    double fgBest = suma(D,16);

    for(int i=0; i<iter; i++){

        for (int ii=0; ii<partc; ii++){
            int paux = -1;
            for (int j = 0; j<RP; j++){if (RECP[j][0]==x[ii]){paux = j;
                break;}}
```

```

    if (paux > -1){f = RECP[paux][1];}
    else {
        Trafo = (int) x[ii];
        calculoDV();
        f = suma(D,16);
        RECP[RP][0]=x[ii];  RECP[RP][1]=f; RP++;}

    if (f < fpBest[ii]){ //Best local result
        pBest[ii]=x[ii]; fpBest[ii]=f;}

    if (fpBest[ii] < fgBest){
        gBest = pBest[ii]; fgBest = fpBest[ii];}
}

for(int ii=0; ii<partc; ii++){
    double w = wmax-(wmax-wmin)*i/iter; //Velocity
    vx[ii]=w*vx[ii]+C1*Math.random()*(pBest[ii]-
        x[ii])+C2*Math.random()*(gBest-x[ii]);

    if (vx[ii] > vmax_x){vx[ii] = vmax_x;}
    else if (vx[ii] < vmin_x){vx[ii]=vmin_x;}

    x[ii] = x[ii]+vx[ii]; //Actualization of position

    if (x[ii] > xlim[1]){x[ii] = xlim[1]-Math.abs(vx[ii]);}
    else if (x[ii] < xlim[0]){x[ii] = xlim[0]+Math.abs(vx[ii]);}

    x[ii] = Math.round(x[ii]);
}

//Stop criterion
double prom = 0;
for (int ii = 0; ii < partc; ii++){prom = prom + x[ii];}
prom = Math.abs(prom/partc);
double ccc = 0;
for(int ii=0; ii<partc; ii++){
    double cc = (x[ii]-prom)*(x[ii]-prom);
    ccc = ccc+cc;
}
ccc = ccc*ccc/partc;
if (ccc < 1){break;}
}
}

```

## Published Papers

- J. Avilés, J. C. Mayo-Maldonado, and O. Micheloud, “*A Hybrid Evolutionary Approach to Design Off-Grid Electrification Projects with Distributed Generation*,” Mathematical Problems in Engineering, vol. 2018, Article ID 9135842, 12 pages, 2018. <https://doi.org/10.1155/2018/9135842>.
- J. Avilés, J. C. Mayo-Maldonado, and O. Micheloud, “*A multi-objective evolutionary approach for planning and optimal condition restoration of secondary distribution networks*”, Applied Soft Computing, (under review), 2018.
- J. Avilés, O. Erives, and O. Michleoud, “*Optimal Design of Low Voltage Distribution-Networks Using a PSO-PRIM Algorithm*”, in 2018 IEEE Third Ecuador Technical Chapters Meeting (ETCM), 2018, pp. 1-6.





## **Curriculum Vitae**

Juan Pablo Avilés was born in Cuenca – Ecuador in 1987. He received his MSc in Energy Engineering from the Instituto Tecnológico y de Estudios Superiores de Monterrey in 2015, under a scholarship from the Ecuadorian government. He received his B.S. in Electrical Engineering from the Universidad Politécnica Salesiana in 2011 and has proven experience in the design of distribution lines and electrical maintenance of power transformers. Currently he is pursuing his Ph.D. at the Tecnológico de Monterrey focused in microgrids and design of electrical systems using metaheuristics methods.



## References

- [1] A. d. R. y. C. d. Electricidad, "Perspectiva y Expansión del Sistema Eléctrico Ecuatoriano,," vol. 3, C. Consejo Nacional de Electricidad, Ed., ed, 2013.
- [2] (2013). *Plan Maestro de Electrificación 2013-2022*. Available: <http://www.regulacionelectrica.gob.ec/plan-maestro-de-electrificacion-2013-2022/>
- [3] HowStuffWorks. (2018, 20/09). *How Power Grids Work*. Available: <https://science.howstuffworks.com/environmental/energy/power5.htm>
- [4] H. W. Beaty, *Electric power distribution systems: a nontechnical guide*. PennWell Books, 1998.
- [5] M. A. and B. H., "Search for a minimal-loss operating spanning tree configuration in an urban power distribution system," presented at the 5th Power System Computation Conf., Cambridge, UK, 1975.
- [6] B. J. Cory and M. R. Irving, "Chapter 13 - The power system," in *Newnes Electrical Power Engineer's Handbook (Second Edition)*, D. F. Warne, Ed. Oxford: Newnes, 2005, pp. 375-390.
- [7] E. E. R. d. S. S.A. (2012, 09/25). *Normas técnicas para el diseño de redes eléctricas urbanas y rurales*. Available: <https://es.scribd.com/document/88804962/Indice-Normas-Tecnicas-2006-Para-El-Diseno-Redes-Elctricas-Urbanas-y-Rurales>
- [8] V. Tech. (2007, September 20). *Introduction to Distributed Generation*. Available: <https://www.dg.history.vt.edu/ch1/introduction.html>
- [9] N. A. o. C. A. A. NACAA. (2018, 09/26). *Reduce Losses in the Transmission and Distribution System* Available: [http://www.4cleanair.org/sites/default/files/Documents/Chapter\\_10.pdf](http://www.4cleanair.org/sites/default/files/Documents/Chapter_10.pdf)
- [10] W. Caisheng and M. H. Nehrir, "Analytical approaches for optimal placement of distributed generation sources in power systems," *IEEE Transactions on Power Systems*, vol. 19, no. 4, pp. 2068-2076, 2004.
- [11] B. Khorshid-Ghazani, H. Seyedi, B. Mohammadi-ivatloo, K. Zare, and S. Shargh, "Reconfiguration of distribution networks considering coordination of the protective devices," *IET Generation, Transmission & Distribution*, vol. 11, no. 1, pp. 82-92, 2017.
- [12] T. M. Masaud, G. Nannapaneni, and R. Chaloo, "Optimal placement and sizing of distributed generation-based wind energy considering optimal self VAR control," *IET Renewable Power Generation*, vol. 11, no. 3, pp. 281-288, 2017.
- [13] M. Nick, R. Cherkaoui, and M. Paolone, "Optimal Planning of Distributed Energy Storage Systems in Active Distribution Networks Embedding Grid Reconfiguration," *IEEE Transactions on Power Systems*, vol. 33, no. 2, pp. 1577-1590, 2018.
- [14] R. A. Jabr, D. I, x017E, afi, x, and I. Huseinagi, "Real Time Optimal Reconfiguration of Multiphase Active Distribution Networks," *IEEE Transactions on Smart Grid*, pp. 1-1, 2018.
- [15] M. E. Baran and F. F. Wu, "Network reconfiguration in distribution systems for loss reduction and load balancing," *IEEE Transactions on Power Delivery*, vol. 4, no. 2, pp. 1401-1407, 1989.

- [16] R. Siddaiah and R. P. Saini, "A review on planning, configurations, modeling and optimization techniques of hybrid renewable energy systems for off grid applications," *Renewable and Sustainable Energy Reviews*, vol. 58, pp. 376-396, 5// 2016.
- [17] B. Y. Bagde, B. S. Umre, R. D. Bele, and H. Gomase, "Optimal network reconfiguration of a distribution system using Biogeography Based Optimization," in *2016 IEEE 6th International Conference on Power Systems (ICPS)*, 2016, pp. 1-6.
- [18] A. Tandon and D. Saxena, "Optimal reconfiguration of electrical distribution network using selective particle swarm optimization algorithm," in *2014 International Conference on Power, Control and Embedded Systems (ICPCES)*, 2014, pp. 1-6.
- [19] S. Bahadoorsingh, J. V. Milanovic, Y. Zhang, C. P. Gupta, and J. Dragovic, "Minimization of Voltage Sag Costs by Optimal Reconfiguration of Distribution Network Using Genetic Algorithms," *IEEE Transactions on Power Delivery*, vol. 22, no. 4, pp. 2271-2278, 2007.
- [20] A. Kouzou and R. D. Mohammadi, "Optimal reconfiguration of a radial power distribution network based on Meta-heuristic optimization algorithms," in *2015 4th International Conference on Electric Power and Energy Conversion Systems (EPECS)*, 2015, pp. 1-6.
- [21] Y. Wu, C. Lee, L. Liu, and S. Tsai, "Study of Reconfiguration for the Distribution System With Distributed Generators," *IEEE Transactions on Power Delivery*, vol. 25, no. 3, pp. 1678-1685, 2010.
- [22] S. Huang, Q. Wu, L. Cheng, and Z. Liu, "Optimal Reconfiguration-Based Dynamic Tariff for Congestion Management and Line Loss Reduction in Distribution Networks," *IEEE Transactions on Smart Grid*, vol. 7, no. 3, pp. 1295-1303, 2016.
- [23] A. Tiguercha, A. A. Ladjici, and M. Boudour, "Optimal radial distribution network reconfiguration based on multi objective differential evolution algorithm," in *2017 IEEE Manchester PowerTech*, 2017, pp. 1-6.
- [24] T. T. Nguyen, T. T. Nguyen, A. V. Truong, Q. T. Nguyen, and T. A. Phung, "Multi-objective electric distribution network reconfiguration solution using runner-root algorithm," *Applied Soft Computing*, vol. 52, pp. 93-108, 2017/03/01/ 2017.
- [25] M. Kaur and S. Ghosh, "Network reconfiguration of unbalanced distribution networks using fuzzy-firefly algorithm," *Applied Soft Computing*, vol. 49, pp. 868-886, 2016/12/01/ 2016.
- [26] T. Kaboodi, J. Olamaei, H. Siahkali, and R. Bitai, "Optimal distribution network reconfiguration using fuzzy interaction and MPSO algorithm," in *2014 Smart Grid Conference (SGC)*, 2014, pp. 1-5.
- [27] T. Subas Ratna, S. Jai Govind, and O. Weerakorn, "Multi-objective approach for distribution network reconfiguration with optimal DG power factor using NSPSO <br/>," (in English <br/>), vol. 10 <br/>, no. 12 <br/>, p. 2842 <br/>, 2016.
- [28] P. S. Georgilakis and N. D. Hatziargyriou, "Optimal Distributed Generation Placement in Power Distribution Networks: Models, Methods, and Future Research," *IEEE Transactions on Power Systems*, vol. 28, no. 3, pp. 3420-3428, 2013.

- [29] S. Sultana and P. K. Roy, "Krill herd algorithm for optimal location of distributed generator in radial distribution system," *Applied Soft Computing*, vol. 40, pp. 391-404, 2016/03/01/ 2016.
- [30] B. Das, V. Mukherjee, and D. Das, "DG placement in radial distribution network by symbiotic organisms search algorithm for real power loss minimization," *Applied Soft Computing*, vol. 49, pp. 920-936, 2016/12/01/ 2016.
- [31] A. S. Bouhouras, P. A. Gkaidatzis, and D. P. Labridis, "Optimal application order of network reconfiguration and ODGP for loss reduction in distribution networks," in *2017 IEEE International Conference on Environment and Electrical Engineering and 2017 IEEE Industrial and Commercial Power Systems Europe (EEEIC / I&CPS Europe)*, 2017, pp. 1-6.
- [32] M. Ahmadigorji, N. Amjadi, and S. Dehghan, "A novel two-stage evolutionary optimization method for multiyear expansion planning of distribution systems in presence of distributed generation," *Applied Soft Computing*, vol. 52, pp. 1098-1115, 2017/03/01/ 2017.
- [33] P. P. Biswas, R. Mallipeddi, P. N. Suganthan, and G. A. J. Amaratunga, "A multiobjective approach for optimal placement and sizing of distributed generators and capacitors in distribution network," *Applied Soft Computing*, vol. 60, pp. 268-280, 2017/11/01/ 2017.
- [34] W. Sheng, K. Liu, Y. Liu, X. Meng, and Y. Li, "Optimal Placement and Sizing of Distributed Generation via an Improved Nondominated Sorting Genetic Algorithm II," *IEEE Transactions on Power Delivery*, vol. 30, no. 2, pp. 569-578, 2015.
- [35] Y. Xu, Z. Y. Dong, K. P. Wong, E. Liu, and B. Yue, "Optimal Capacitor Placement to Distribution Transformers for Power Loss Reduction in Radial Distribution Systems," *IEEE Transactions on Power Systems*, vol. 28, no. 4, pp. 4072-4079, 2013.
- [36] M. Mohammadi, "Bacterial foraging optimization and adaptive version for economically optimum sitting, sizing and harmonic tuning orders setting of LC harmonic passive power filters in radial distribution systems with linear and nonlinear loads," *Applied Soft Computing*, vol. 29, pp. 345-356, 2015/04/01/ 2015.
- [37] M. Ranaboldo, A. García-Villoria, L. Ferrer-Martí, and R. Pastor Moreno, "A meta-heuristic method to design off-grid community electrification projects with renewable energies," *Energy*, vol. 93, Part 2, pp. 2467-2482, 12/15/ 2015.
- [38] V. Miranda, J. V. Ranito, and L. M. Proenca, "Genetic algorithms in optimal multistage distribution network planning," *IEEE Transactions on Power Systems*, vol. 9, no. 4, pp. 1927-1933, 1994.
- [39] V. F. Martins and C. L. T. Borges, "Active Distribution Network Integrated Planning Incorporating Distributed Generation and Load Response Uncertainties," *IEEE Transactions on Power Systems*, vol. 26, no. 4, pp. 2164-2172, 2011.
- [40] K. Deb, A. Pratap, S. Agarwal, and T. Meyarivan, "A fast and elitist multiobjective genetic algorithm: NSGA-II," *IEEE Transactions on Evolutionary Computation*, vol. 6, no. 2, pp. 182-197, 2002.
- [41] Q. Zhang and H. Li, "MOEA/D: A Multiobjective Evolutionary Algorithm Based on Decomposition," *IEEE Transactions on Evolutionary Computation*, vol. 11, no. 6, pp. 712-731, 2007.

- [42] J. E. S. A.E. Eiben, *Introduction to Evolutionary Computing*. (Natural Computing Series). Springer, 2015
- [43] Y. d. Valle, G. K. Venayagamoorthy, S. Mohagheghi, J. C. Hernandez, and R. G. Harley, "Particle Swarm Optimization: Basic Concepts, Variants and Applications in Power Systems," *IEEE Transactions on Evolutionary Computation*, vol. 12, no. 2, pp. 171-195, 2008.
- [44] PROGRAMIZ. (2018, 18/09). *Prim's Algorithm*. Available: <https://www.programiz.com/dsa/prim-algorithm>
- [45] E. E. R. C. Sur, "PRECIOS UNITARIOS VIGENTES DESDE 01-AGOSTO-2009," ed, 2017.
- [46] Alibaba. (2018, November 15). *Alibaba, Electrical Equipment and Supplies*. Available: <https://www.alibaba.com/showroom/15kw-inverter.html>
- [47] AutoSolar. (2018 8/08). *AutoSolar, Solar Energy*. Available: <https://autosolar.es/paneles-solares>
- [48] J. J. Grainger and C. Lozano Sousa, *Análisis de sistemas de potencia / John J. Grainger, William D. Stevenson ; traductor Carlos Lozano Sousa*. México : McGraw-Hill, 1996., 1996.
- [49] A. S. D. CENTER. (26 March 2008, 5 11). *Surface meteorology and Solar Energy*. Available: <https://eosweb.larc.nasa.gov/sse/RETScreen/>
- [50] EERCS. (2018, 06/01). *Geoportal*. Available: [geoportal.centrosur.com.ec/geoportal/arcgisfroautocad.aspx](http://geoportal.centrosur.com.ec/geoportal/arcgisfroautocad.aspx)
- [51] L. B. N. L. (LBNL). (2016, 10/05). *DER-CAM User Manual*. Available: <https://building-microgrid.lbl.gov/sites/all/files/DER-CAM User Manual V4-414 0.pdf>